METRO RAIL TRANSIT CONSULTANTS
DMJM/PBQD/KE/HWA

FOR

SOUTHERN CALIFORNIA RAPID TRANSIT DISTRICT

SUPPLEMENTAL CRITERIA FOR SEISMIC DESIGN OF UNDERGROUND STRUCTURES

LOS ANGELES

231

215896L+

SUPPLEMENTAL CRITERIA FOR SEISMIC DESIGN OF UNDERGROUND STRUCTURES

JUNE 1984

Prepared by

METRO RAIL TRANSIT CONSULTANTS

<u>TABLE OF CONTENTS</u>

TABLE OF CONTENTS (CONT'D)

LIST OF TABLES

LIST OF FIGURES

SOUTHERN CALIFORNIA RAPID TRANSIT DISTRICT

NOVEMBER 1983

RTD

METRO RAIL PROJECT

PROJECT UNIT INDEX

- Detail Design Units
- CONSTRUCTION CONTRACT UNITS:
  - STATION-STAGE II
  - ALL OTHER CONTRACTS

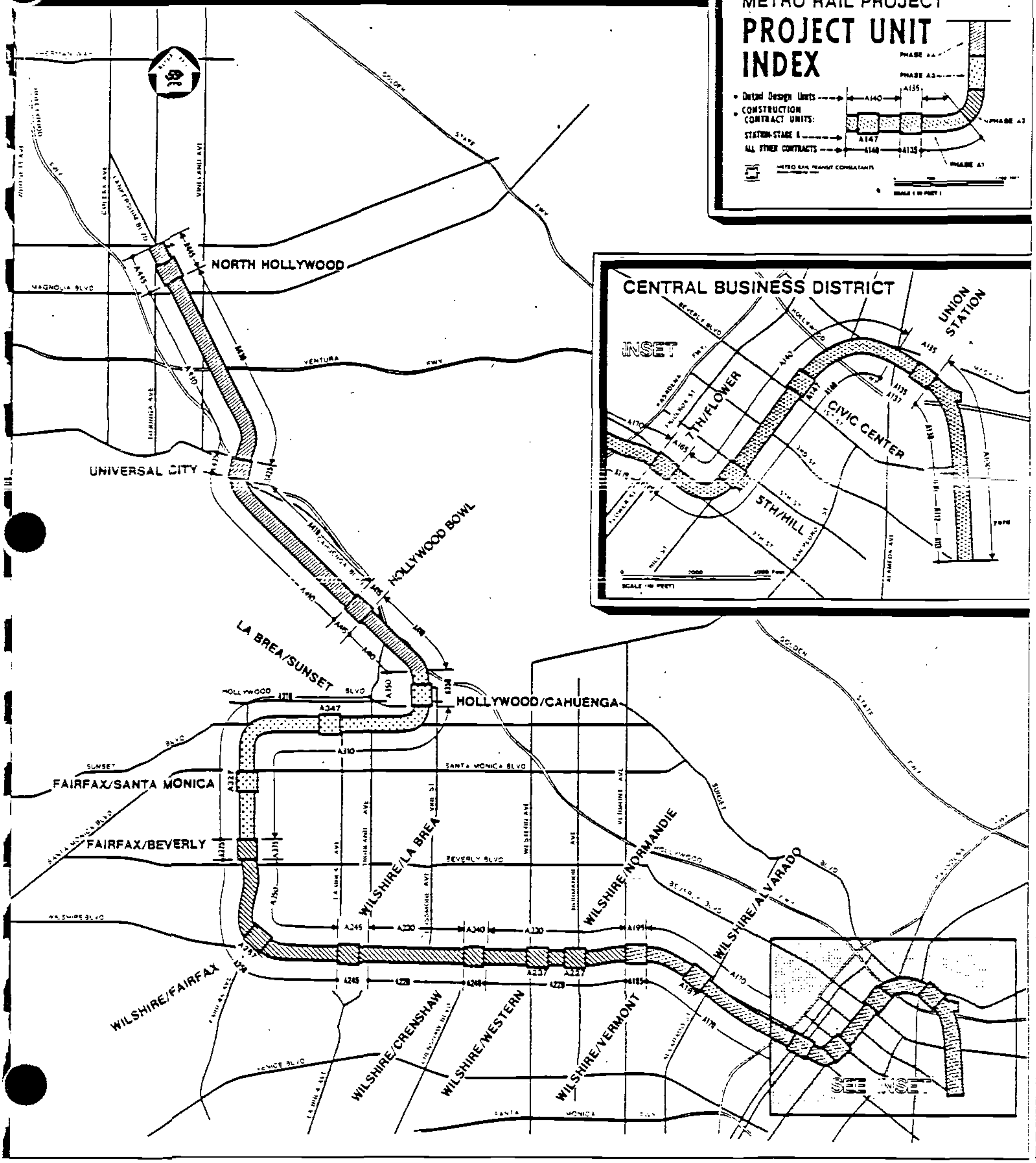

I. INTRODUCTION

A. BACKGROUND

Except for the contents of structures, this document provides structural seismic design criteria for underground structures of the Southern California Rapid Transit District (SCRTD) Metro Rail Project. For the sake of clarity, this document was written as a complete criteria for the seismic design of underground structures and as such replaces Section 4.3 and subsection 4.4.6 of Part II, Appendix A, Seismological Investigation & Design Criteria (Converse, 1983; hereinafter referred to as Appendix A). Portions of Appendix A are incorporated by reference.

This document has been written to address the general seismic design conditions that apply to the underground structures of the Metro Rail Project. It is recognized that special problems may arise for individual section design. Representative examples of such special problems are change of materials from "rock" to alluvium, fault crossings, and joints between tunnels and stations. Section designers are to review their site-specific conditions for these types of problems and identify those that cannot be solved by direct application of all applicable criteria and standard and directive drawings. Solutions to these remaining problems shall then be subject to further discussion between the section designer, SCRTD, and SCRTD's consultants.

B. GENERAL EFFECTS OF EARTHQUAKES

The effects of earthquakes on underground structures may be broadly grouped into two general classes -- shaking and faulting.

1. Shaking

In response to earthquake motion of bedrock (shaking), the soil transmits energy by waves. Seismologists identify various types of earthquake waves; structural engineers are generally interested in the effects of shear waves, which produce a displacement of the ground transverse to the axis of wave propagation.

The orientation of propagation is generally random with respect to any specific structure. Waves propagated parallel to the long axis of a linear structure, such as a subway tunnel, will tend to force a corresponding transverse distortion on the structure. Waves traveling at right angles to the structure will tend to move it back and forth longitudinally, and may tend to pull it loose at zones of abrupt transitions in soil conditions, where wave properties may vary. Diagonally impinging waves subject different parts of a linear structure to out-of-phase displacements. This results in a longitudinal compression-rarefaction wave that travels along the structure.

2. Faulting

Faulting generally represents primary shearing displacements of bedrock, which may pass through the overburden layer(s) to the ground surface. Such physical shearing of the rock or soil is generally limited to relatively narrow seismically active fault zones, which may be identified by geological and seismological surveys. From a structural viewpoint, faulting may evidence itself as major soil displacements, for example, liquefaction or landslide.

In general, it is not feasible to design structures to restrain major soil displacements. Useful design measures are limited to identifying and avoiding sensitive areas, or if this is not possible, accepting the displacement, localizing and minimizing damage, and providing means to facilitate repairs.

C. EFFECTS ON UNDERGROUND STRUCTURES

Past performance of underground structures during seismic events indicates that damage may result from primary or secondary effects of earthquakes, including the following:

- Strong ground motions
- Fault rupture
- Regional tectonic movements
- Landslides
- Liquefaction
- Differential compaction or consolidation of sediments.

Instances of complete tunnel closure were associated with combined primary and secondary effects of earthquakes, such as fault rupture and slope failure. However, in general, tunnels are safer than aboveground structures for a given level of shaking.

A major contributor to deformations and corresponding stresses in long linear structures, such as tunnels, is traveling wave effects, which can be accounted for by assuming that the tunnel and surrounding soil move together as the wave passes, and that motion from point to point along the route follows the wave pattern and differs from point to point only due to a time lag.

It is important that the designer recognize that the effect of an earthquake on underground structures is the imposition of a deformation which cannot be changed substantially by strengthening the structure. Therefore, the structural design solution is provision of sufficient ductility to absorb the imposed deformation without losing the capacity to carry static loads, rather than designing to resist inertial loads at a specified unit stress.

Nonetheless, it should also be recognized that although the absolute amplitude of earthquake <u>displacement</u> may be large, this displacement is spread over a long length. The gradient of earthquake <u>distortion</u> is generally small, and often within the elastic deformation capacity of the structure. If it can be established that the maximum deformation imposed by the specified earthquake, when combined with other appropriate loading conditions, will not strain the structure beyond the elastic range, no further provisions are required. If certain parts of the structure are strained into the plastic range, the ductility of such parts should be investigated.

Plastic straining in conformance with shearing distortion of the ground may affect the elastic properties of the structure. If continuity of the structure has been assumed in the design for static loads, the effects of plastic distortions will require special consideration as outlined in these criteria.

In the following sections, the effects of shaking and faulting on underground structures are considered and methods of analyzing their impact on structural design are presented.

II. ENVIRONMENTS

This section provides criteria for the earthquake-related environment applicable to the design of underground structures on the Metro Rail Project. Except where specifically referenced, this section takes precedence over Section 4.3, Appendix A.

A. DESIGN PARAMETERS

Design ground motion values for the underground structures are given in Table II-1 (from Appendix A, Converse, 1983).

TABLE II-1

DESIGN EARTHQUAKE PARAMETERS

Design Earthquake	Foundation Condition	DESIGN GROUND MOTION PARAMETERS: Acceleration (a_{max}) (g) Hor.	Acceleration (a_{max}) (g) Vert.	Velocity (v_{max}) (ft/sec) Hor.	Velocity (v_{max}) (ft/sec) Vert.	Dispalcement (ft) Hor.	Dispalcement (ft) Vert.
ODE	Soil	0.30	0.20	1.4	1.0	1.6	1.0
	Rock	0.30	0.20	0.8	0.6	0.5	0.3
MDE	Soil	0.60	0.40	3.2	2.1	3.3	2.2
	Rock	0.60	0.40	1.9	1.3	1.0	0.7

The shearing distortion of the ground shall be determined as given in Figures III-1 and III-2. (These figure are reproduced from Part II of the Seismological Investigation, and are shown there as Figures 4-2 and 4-3. For the purposes of this report, curves have been added for New Alluvium.) Unless more site-specific data are available from dynamic laboratory or field tests, as given in the individual geotechnical report for each design section, the velocity of propagation of the earthquake shear waves shall be taken for design purposes as shown in Table II-2.

TABLE II-2

SHEAR-WAVE SEISMIC VELOCITIES

(FOR USE IF SPECIFIC DATA ARE UNAVAILABLE)

Soil Classification	Shear Wave Seismic Velocity, C_s
New Alluvium	900 fps
Old Alluvium	1200 fps
"C" Units	1700 fps
Basalt	5000 fps

Design for fault displacement is required only for maximum design earthquake (MDE) conditions. Where actual surface faulting may be expected to occur, at the Santa Monica and Hollywood faults, the MDE fault displacement shall be taken as 6.6 ft. and 4.9 ft., respectively, for these faults (Appendix A). The MDE Richter magnitude is 7.0 for Santa Monica and 6.5 for Hollywood. Table A-3 of Appendix A contains additional details of fault displacements.

B. APPROACH

Table II-3 provides the recommended general value for strain to be used in design for earthquake inputs (line 3, column 3); this table also gives representative values for Old Alluvium with a shear wave velocity of 1200 fps. Pseudostatic procedures may be used for the design of all underground structures.

It is recognized that the use of the component of effective shear-wave velocity in the direction of the axis of the structure, as used in Table II-3 and in Annex A, is more conservative than the use of apparent wave velocity in the design of buried lifelines to resist earthquake shaking motions. It is further recognized that lifelines are critical structures whose survival is desired in the immediate postearthquake period, especially for fighting fires and maintaining safety. However, in terms of potential loss of lives, an underground metro often presents a higher risk than failure of a typical lifeline system. Measured in terms of depth of burial relative to diameter of opening, an underground metro is generally closer to the surface than other lifelines; for some conditions, this shallow relative depth can increase distress due to earthquake.

Therefore, the writers of these supplemental criteria adopted the more conservative approach. As noted in the brief study in Supplement F, this approach may produce strains in the structures approaching a factor of two higher than might be the actual case. However, given the inherent variability in properties of natural earth materials, the large combination of conditions that are expected to occur throughout the Metro Rail Project, and the lack of actual measurements in metro tunnels subjected to earthquakes, the conservative approach is deemed appropriate.

Using the assumption that the soil does not lose its integrity during the design earthquake, the basic concept governing the response of underground structures is that the soil is generally stiff when compared to the structure and, therefore, the earthquake deformation of the soil is imposed on the structure, which must conform to this deformation. For very soft soils, interaction between the soil and the structure may be considered, but for any reasonably competent soil this interaction may be neglected, and the structures should be designed to conform to the free soil deformations. Ignoring interaction generally induces larger deformation and strain; thus, it is conservative to neglect interaction.

The imposed deformations are of two types -- curvature and shearing. The former represents the direct imposition of the soil curvature on the structure, which must have the capacity to absorb

TABLE II-3

SELECTED PRINCIPAL EFFECTS OF EARTHQUAKE GENERATED WAVES ON FLEXIBLE UNDERGROUND STRUCTURES

Wave Type	Propagation Direction Relative to Tunnel Axis (θ)	Effect of Combined Waves Axial Strains Induced in Medium: General Formula[a]	Effect of Combined Waves Axial Strains Induced in Medium: Representative Numerical Value for Old Alluvium (in/in)	Remarks (See Annex B)
Dilational (P-) Wave	0°	$\varepsilon_p \cong \pm \frac{v_{max}}{c_{pe}}$	± 0.0017 [b,c]	No curvature is induced for 0° incidence.
Shear (S-) Wave	45°	$\varepsilon_a \cong \pm \frac{v_{max}}{2c_{se}} \pm 0.7 R \frac{a_{max} g}{c_{ae}^2}$	± 0.0018 [b]	R = 10' (assumed)[d]
Recommended Value	Shear Wave at 45°	$\bar{\varepsilon}_1 \cong \pm \frac{v_{max}}{2c_{ae}} \pm 0.7 R \frac{a_{max} g}{c_{se}^2}$	± 0.0018 [b]	R = 10' (assumed)[d]

[a] Assumes a_{max} and v_{max} are produced only by the wave considered and they occur simultaneously which is physically impossible but an acceptable conservative approximation.

[b] For Old Alluvium and MDE; c_s = 1200 fps and C_{se} = 0.8 x 1200 = 960 fps (See Annex A)

[c] $c_p = 2c_s$ for $u = 1/3$; this is a better approach for deriving strain in the soil than a measured valued in saturated or nearly saturated soil for which c_p approaches that for the water in the interstices. For dry soils $c_p \neq 2c_s$

[d] Coefficient includes required trigonometric terms for angle of incidence.

the resulting strains. The latter represents the displacement of the soil in response to a base acceleration imparted to it through the bedrock.

C. APPLICATION

Application of the design methods for underground station structures is discussed in Sections III through V and for circular running tunnels in Section VI. Section VII contains design methods for structural connections and other special considerations. The special design cases for fault crossings, landslides, and liquefaction are presented in Section VIII. Section Designers are responsible for implementation of criteria in Sections III, IV, V, and VII. The General Architectural/Engineering Consultant (MRTC) will implement the criteria in Section VI. Section Designers shall identify the location(s) of special problems discussed in Section VIII; the resolution of these special conditions shall be agreed upon among SCRTD, MRTC, and the Section Designers.

III. EARTHQUAKE DESIGN OF STATIONS AND OTHER SHALLOW, RECTANGULAR, FRAMED STRUCTURE

The effect of earthquake racking (see Section IV) on the structure requires that the structure conform to the free-field soil deformation. If it can be established that the maximum deformation imposed by the specified earthquake will not strain the structural frame beyond yield at any point, using the loads of Equation (Eq.) IV-2 or IV-3, no further provisions to resist the deformation are required. If certain joints are strained into the plastic range by the MDE, the structure shall be checked, and redesigned as necessary, to ensure that no plastic hinge combinations can be formed that are capable of leading to a collapse mechanism.

A. GENERAL PROCEDURE

1. Base initial size of members on static design, Eq. IV-1 or Eq. V-1, and appropriate strength requirements. Building code design methods shall be applied, recognizing that the structure is surrounded by geologic materials.

2. Impose earthquake deformation (racking) on the structure using data from Figures III-1 and III-2, following the concept shown in Figure III-3. These racking deformations induce moments and internal forces in the structure. These effects, treated as values of Q in Sections IV and V, are to be added to those from the static analysis in accord with the complete equations defining demand, also in Sections IV and V. Follow ACI, Los Angeles City Building Code (LACBC), or Uniform Building Code as appropriate for determining member stiffnesses. Pseudohorizontal loads, to provide racking deformations equal to that of Figure III-3a, may be applied at the floor levels (Figure III-3b) for analysis purposes. It

is essential that these loads be adjusted to account for the changes in member stiffness and the effect of the surrounding soil in limiting the racking of the structure.

3. Impose a dynamic soil-pressure increment on the structure (Appendix A, Converse, 1983; Seed and Whitman, 1970). These effects, treated as values of Q in Sections IV and V, are to be added to those from the static analysis in accord with the complete equations defining demand (Sections IV and V). Follow ACI, Uniform Building Code, or LACBC as appropriate for determining member stiffness.

4. Evaluate conditions in the structure applying Eqs. IV-2 or IV-3 or Eqs. V-2 or V-3, and Steps 1 and 2, and then 1 and 3. The more critical (Step 1 plus Step 2, or Step 1 plus Step 3) shall apply.

5. Design completed if adequate strength conditions in the context of the appropriate building code(s) exist at all points for static and ODE conditions. Design completed when ultimate conditions in the context of plastic design as hereinafter provided are not exceeded at any point for MDE conditions.

6. Evaluate possible mechanisms for MDE conditions (see Figure III-4). Conditions with only two hinges in any one member, such as illustrated in Figure III-4a, are acceptable because a failure (collapse) mechanism has not formed. Conditions with four hinges, such as illustrated in Figure III-4b, are acceptable because collapse is prevented by the surrounding material, even though such a structure would collapse if it were aboveground. However, formation of any of mechanisms such as 1, 2, 3, 4, or 5 in Figure III-4c, would lead to collapse and these mechanisms are, therefore, not acceptable. Similarly, if soils are susceptible to

liquifaction, the conditions of Figure III-4b could lead to collapse and are not acceptable.

7. Check the structure for strain in the longitudinal direction resulting from frictional soil drag (see Appendix 1). This strain from soil drag is the upper limit on strain in the longitudinal direction.

8. Modify the structure elements as necessary so that an acceptable design results.

FIGURE III-1

HORIZONTAL SHEAR DEFORMATION IN VARIOUS GEOLOGIC UNITS

(OPERATING DESIGN EARTHQUAKE)

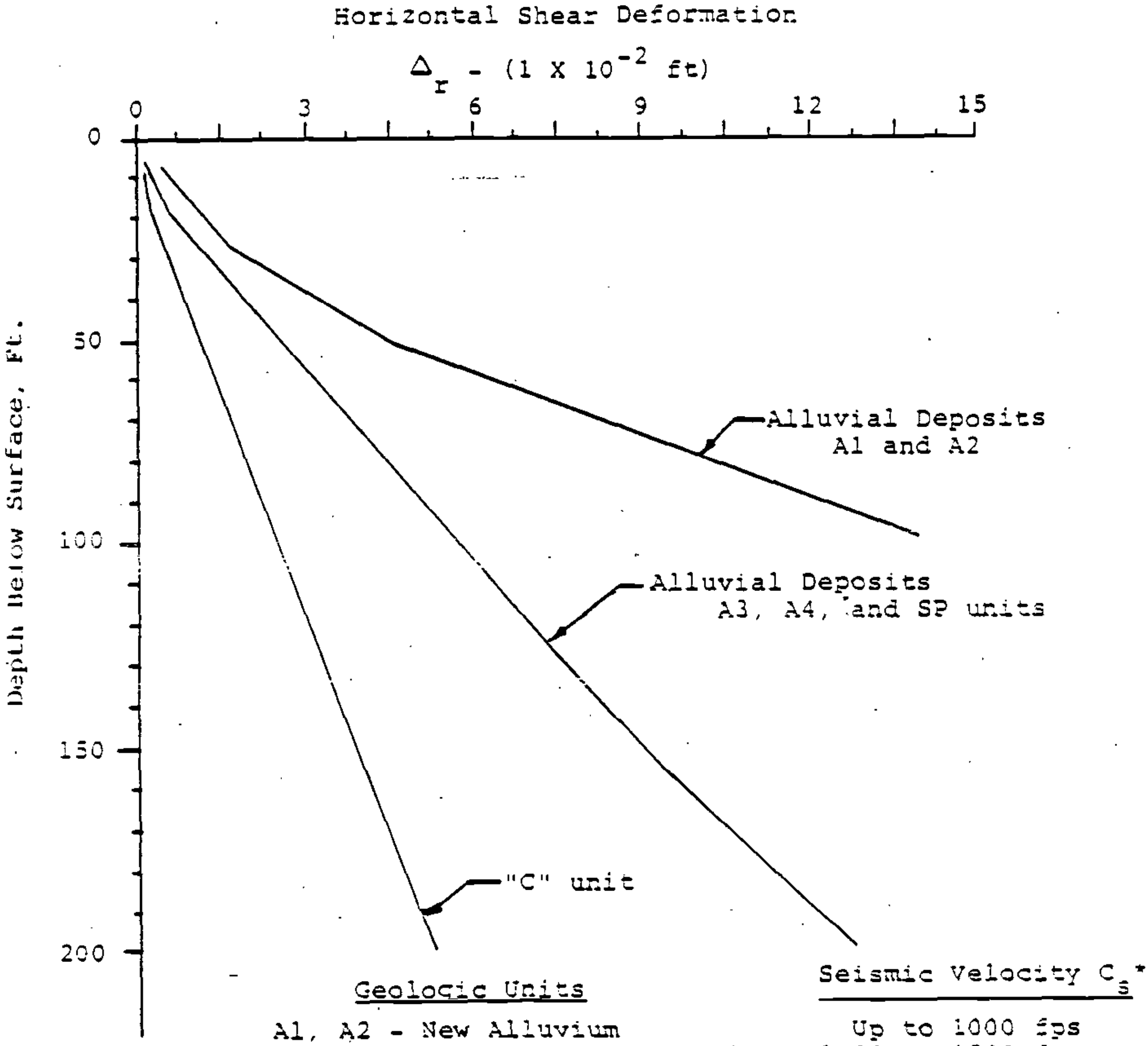

Geologic Units	Seismic Velocity C_s*
A1, A2 - New Alluvium	Up to 1000 fps
A3, A4 - Old Alluvium	1000 to 1500 fps
SP - San Pedro Formation	1000 to 1500 fps
C - Fernando Formation	1500 to 1900 fps

*See Table II-2

Modified from Converse Consultants (Part II, 1983) by addition of curve for Alluvial Deposits A1 and A2 from SHAKE solution by change in titles of scales, and by adding tabulation of seismic velocities.

FIGURE III-2

HORIZONTAL SHEAR DEFORMATION IN VARIOUS GEOLOGIC UNITS

(MAXIMUM DESIGN EARTHQUAKE)

Horizontal Shear Deformation

Δ_r - (1×10^{-1} ft)

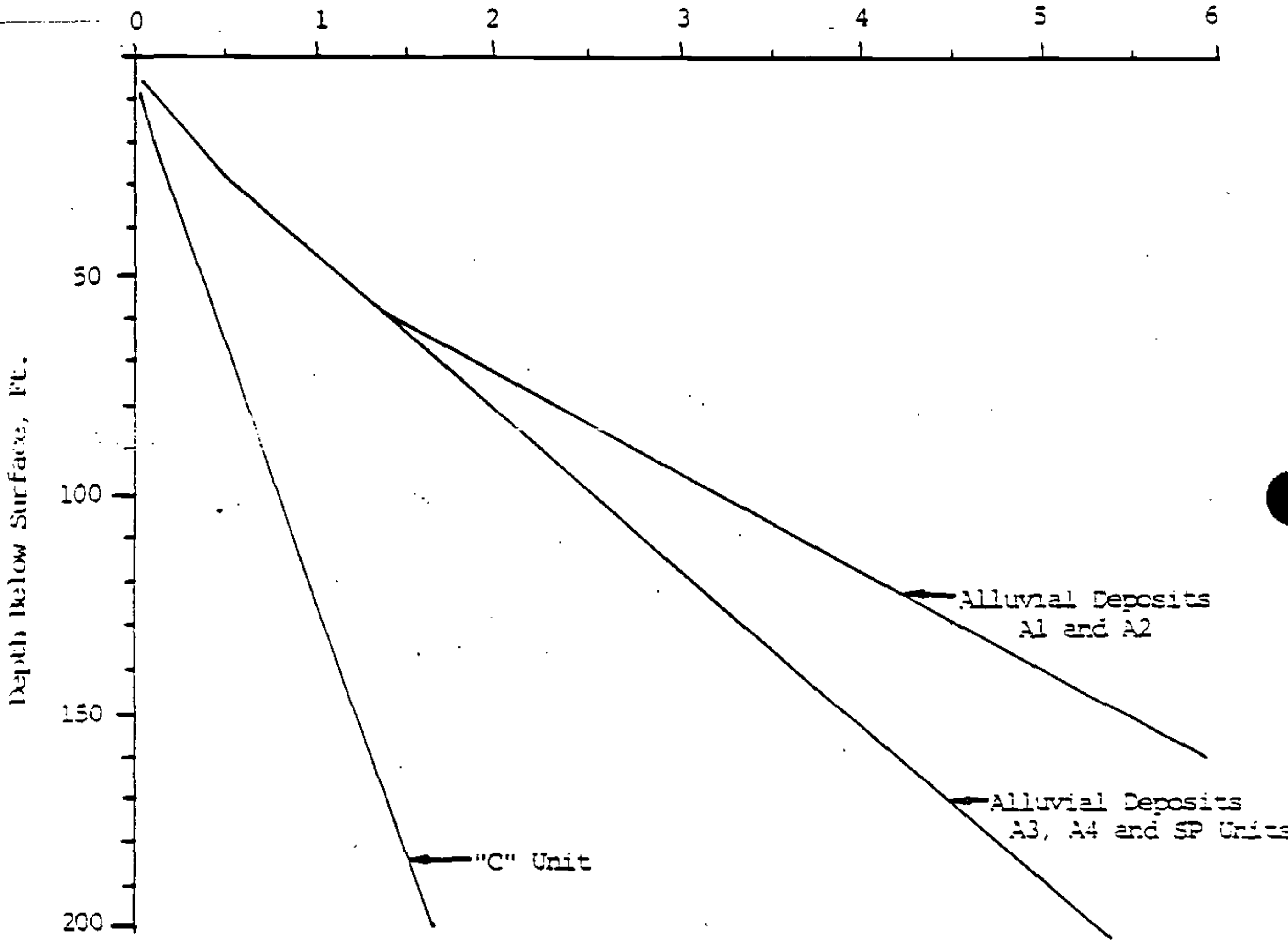

Geologic Units	Seismic Velocity C_s*
A1, A2 - New Alluvium	Up to 1000 fps
A3, A4 - Old Alluvium	1000 to 1500 fps
SP - San Pedro Formation	1000 to 1500 fps
C - Fernando Formation	1500 to 1900 fps

Modified from Converse Consultants (Part II, 1983) by addition of curve for Alluvial Deposits A1 and A2 from SHAKE solution by change in titles of scales, and by adding tabulation of seismic velocities.

*See Table II-2

FIGURE III-3

APPLICATION OF IMPOSED EARTHQUAKE DEFORMATION

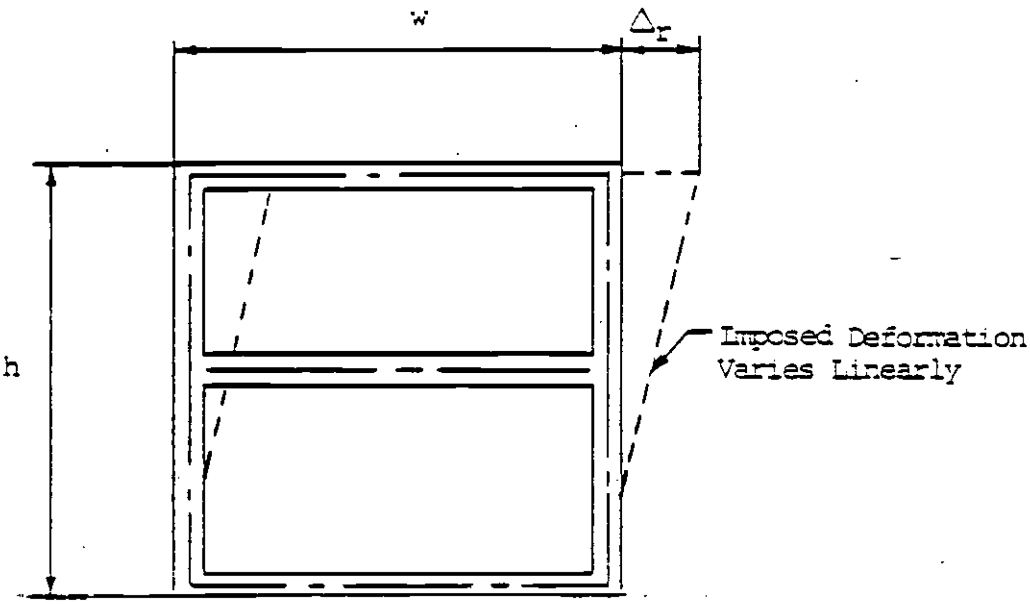

a. Imposed Horizontal Deformation

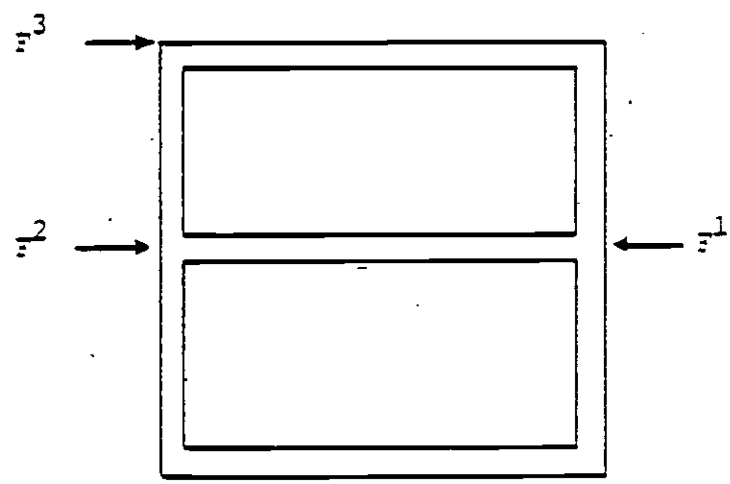

b. Pseudo horizontal loads applied to structure to provide imposed deformation of Figure III-3a.

Note: Δ_r (slope of curve times height of story or of structure) from Fig. III-1 or Fig. III-2

FIGURE III-4

STRUCTURE MECHANISMS FOR MDE

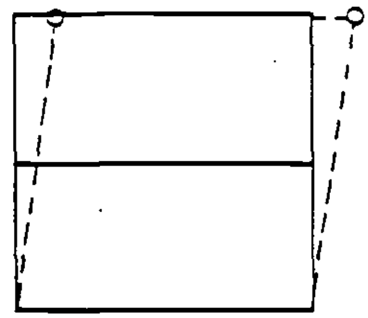

a. Acceptable Condition - Two Hinges

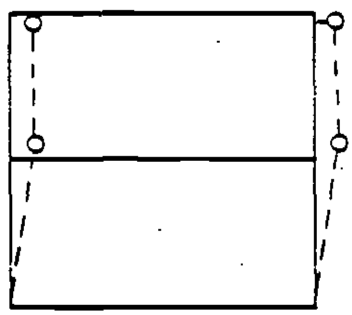

b. Acceptable Condition - Four Hinges

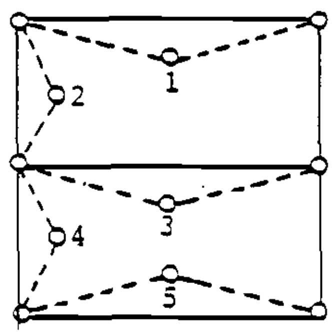

c. Unacceptable Conditions - Three Hinges in Any Member

IV. DESIGN OF STATION AND OTHER SHALLOW, RECTANGULAR, FRAMED CONCRETE STRUCTURES

A. STATIC LOADING CONDITIONS

Stations shall be designed for static loading conditions following the direction given in SCRTD Design Criteria and on directive drawings. Reinforced concrete design shall follow ACI 381-83, the commentary to ACI 318-83, the LACBC, Division 26, and the following:

$$U = 1.4D + 1.7L + 1.7H \qquad \text{Eq. IV-1}$$

where: U = Required strength to resist factored loads or related internal moments and forces.

D = Dead loads due to soil, water in soil, structural components, or other materials, or related internal moments and forces

L = Live loads or related internal moments and forces.

H = Loads due to horizontal pressure of soil, water in soil or other materials, or related internal moments and forces.

B. DYNAMIC LOADING CONDITIONS

Station designs shall then be checked for dynamic loading conditions using ACI 318-83 and the following:

$$U = D + L + H + Q \qquad \text{Eq. IV-2}$$

for the maximum design earthquake, and

$$U = 0.75\ [1.4D + 1.7L + 1.7H + 1.87Q] \qquad \text{Eq. IV-3}$$

for the operating design earthquake (ODE).

where: U, D, L, and H are as defined in IV.A, Q being the effects induced by the earthquake.

C. DESIGN DETAILS

1. Designer shall select the design tension steel percentage, p, to avoid brittle behavior.

2. Redistribution of moments in accordance with ACI 318-83, Section 8.4, is acceptable for ODE.

3. Consideration of plastic hinges is acceptable for MDE and shall follow procedures such as given in Blume, et al (1961), Rosenblueth (1980), and Park and Paulay (1975). Stability considerations are applied at the ultimate-limit state and stiffnesses should be representative of this state. In lieu of more precise values, calculate EI following procedures in Sections 10.10 and 10.11 (paragraph a) of the ACI Commentary (1983), and Section 10.3.3 of ACI (1983).

4. The earthquake design of underground structures shall consider the more critical of the following two conditions:

a. Applicable static loading conditions plus the racking effects described herein.

b. Applicable static loading conditions plus a dynamic soil-pressure increment (Appendix A and Seed and Whitman, 1970).

5. Vertical loads from soil backfill, water in soil, structural components, or other materials over cut-and-cover structures shall be increased by 20 percent and 40 percent for operating design and maximum design earthquakes, respectively (Table II-1).

V. DESIGN OF STATIONS AND OTHER SHALLOW, RECTANGULAR, FRAMED STEEL STRUCTURES

A. STATIC LOADING CONDITIONS

Stations shall be designed for static loading conditions following the direction given in SCRTD Design Criteria and on directive drawings. Steel design shall follow AISC (1978), LACBC (Division 27), Uniform Building Code, Chapter 27 (1982), and the following:

$$U = 1.7\ (D + L + H) \qquad \text{Eq. V-1}$$

where the terms are as defined in Section IV.

B. DYNAMIC LOADING CONDITIONS

Station designs shall then be checked for dynamic loading conditions using the following:

$$U = D + L + H + Q \qquad \text{Eq. V-2}$$

for the maximum design earthquake, and

$$U = 1.3\ (D + L + H + Q) \qquad \text{Eq. V-3}$$

for the operating design earthquake.

C. DESIGN DETAILS

1. Designer shall proportion steel structures under static loading conditions in accordance with provisions of AISC (1978), Section 2702 of the Uniform Building Code (1982), and LACBC, Division 27.

2. Designer may proportion steel structures under dynamic loading conditions in accordance with provisions of Sections 2721 and 2722 of the Uniform Building Code, and Division 27, LACBC. Requirements for Seismic Zone 4 shall apply, with plastically designed members permitted.

3. The earthquake design of underground structures shall consider the more critical of the following two conditions:

   a. Applicable static loading conditions plus the racking effects described herein.

   b. Applicable static loading conditions plus a dynamic soil-pressure increment (Appendix A; Seed and Whitman, 1980).

4. Vertical loads from soil backfill, water in soil, structural components, or other materials over cut-and-cover structures shall be increased by 20 percent and 40 percent for operating design and maximum design earthquakes, respectively (Table II-1).

VI. DESIGN OF CIRCULAR RUNNING TUNNELS

A. STATIC LOADING CONDITIONS

The current specified concrete segments for circular running tunnels have been designed by MRTC (following O'Rourke, 1984) for static loading conditions existing at all soil or soft rock sites along the alignment.* Linings for tunnel sections in the Topanga Formation will be designed by that section's designer.

B. DYNAMIC LOADING CONDITIONS

The adequacy of these designs to resist the possible static plus superimposed dynamic loading conditions must be checked following the steps given below.

The running tunnel structure is more flexible than the surrounding medium with respect to distortions in planes perpendicular to the axis of the structure (Annex D and Appendix 1). These distortions are, thus, the same as those of the surrounding medium. Although the running line structure is longitudinally stiffer than the surrounding medium, imposing the motions induced in the medium onto the structure is generally conservative.

C. STEPS IN DESIGN

1. Designer shall determine the applicable shear-wave velocity, c_s, for each segment of the running line considering the appropriate geotechnical data. If more specific data are not available, use Table II-2.

---

* Soil or soft rock describes all ground conditions except the Topanga Formation.

2. Define appropriate value of <u>effective</u> shear-wave velocity, c_{se}, consistent with the strain level expected. In general, unless explicit data are available, c_{se} shall be 0.9 c_s for ODE and 0.8 c_{se} for MDE; however, in isolated cases where the line is within new alluvium, c_{se} shall be 0.75 c_s for ODE and c_{se} = 0.5 c_s for MDE (see Annex A).

3. Compute maximum induced longitudinal strains using "recommended value" from Table II-3 for the ODE and MDE. Frictional soil drag should be checked as in Step 7 for the station. The maximum usable compressive strain for this case is 0.002 (Park and Paulay, 1975; Ford, et al, 1981 a, b, and c).

4. Assess the longitudinal capabilities of the lining to provide for no adverse distress for ODE and no collapse for MDE, explicitly considering effects and capabilities of articulation (O'Rourke, 1984). Ductile bolts shall be used in all cases.

5. When necessary, modify longitudinal reinforcement, bolts, and/or joint filler details to ensure no adverse distress for ODE conditions and no collapse for MDE conditions. The minimum reinforcing percentage for concrete segmental linings shall be 0.003 in either direction.

6. Check strains in plane perpendicular to the axis of the tunnel produced by excavation using Figure VI-1 (Ranken et al, 1978, Figure 3.8) in combination with racking deformation (see Appendix 1). The strain due to racking deformation is that produced by a shear wave with principal distortion in the plane of the tunnel which is perpendicular to the axis of the tunnel.

The strains are approximately:

$$\varepsilon_{rack} = \left(\frac{v_s}{c_{se}}\right) \left[2 \left(\frac{t}{R}\right) + \frac{3}{16} \left(\frac{E_m}{E_\ell}\right) \left(\frac{R}{t}\right)\right] \qquad \text{Eq. VI-1}$$

in compression, and

$$\varepsilon_{rack} = 2 \left(\frac{v_s}{c_{se}}\right) \left(\frac{t}{R}\right) \qquad \text{Eq. VI-2}$$

in tension.

where: v_s = Peak particle velocity produced by earthquake (Table II-1).

c_{se} = Effective shear-wave velocity for the value of v_s (see Grant and Brown, 1981).

t = Thickness of lining.

R = Mean radius of lining.

E_m = Modulus of elasticity of medium.

E_ℓ = Modulus of elasticity of lining (cylinder).

The at-rest condition, $K_o = 0.5$, shall be assumed. The average compression (average $K_o = 0.5$ in Figure VI-1) produces a uniform strain of $\Delta D/D$. It is recommended for horizontal and vertical displacement that the average for no- and full-slippage be assumed. The strain due to average compression should be superimposed on the strain due to horizontal or vertical displacement. Note that these last values of strain are due to flexure and that the maximum strains are as follows:

$$\varepsilon_{\theta_{outside}} = \frac{3}{2} \left(\frac{\Delta D}{D}\right) \left(\frac{t_{outside}}{R}\right) \qquad \text{Eq. VI-3}$$

$$\varepsilon_{\theta_{inside}} = \frac{3}{2} \left(\frac{\Delta D}{D}\right) \left(\frac{t_{inside}}{R}\right) \qquad \text{Eq. VI-4}$$

where:

$\varepsilon_{\theta_{outside}}$ = Strain on the outside of the lining.

$\varepsilon_{\theta_{inside}}$ = Strain on the inside of the lining.

$\Delta D/D$ = Appropriate value from Figure VI-1.

$t_{outside}$ = Distance from geometric axis to outside of cylinder.

t_{inside} = Distance from geometric axis to inside of cylinder.

R = Mean radius of cylinder.

The maximum usable compressive strain, ε_c, for flexure shall be 0.004 (Ford et al, 1981 a, b, and c).

7. Check strain due to loosening of medium above the structure in combination with racking distortions for lateral distortions (Appendix 1). The diameter change due to loosening load may be approximated from Figure VI-2. This change produces a flexural strain which is treated as above in Step 6.

8. Check strains for combination of out-of-round tolerance and racking. The out-of-round tolerance shall not exceed 0.005D.

9. Compare circumferential strains for Steps 6, 7, and 8 with allowable values. Modify reinforcement and joint details if necessary (O'Rourke, 1984). In no case should the reinforcing ratio exceed three-fourths of the balanced reinforcing ratio.

FIGURE VI-1

VARIATION OF DIAMETER CHANGE COEFFICIENT WITH FLEXIBILITY RATIO

(From Ranken, 1977)

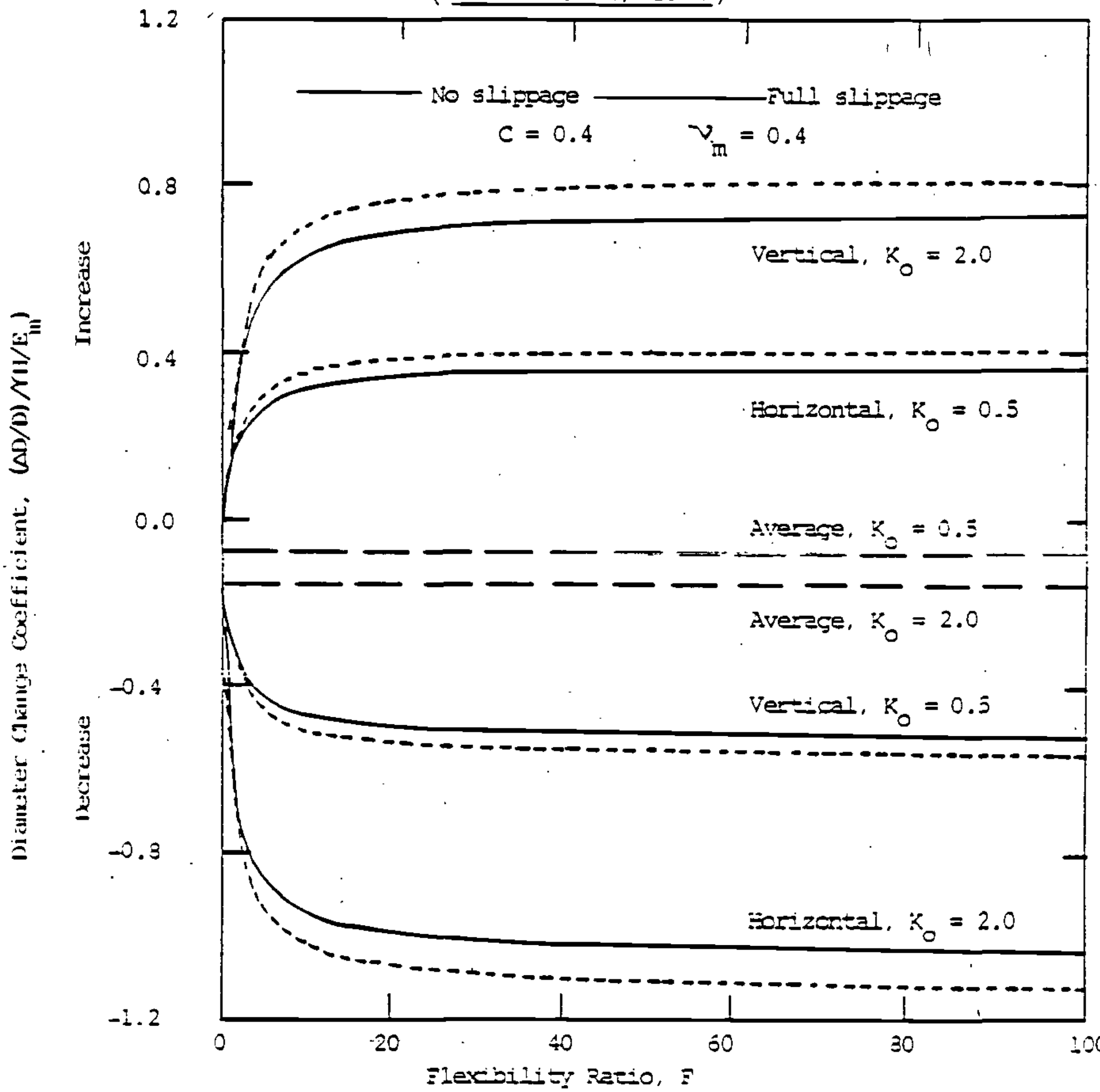

C = Compressibility Ratio (See Peck et al (1972), Annex D, and the Appendix

K_o = Ratio of Lateral to Vertical Stress in Medium

ν_m = Poisson's Ratio of Medium

E_m = Modulus of Elasticity of Medium

γ = Unit Weight of Medium

ΔD = Diameter Change of Cylinder

D = Diameter of Cylinder

H = Depth to Springline

F = Flexibility Ratio (See Peck et al (1972), Annex D, and the Appendix)

FIGURE VI-2

VARIATION OF APPROXIMATE DIAMETER CHANGE
WITH FLEXIBILITY RATIO FOR LOOSENING LOAD

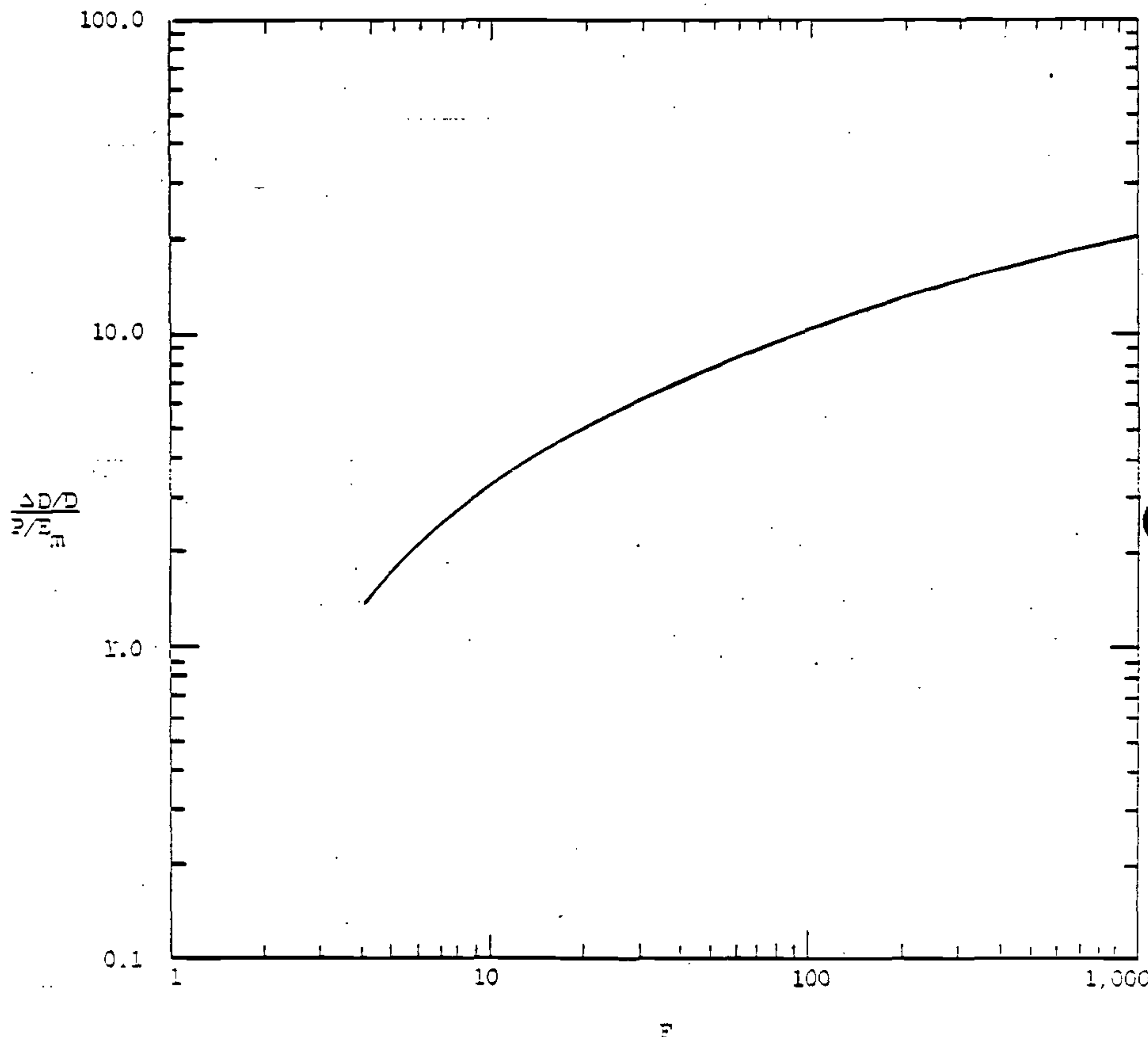

F = Flexibility Ratio (See Peck et al (1972))
P = Intensity of Loosening Load, Assumed to be a Triangular Distribution over a Central Angle of 90°. (for γ = 120 pcf and R = 9.5 ft., p = 3.5 psi) (see Figure E.15, Annex E)
E_m = Modulus of Elasticity of Medium
ΔD = Diameter Change of Cylinder
D = Diameter of Cylinder

VII. CONNECTIONS AND OTHER SPECIAL CONSIDERATIONS

A. STATION END WALLS

For all cases, the end walls shall be designed integrally with the walls, roof, and floor but separate from the tunnels. In developing the design, the section designer shall consider the following items:

1. End walls will behave generally as shear walls. They generally will not experience sidesway since they are stiff relative to the soil in resisting the imposed shear distortion of the soil.

2. Loading conditions described in Section III shall be applied to the framed structures to design the end walls.

3. The standard design provides a reinforced concrete foundation "approach span" transition where the tunnels enter the station to minimize the differential movements at that point. Polystyrene or other materials to accommodate shears shall be used.

B. THREE-DIMENSIONAL UNDERGROUND STRUCTURES

The geometry of some underground structures may require that they be considered three-dimensional rather than two-dimensional. When that is the case, designer shall apply the imposed racking deformations or incremental earth loadings consistent with those presented in Section III. The following cases and the effects of each must be evaluated:

1. One hundred percent in the first axial direction.

2. One hundred percent in the second axial direction.

3. Seventy percent superimposed in each of the two axial directions simultaneously.

C. DUCTILITY

The prime consideration in earthquake design is to provide a structure capable of behaving in a ductile manner when subjected to several cycles of earthquake deformations. Thus, even more than in usual design, the ultimate success of the structure is dependent upon attention to details in both design and construction. This set of criteria cannot address all the considerations to be applied by the designer, who should be familiar with the available information for aboveground structures and apply appropriate procedures to the underground structures.

As a minimum, the designer shall follow the most stringent of the following:

- o Steel - LACBC Specification, Part 2 (1978) or the LACBC, Division 26
- o Concrete - ACI, Appendix A (1983) or the LACBC, Division 26

Other applicable references include: ACI 318-83 and Commentary, UBC, 1982; Housner and Jennings, 1982; Newmark and Rosenblueth, 1971; Park and Paulay, 1975; Wiegel, 1970; Blume, et al, 1961; Rosenblueth, 1980; and Newmark and Hall, 1982.

VIII. FAULT AND RELATED CROSSINGS, LANDSLIDES, AND LIQUEFACTION

Design of systems that cross faults capable of offset, as expected at the Santa Monica and Hollywood fault crossings, is a difficult problem. As already noted, it is virtually impossible to provide a structure that will impede fault or related abrupt lateral motion; thus, the structure must be capable of accommodating the motion without collapse. These design solutions are expensive and they become even more expensive if an abrupt fault exists but, as in this case, its exact location is unknown.

Use of the standard steel lining becomes a question primarily of the total length of steel lining required. In turn, this total length depends on the distance required to develop sufficient angle change to accommodate conservatively that lateral displacement(s) specified for the MDE (6.6 ft.) in Section II. The geometry of the distorted running line is shown in Figure VIII-1, and the critical dimensions of the standard steel lining in general terms are shown in Figure VIII-2 (see also Annex B).

In all soils (Nyman, 1983) and in rock where the shear zone associated with a fault is distributed over hundreds of feet, the lining will tend to conform to the distributed displacement of the medium.

Landslides may develop only where alluvium with sufficient surface slope and water content intersects the axis of a structure. MRTC has conducted a review of the City of Los Angeles Planning Department's Seismic Safety Element Report (1974) and their Preliminary Geologic Maps (1964). These documents identify possible slide areas in the City of Los Angeles. During this review no significant existing landslide areas or areas susceptible to landslides from earthquakes were identified along the alignment of the SCRTD Metro Rail Project. This preliminary finding, however, does not relieve the section designer of the responsibility of evaluating the potential of and providing mitigation against landslide(s) along each specific section.

The final special design condition of potential concern is liquefaction. Current data regarding possible areas of liquefaction are presented in individual design unit geotechnical engineering reports. Where concern regarding liquefaction is expressed, the section designer shall assess the effects of such behavior on design and ensure that the structures are not adversely impacted.

FIGURE VIII-1

DISTORTION OF RUNNING LINE
FROM FAULT OFFSET

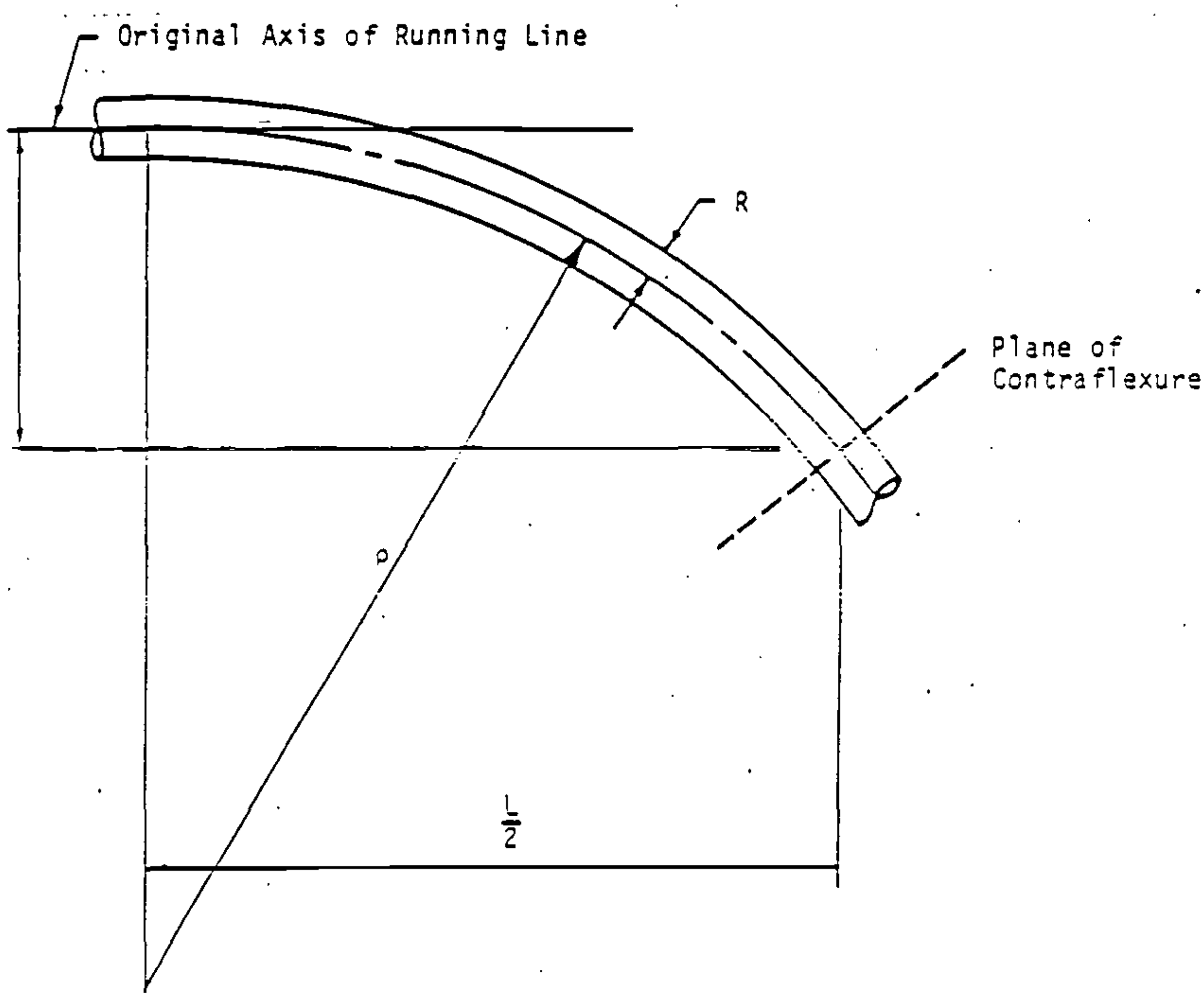

FIGURE VIII-2

CRITICAL DIMENSIONS OF STANDARD

STEEL LINING SEGMENTS

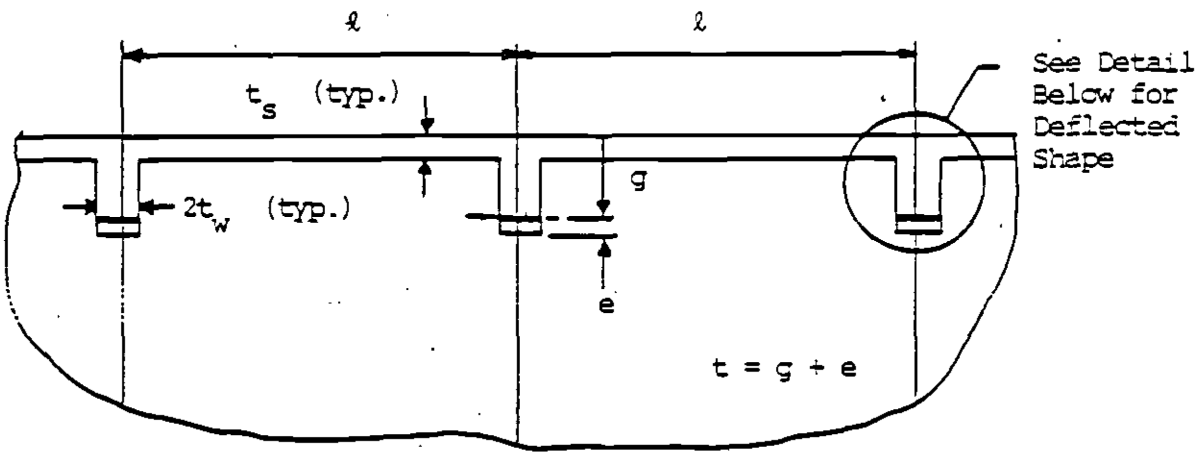

Longitudinal Wall Section

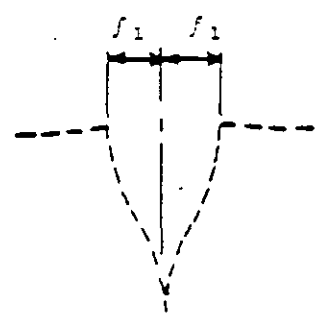

REFERENCES

ACI Committee 318 (1983), Building Code Requirements for Reinforced Concrete (ACI 318-83), American Concrete Institute, Detroit.

ACI Committee 318 (1983), Commentary on Building Code Requirements for Reinforced Concrete (ACI 318-83), American Concrete Institute, Detroit.

AISC (1978), Specification for the Design, Fabrication & Erection of Structural Steel for Buildings, American Institute of Steel Construction, New York.

ATC (1978), "Tentative Provisions for the Development of Seismic Regulations for Buildings. A Cooperative Effort with the Design Professions, Building Code Interests and the Research Community," Applied Technology Council Publication ATC 3-06, NBS Special Publication 510, NSF Publication 78-8.

Blume, J.A. et al (1961), Design of Multistory Reinforced Concrete Buildings for Earthquake Motions, Portland Cement Association, Chicago.

City of Los Angeles (1974), "Seismic Safety Element - Planning Department," J. H. Wiggins Company Technical Report 74-1199-1.

City of Los Angeles (1964) "Preliminary Geologic Maps - Santa Monica Mountains", Sheets 74, 93, 94, 95, 114, 115, 116, 136, 137, 158, 159, 181, O, P.

Converse Consultants (1983), Seismological Investigation & Design Criteria, Southern California Rapid Transit District Metro Rail Project.

Ellingwood, B. et al. (1980), "Development of a Probability Based Load Criterion for American National Standard A58," NBS Special Publication 577, Washington, DC.

Ford, J.S. et al. (1981a), "Behavior of Concrete Columns Under Controlled Lateral Deformation," Journal of the American Concrete Institute, January-February 1981, No. 1, Proceedings V.78, pp. 3-20.

Ford, J.S. et al. (1981b), "Experimental and Analytical Modeling of Unbraced Multipanel Concrete Frames," Journal of the American Concrete Institute, January-February 1981, No. 1, Proceedings V.78, pp. 21-35.

Ford, J.S. et al. (1981c), "Behavior of Unbraced Multipanel Con crete Frames," Journal of the American Concrete Institute, March-April 1981, No. 2, Proceedings V.78, pp. 99-115.

Grant, W.P. and Brown, F.R., Jr. (1981), "Dynamic Behavior of Soil from Field and Laboratory Test," Proceedings, International Conference on Recent Advances in Geotechnical Earthquake Engineering and Soil Dynamics, University of Missouri at Rolla, pp. 591-596.

Hognestad, E. (1951), "A Study of Combined Bending and Axial Load in Reinforced Concrete Members," University of Illinois Bulletin, Volume 49, Number 22, November 1951, Bulletin Series No. 399.

Housner, G.W. and Jennings, P.C. (1982), "Earthquake Design Criteria," Earthquake Engineering Research Institute, Volume Four of a series titled: Engineering Monographs on Earthquake Criteria, Structural Design, and Strong Motion Records.

Newmark, N.M. and Rosenblueth, E. (1971), Fundamentals of Earthquake Engineering, Prentice-Hall, Englewood Cliffs, N.J.

Newmark, N.M. and Hall, W.J. (1982), "Earthquake Spectra and Design," Earth Engineering Research Institute, Berkeley, California.

Nyman, D.J. (1983), Private Communication.

O'Rourke, T.D., editor (1984), "Guidelines for Tunnel Lining Design," Underground Technology Research Council, American Society of Civil Enginers, N.Y.

Park, R. and Paulay, T. (1975), Reinforced Concrete Structures, John Wiley & Sons, New York.

Peck, R.B. et al. (1972), "State of the Art of Soft Ground Tunneling," First North American Rapid Excavation and Tunneling Conference, ASCE-AIME, Chicago.

Ranken, R.E. et al (1978), "Analysis of Ground-Liner Interaction for Tunnels," U. S. Department of Transportation Report No. UMTA-IL-06-0043-78-3, Department of Civil Engineering, University of Illinois at Urbana-Champaign, Report No. UILU-ENG-78-2021.

Rosenblueth, E. (1980), Design of Earthquake Resistant Structures, John Wiley & Sons, New York.

Roy, H.E.H. and Sozen, M.A. (1964), "Ductility of Concrete," Flexural Mechanics of Reinforced Concrete, Proceedings of the International Symposium, Miami, Florida, 10-12 November 1964, sponsored by ASCE//ACI, pp. 213-235.

Seed, H.B. and Whitman, R.V. (1970), "Design of Earth Retaining Structures for Dynamic Loads," presented at the 1970 Specialty Conference: Lateral Stresses in the Ground and Design of Earth-Retaining Structures, sponsored by ASCE, 22-24 June 1970 at Cornell University, Ithaca, N.Y., pp. 103-147.

Uniform Building Code (1982), International Conference of Building Officials, Whittier, California.

Wiegel, R.L. et al. (1970), Earthquake Engineering, Prentice Hall, Englewood Cliffs, N.J.

APPENDIX 1

DESIGN EXAMPLES

APPENDIX 1

This appendix is provided for information only. It has no contractual implication, but provides numerical examples to illustrate the application of the supplemental criteria. Because the examples are illustrative and are focused on the problem at hand, the calculations have been kept as simple as possible.

Based upon the considerations reflected by these illustrations, it is expected that the greatest impact from earthquakes will occur for underground structures located totally or partially in New Alluvium. Nevertheless, each Section Designer is responsible for applying these criteria to his site specific conditions.

Design Examples

(All examples use numbers rounded to two significant figures.)

A. LONGITUDINAL STIFFNESS OF STATION

1. Compare longitudinal stiffnesses of station and replaced ground. For illustration, assume a structure 55 ft. wide by 43 ft. high with 2 ft. walls, 4 ft. top and bottom, and 2 ft. intermediate level. Assume effective modulus of elasticity of soil of 50,000 psi, representative of alluvium, and modulus of elasticity of concrete of 3.6×10^6 psi.

$$\frac{AE\ (\text{Station})}{AE\ (\text{Soil})} = \frac{(2\text{x}55\text{ft.x}4\text{ft.}+55\text{ft.x}2\text{ft.}+2\text{x}33\text{ft.x}2\text{ft.})\text{x}144\text{in}^2/\text{ft.}^2\text{x}3.6\text{x}10^6\text{psi}}{55\text{ ft. x }43\text{ ft. x }144\text{ in}^2/\text{ft.}^2\text{ x }50{,}000\text{ psi}} = 21$$

Therefore, the station is relatively stiff compared to the soil, so that the soil would be compressed more than the structure by a longitudinal wave. Thus, the structure would experience the full frictional drag exerted by the soil which tends to be the upper bound (see Annex B).

2. Compute the strain resulting from frictional drag.

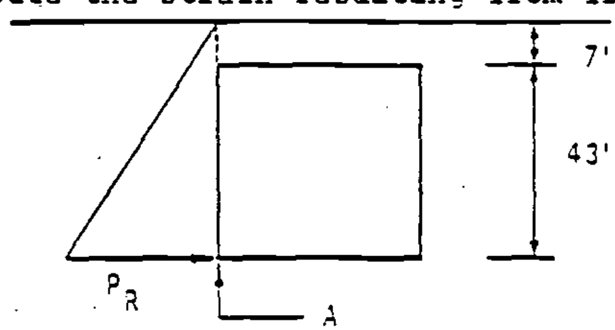

The at-rest pressure at the base of the structure is:

50 ft. x 120 pcf x (0.5 = Ko) = 3000 psf.

(K_o, the at-rest coefficient, is taken equal to 0.5).

3. Estimate the length of structure over which to sum strains as one-quarter the wave length. Assume the frequency

of the earthquake wave to be approximately three cycles/second from El Centro records. Then wave length = $\frac{c_s}{3} = \frac{1000}{3}$ = 300 ft., and the involved length of structure 75 ft.

4. Calculate the indicated strain in the concrete at point A, using a conservative soil friction of tan 40°:

$$\frac{300 \text{ psf} \times 1 \text{ ft.} \times 75 \text{ ft.} \times \tan 40°}{2\text{ft.} \times 1\text{ft.} \times 144\text{sq.in./sq.ft.} \times 3.6\times10^6\text{psi}} = 0.0002 \text{ in./in.}$$

5. Assume the allowable strain in tension is ten percent that in compression, and considering these to be axial strains, the allowable strain is 0.10 x 0.002 = 0.0002 in./in.

6. Therefore, for this example, the indicated strain equals the allowable and no provision for axial strain need be made in the design.

7. Designer shall analyze the actual structures in light of site-specific conditions and properties.

B. HORIZONTAL RACKING OF SHALLOW RECTANGULAR FRAMED STRUCTURE

1. Make a preliminary design of the structure. For this example assume centerline dimensions and member thicknesses are as follows:

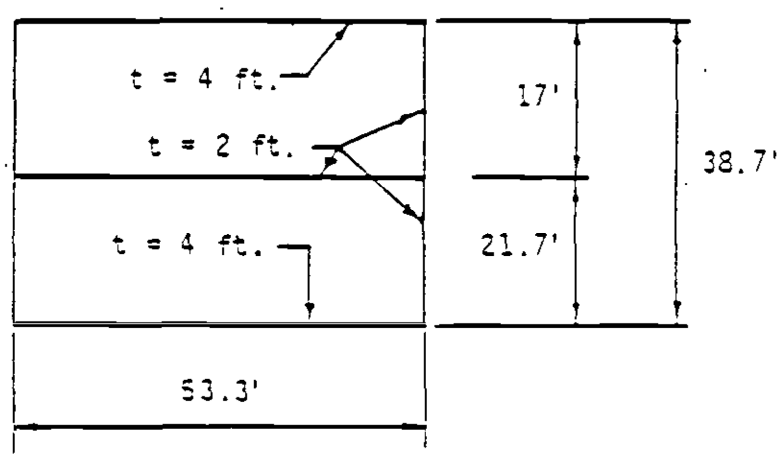

2. Calculate the differential horizontal racking distortions from bottom to top of structure. Using Figure III-2 (assuming the top 50 ft. of the curves for alluvium as an illustration), the racking deformation is estimated by taking the slope of the curve for Old Alluvium, approximately one in 400. Therefore, for the 38.7 ft. high structure the total racking is $\frac{38.7}{400}$ = 0.097 ft. (say 0.1 ft).

3. Calculate the relative racking distortion of each floor of the structure:

$$\text{Bottom floor} = \frac{21.7}{38.7} \times 0.1 = 0.056 \text{ ft.}$$

$$\text{Top floor} = \frac{17}{38.7} \times 0.1 = 0.044 \text{ ft.}$$

4. Impose these horizontal racking distortions on the structure and bring the structure to equilibrium, obtaining the following rounded moments (in in.-kips) at the points indicated:

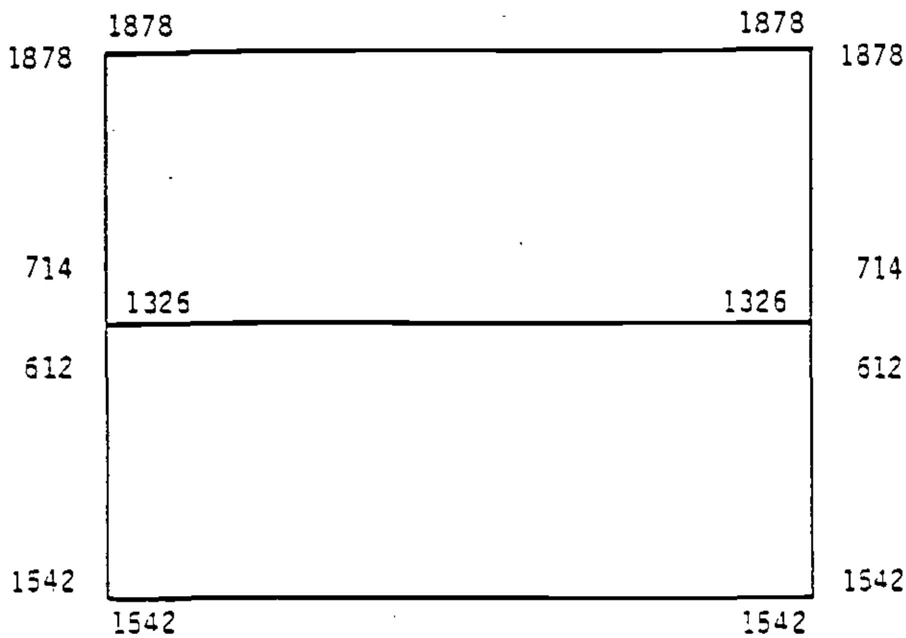

5. The above moments resulting from the dynamic racking shall then be combined with the static moments and thrusts defined previously to check the members. As an approximate check, calculate the approximate capacity at yield of the two-ft. thick section :

$M_{cap} = 0.9\ pbd^2 f_y$ (ignoring for this illustration capacity reduction factor and p')

$$= 0.9(0.02)(12\ in)\ (21\ in.)^2\ 60,000 = 5,720\ in\ kip$$

$$\therefore\ U = 5,720 = (1.4D + 1.7L + 1.7H)\ static$$

$$U = 1.0\ (1.0D + 1.0L + 1.0H + 1.0Q)\ dynamic$$

Obviously, the static loading can be no greater than 5,720/1.4 = 4,080 in kip. Therefore the dynamic (MDE) loading is no greater than

$$U = 4,080 + 1,880 = 5,960$$

or approximately four percent over the static capacity.

6. Obviously, for this example it appears necessary to raise the section capacity slightly so that the addition of the dynamic racking does not impose a bending requirement in excess of the static section capacity. Before making such a change, the designer shall consider the redistribution of bending stresses brought about by the formation of plastic hinges and compare with conditions shown in Figure III-4. If the resulting structural capacity still is less than the requirement, then the design shall be modified as required to satisfy the combined conditions.

The designer shall perform and complete such analyses for all appropriate conditions and combinations on a site-specific basis.

C. PLAN VIEW RACKING OF A THREE DIMENSIONAL STRUCTURE

1. Make a preliminary design of the structure. For this example assume centerline dimensions as follows (plan view):

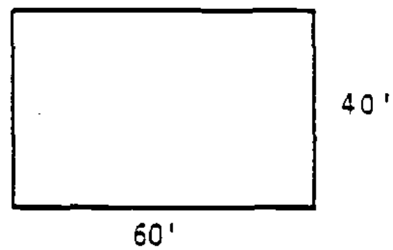

2. Review geotechnical data to define soil classification(s) encountered for the reaches and depths under consideration. Assume for this example that the structure is located in "C" units.

3. From Table II.2, define seismic velocity, $c_s = 1{,}700$ fps.

4. Define C_{se} from Annex A:

   for ODE, $c_{se} = 0.9c_s = 1{,}530$ fps

   for MDE, $c_{se} = 0.8c_s = 1{,}360$ fps

5. Estimate the racking strain by:

   $\gamma = \dfrac{v}{c_s}$ where v is from Table II.1

   for ODE, v = 1.4 fps, $\gamma = \dfrac{1.4}{1{,}530} = 0.00092$

   for MDE, v = 3.2 fps, $\gamma = \dfrac{3.2}{1{,}360} = 0.0024$

For illustration, use the MDE.

6. Calculate the racking distortion in the first major direction:

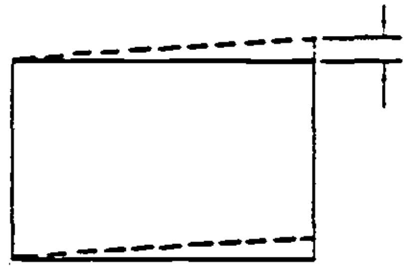

$\Delta = 0.0024 \times 60 = 0.144$ ft.

7. Calculate the racking distortion in the second major direction:

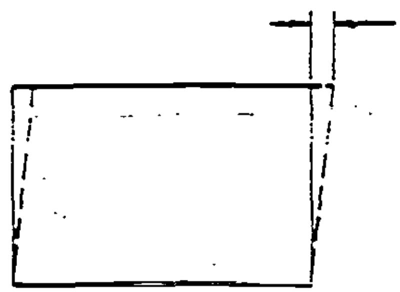

$\Delta = 0.0024 \times 40 = 0.096$ ft.

8. Calculate 0.70 of the distortion in each major direction and superimpose:

$0.096 \times 0.7 = 0.07$ ft.

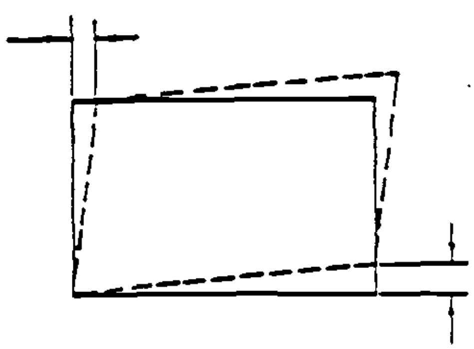

$0.144 \times 0.7 = 0.10$ ft.

9. Impose these racking distortions (steps 6, 7, and 8) on the structure and bring the structure to equilibrium under each, obtaining moments in each major structural member.

10. The moments and thrusts resulting from the dynamic racking shall then be combined (in turn if necessary, or using the maximum if obvious) with the static moments and thrusts defined previously to check the members.

11. Consider the redistribution of bending stresses brought about by the formation of plastic hinges. If the resulting structural capacity is less than the requirement, modify the static design to satisfy the requirement.

12. Perform and complete such analyses for all appropriate conditions and combinations on a site-specific basis.

D. EARTHQUAKE RESPONSE OF RUNNING LINE IN HOMOGENEOUS MEDIA

(The following examples applies Steps 1 through 9 of Chapter VI.)

NOTE: For illustration only, it has been assumed here that the data for the "C" units indicate a shear wave seismic velocity near the upper limit of the specified range -- or c_s = 1700 fps.

1. Review geotechnical data available to define soil classification(s) encountered for the reaches and depths under consideration. Assume for this example that all of the structure will be located in "C" units.

2. For Table II.3 and Figs. III.1 and III.2, define seismic velocity for "C" units:

c_s = 1700 fps (see above)

2.a Define c_{se}:

From more complete data, including techniques used by Grant and Brown (1981), or, if more data are not available, Annex A (Annex A is used here):

For ODE, $c_{se} = 0.9\ c_s = 1{,}530$ fps

For MDE, $c_{se} = 0.8\ c_s = 1{,}360$ fps

3. Compute axial strains induced:

From Table B.1:

$$\epsilon_{max} = \pm \frac{v_{max}}{2c_{se}} \pm 0.7\ R\ \frac{a_{max}\ g}{c_{se}^2}$$

From Table II-3:

For ODE, v_{max} = 1.4 fps and a_{max} = 0.3 g

For MDE, v_{max} = 3.2 fps and a_{max} = 0.6 g

Thus, for ODE:

$$\epsilon_{max} = \pm \frac{1.4 \text{ fps}}{2 \times 1{,}530 \text{ fps}} \pm 0.7 \times 10 \text{ ft.} \frac{0.3\ g \times 32.2\ \frac{\text{ft.}}{\text{sec}^2}}{(1{,}530 \text{ fps})^2} = \pm 0.0005$$

(Assumed radius of tunnel is 10 ft.)

If more complete data were available, the designer would now compare this strain with that assumed in Step 2a. If they were not consistent, the computed value here would be used to define a new value of c_{se}. By iteration, the appropriate c_{se} and corresponding ε_{max} would be defined.

For MDE,

$$\varepsilon_{max} = \pm \frac{3.2 \text{ fps}}{2 \times 1{,}360 \text{ fps}} \pm 0.7 \times 10 \text{ ft.} \frac{0.6 \text{ g} \times 32.2 \frac{\text{ft.}}{\text{sec}^2}}{(1{,}360) \text{ fps})^2} = \pm 0.0012$$

Again, if more data were available, the iterative process mentioned above would be used.

4. Compare with maximum usable strains:

For ODE in compression, $\varepsilon_{allow} = 0.002$ since strain is nearly purely axial. Also since $0.0005 < 0.002$ ok.

Since $|-0.0005 > |-0.0002|$, a plain concrete lining would crack in tension for the ODE; however, the segmented linings are reinforced and this tension strain (0.0005) is well below the minimum yield value of 0.0014. Therefore, any small cracks that tend to open in the segments will be closed by the reinforcing steel. Thus ok.

For MDE in compression, $\varepsilon_{allow} = 0.002$ since again strain is almost purely axial. Also since $0.0012 < 0.002$ ok.

Since $|-0.0012 > |-0.0002|$, a plain concrete lining would crack in tension for the MDE also; however, the segmented linings are reinforced and this tensile strain (0.0012) is still less than the minimum yield value of 0.0014. Thus ok.

Should a continuous liner be used for the tunnel passing through the basalt in the Hollywood Hills, it will require minimum reinforcement ($p = p' = 0.002$ as specified in Chapter VI). Such reinforcement will adequately distribute tension cracks induced by either the ODE or MDE.

5. Since no adverse distress is induced, no modification is required.

6. According to Ranken et al. (1978), the average diameter change coefficient for an assumed $K_o = 0.5$, from Figure VI.1, is:

$$\frac{(\Delta D)}{D} \frac{(E_m)}{\gamma H} = 0.08$$

(inward displacement) for all flexibility ratios of interest. Thus,

$$\frac{\Delta D}{D} = \varepsilon_{\theta_{ave}} = 0.08 \frac{\gamma H}{E_m}$$

or

$$\varepsilon_{\theta_{ave}} = 0.08 \frac{120 \text{ pcf} \times 50 \text{ ft.}}{50{,}000 \text{ psi} \times 144 \text{ in.}^2/\text{ft.}^2} = 0.000067$$

(shortening causes compression) for an average depth to springline of 50 ft.

From the same figure, the varying component of diameter change is approximately:

$$\left(\frac{\Delta D}{D}\right)\left(\frac{E_m}{\gamma H}\right) = 0.5 \quad \text{(shortening of vertical diameter)}$$

Thus, at the springline:

$$\frac{\Delta D}{D} = 0.5 \, \frac{120 \text{ pcf} \times 50 \text{ ft.}}{50{,}000 \text{ psi} \times 144 \text{ in.}^2/\text{ft.}^2} = 0.00042$$

Since:

$$\varepsilon_{\theta_{var}} = \frac{3}{2}\left(\frac{t}{R}\right)\left(\frac{\Delta D}{D}\right)^* = \frac{3}{2} \times \frac{8 \text{ in.}}{10 \text{ ft.} \times 12 \text{ in./ft.}} \times 0.00042 = 0.000042$$

The maximum strain produced by excavation is obtained by summing $\varepsilon_{\theta_{ave}}$ and $\varepsilon_{\theta_{var}}$

Thus:

$$\varepsilon_{max} = 0.000067 + 0.000042 = 0.00011.$$

Similarly, the minimum strain is approximately (Figure VI.1) =

$$\frac{\Delta D}{D} = -0.3 \, \frac{120 \text{ pcf} \times 50 \text{ ft.}}{50{,}000 \text{ psi} \times 144 \text{ in.}^2/\text{ft.}^2} = -0.00025 \text{ at the crown}$$

and invert.

$$\varepsilon_{\theta_{var}} = \frac{3}{2}\left(\frac{t}{R}\right)\left(\frac{\Delta D}{D}\right) = \frac{3}{2} \times \frac{8 \text{ in.}}{10 \text{ ft.} \times 12 \text{ in./ft.}} \times (-0.00025) =$$

$$-0.000025 \text{ and } \varepsilon_{min} = 0.000067 - 0.000025 = 0.000042.$$

---

* Curvature of a circular section = $\alpha = 3 \frac{\Delta R}{R^2} = 3 \left(\frac{\Delta D}{D}\right)\left(\frac{1}{R}\right)$ and strain = $\varepsilon_{\theta_{var}} = \alpha \frac{t}{2}$ or $\varepsilon_{\theta_{var}} = \frac{3}{2}\left(\frac{t}{R}\right)\left(\frac{\Delta D}{D}\right)$

The racking deformation causing compressive strain for combination with strain reproduced by excavation is defined by Equation B.17 in Annex B; that causing tensile strain by Equation B.18. In both cases the Poisson's Ratio was assumed to be one-third. If better values exist, they should be used and the equations modified as indicated in Annex B.

$$\varepsilon_{tot} = \left(\frac{V_s}{C_{se}}\right) \left[2 \left(\frac{t}{R}\right) + \frac{3}{16} \left(\frac{R}{t}\right) \left(\frac{E_m}{E_\ell}\right) \right] \qquad \text{Eq. B.17}$$

$$\text{and } \bar{\varepsilon}_{tot} = -2 \left(\frac{t}{R}\right) \left(\frac{V_s}{C_{se}}\right) \qquad \text{Eq. B.18}$$

For ODE, $_{max}$ = 1.4 fps and c_{se} = 1,530 fps (see Steps 2a and 3).

Thus:

$$\varepsilon_{tot} = \left(\frac{1.4 \text{ fps}}{1{,}530 \text{ fps}}\right) \left[2 \left(\frac{8 \text{ in.}}{10 \text{ ft.} \times 12 \text{ in./ft.}}\right) + \frac{3}{16} \left(\frac{10 \text{ ft.} \times 12 \text{ in./ft.}}{8 \text{ in.}}\right) \frac{50{,}000 \text{ psi}}{4.6 \times 10^6 \text{ psi}} \right] = 0.00015$$

$$\varepsilon_{tot} = -2 \left(\frac{8 \text{ in.}}{10 \text{ ft.} \times 12 \text{ in./ft.}}\right) \left(\frac{1.4 \text{ fps}}{1{,}530 \text{ fps}}\right) = -0.00012$$

And the combination of strains due to excavation load and racking are:

$$(\varepsilon_{max}) \text{ combined} = 0.00011 + 0.00015 = 0.00026$$

$$(\varepsilon_{min}) \text{ combined} = 0.000042 - 0.00012 = -0.00008$$

The maximum compressive strain of 0.00026 is well within the maximum allowable value of 0.004 (the allowable value for mainly flexure). The tensile strain of 0.00008 is less than that expected to cause cracking. Thus, no cracking is expected.

For the MDE, v_{max} = 3.2 fps and c_{se} = 1,360 fps (see steps 2a and 3).

Thus:

$$\varepsilon_{tot} = \left(\frac{3.2 \text{ fps}}{1,360 \text{ fps}}\right) \left[2\left(\frac{8 \text{ in.}}{10 \text{ ft.} \times 12 \text{ in./ft.}}\right) + \frac{3}{16} \left(\frac{10 \text{ ft.} \times 12 \text{ in./ft.}}{8 \text{ in.}}\right) \frac{50,000 \text{ psi}}{4.4 \times 10^6 \text{ psi}} \right] = 0.00039$$

$$\bar{\varepsilon}_{tot} = -2 \left(\frac{8 \text{ in.}}{10 \text{ ft.} \times 12 \text{ in./ft.}}\right) \left(\frac{3.2 \text{ fps}}{1,360 \text{ fps}}\right) = -0.00031$$

And the combination of strains due to excavation load and racking are:

$$(\varepsilon_{max}) \text{ combined} = 0.00011 + 0.00039 = 0.00050$$
$$(\varepsilon_{min}) \text{ combined} = 0.000042 - 0.00031 = -0.00027$$

The maximum compressive strain of 0.00050 remains well within the allowable value of 0.004. Although the tensile strain is slightly larger than that normally associated with cracking, it is still much less than that normally encountered in conventional reinforced concrete beams or slabs.

7. According to the approximate procedure given in Annex E, as reflected in Figure VI.2, the maximum strains due to the loosening load are computed as follows:

Compute properties of transformed section. (Because of the irregular section due to bolt pockets, it is probably satisfactory to ignore the presence of compression steel and use an approximate rectangular section with effective depth of 7 in.).

$k = \sqrt{2pn - \overline{pn}^2} - pn$, $p \cong 0.005$, $f_c' = 6{,}500$ psi

$n = \dfrac{29{,}000{,}000 \text{ psi}}{57{,}000 \sqrt{f_c'}} = \dfrac{29{,}000{,}000}{57{,}000 \sqrt{6{,}500}} = 6.3$, $pn = 0.005 \times 6.3 =$

0.032

$k = 0.22$, $kd = 0.22 \times 7 = 1.5$ in., $I_\ell = \dfrac{b(kd)^3}{3} + nA_s (1 - k)^2 d^2$

For b = 1 in.:

$I_\ell = \dfrac{1 \times (1.5)^3}{3} + 6.3 \times 0.005 \times 1 \text{ in.} \times 7 \text{ in.} (1 - 0.22)^2 \times 7^2$

$I_\ell = 7.7 \text{ in.}^4/\text{in.}$

$F = \left(\dfrac{E_m}{E_\ell}\right) \left(\dfrac{a^3}{6I_\ell}\right) \left(\dfrac{1 - \upsilon_\ell^2}{1 + \upsilon_m}\right)$, from Peck, et al (1972), Annex D.

Let $\upsilon_\ell = 0.2$ and $\upsilon_m = 1/3$ as above

$F = \left(\dfrac{50{,}000 \text{ psi}}{4.6 \times 10^6 \text{ psi}}\right) \left[\dfrac{(10 \text{ ft.})^3 \times (12 \text{ in./ft/})^3}{6 \times 7.7 \text{ in.}^4/\text{in.}}\right] \left(\dfrac{1 - 0.2^2}{1 + 1/3}\right)$

$F = 290$

From Figure VI.2 for F = 290:

$\dfrac{\Delta D/D}{P/E_m} = 16$

P = average load intensity (see Annex E)

$P = \text{Area} \times \dfrac{120 \text{ pcf}}{1{,}728 \text{ in.}^3/\text{ft.}^3} \times \dfrac{1}{R \sqrt{2}}$

$\text{Area} = (\sqrt{2} - \frac{\pi}{4}) R^2$ from Figure E.3

$$P = (\sqrt{2} - \frac{\pi}{4})\ R^2 \times \frac{1}{14.4} \times \frac{1}{R\ \sqrt{2}}$$

$P = 3.5$ psi for $R = 120$ in. (10. ft.)

$$\frac{\Delta D}{D} = 16 \times \frac{3.7 \text{ psi}}{50{,}000 \text{ psi}} = 0.0012$$

$$\varepsilon_{\theta_{top}} = \frac{3}{2}\ (\frac{\Delta D}{D})\ (\frac{t}{R})$$ (See above from transformer section) $t = kd$

$$= \frac{3}{2} \times 0.0012 \times \frac{0.22 \times 7 \text{ in.}}{120 \text{ in.}} = 0.000023$$

$$\varepsilon_{\theta_{bottom}} = -\ \frac{3}{2}\ (\frac{\Delta D}{D})\ (\frac{(1 - k)d}{R})$$

$$= -\ \frac{3}{2} \times 0.0012 \times \frac{(1 - 0.22) \times 7 \text{ in.}}{120 \text{ in.}} = -0.000082$$

These strains are produced by the gravity load alone. Since the calculations in Annex E assume linear elasticity, the effect of the vertical acceleration on the loosened material can be computed by first adding the acceleration to the gravity component and then multiplying that number by the strain; thus,

For ODE: (a_{max})vert = 0.2 g

Thus $\varepsilon_{\ell oo}$ = (1 + 0.2) x computed strains = 0.000028 and -0.000098

For MDE: (a_{max})vert = 0.4 g

Thus: $\varepsilon_{\ell oo}$ = (1 + 0.4) x computed strains = 0.000032 and -0.00011.

The strain due to racking is the same as that in the preceding step; thus,

For ODE, $\varepsilon_{tot} = 0.00015$
$\bar{\varepsilon}_{tot} = -0.00012$

And the combination of strains due to the loosening load and racking are:

$$(\varepsilon_{max})\text{combined} = 0.00015 + 0.000028 = 0.00018$$

$$(\varepsilon_{min})\text{combined} = -0.00012 - 0.000098 = -0.00022$$

The maximum compressive strain of 0.00018 remain well within the maximum allowable of 0.004. The tensile strains are just in excess of those associated with cracking, but much less than those normally encountered in beams or slabs.

For MDE: $\varepsilon_{tot} = 0.00039$
$\bar{\varepsilon}_{tot} = -0.00031$

And the combination of strains due to the loosening load and racking are:

$$(\varepsilon_{max})\text{combined} = 0.00039 + 0.000032 = 0.00042$$

$$(\varepsilon_{min})\text{combined} = -0.00031 - 0.000011 = -0.00042$$

Although the compressive strain is obviously larger for MDE compared to ODE, the same conclusion applies. The tensile strain is above that normally associated with cracking, but it is much less than that in normal reinforced beams or slabs.

8. If an out-of-round tolerance of $\Delta D/D$ greater than 0.0012 (value from Step 7) is allowed in the example, the strain equivalent to this tolerance will be greater than that caused by loosening. Since this tolerance implies a value as small as:

$$\Delta D = 0.0012 \times 1 \times 10 \text{ ft.} \times 12 \text{ in./ft.} = 0.29 \text{ in.}$$

it is likely that out-of-round tolerance combined with racking may control. The steps for evaluating this case should be obvious from the two preceding cases.

9. The comparison and allowables has already been made in the three preceding steps (steps 6, 7, and 8). Obviously, for the conditions assumed here, step 7 governs for compression; step 8 for tension unless a tolerance greater than 0.0012 is allowed.

E. EARTHQUAKE RESPONSE OF RUNNING LINE AT FAULT CROSSINGS

The required clear circle within the tunnel cross section is 17.5 ft.; simultaneously the chord length which must be maintained to clear the individual cars is 40 ft. The minimum radius of curve to accommodate the rolling stock is 750 ft. All of these conditions must be considered in addition to the requirement illustrated by the example in Annex B.

TABLE E.1

Run Summary Matrix

Run No.	Load Shape	V_s soil ft./sec.	V_p soil ft./sec.	E soil psi	ν soil psi	K soil psi	G soil psi	E "loosened" zone-psi	G "interface"-psi	f'_c - psi
1	Uniform	1,500	5,000	184,700	0.45	622,300	63,700	18,500	63,700	8,000
5	Triangular	1,500	5,000	184,700	0.45	622,300	63,700	18,500	63,700	8,000
9	Triangular	1,200	2,400	103,600	0.33	103,500	38,900	0.0	38,900	4,000
10	Triangular	1,200	5,000	114,200	0.47	621,800	38,900	0.0	38,900	4,000
11[a]	Triangular	1,200	2,400	103,600	0.33	103,500	38,900	0.0	38,900	4,000
13	Triangular	830	1,670	50,000	0.33	50,000	18,700	0.0	18,700	6,500
14	Triangular	830	1,670	50,000	0.33[b]	50,000	18,700	0.0	1,870	6,500
15	Triangular	830	1,670	50,000	0.33[c]	50,000	18,700	0.0	0.0	6,500
17	Triangular	830	1,670	50,000	0.33	50,000	18,700	5,000	1,870	6,500
18[d]	Triangular	830	1,670	50,000	0.33	50,000	18,700	0.0	1,870	6,500

a Depth of Burial = 65 ft. in this case only, otherwise 140 ft.

b At interface = 0.48

c At interface = 0.50

d Two rings of interface elements

TABLE F.2

Comparison Between Time History Solution and Results Using Yeh's Expressions (Yeh 1974) for the Strain in the Tunnel Wall

Results are presented for the maximum design earthquake (MDE) and the operating design earthquake (ODE) for the five material configurations of Table F.2. The term Yeh-strain is derived by utilizing Equations 16 and 23 of Yeh (1974) with a radius of the tunnel equal to 9.5 feet and the local seismic velocities from Table F.1.

The MDE and ODE levels are defined as follow:

Table 2a - MDE:	Vertical Velocity	= 2.1 ft./sec.
	Horizontal Velocity	= 3.2 ft./sec.
	Vertical Acceleration	= 0.4 G's
	Horizontal Accleration	= 0.6 G's
Table 2b - ODE:	Vertical Velocity	= 1.0 ft./sec.
	Horizontal Velocity	= 1.4 ft./sec.
	Vertical Acceleration	= 0.2 G's
	Horizontal Accleration	= 0.3 G's

METRO RAIL TRANSIT CONSULTANTS
DMJM/PBQD/KE/HWA

FOR

SOUTHERN CALIFORNIA RAPID TRANSIT DISTRICT

INFORMATIONAL ANNEXES TO SUPPLEMENTAL CRITERIA FOR SEISMIC DESIGN OF UNDERGROUND STRUCTURES

INFORMATIONAL ANNEXES TO SUPPLEMENTAL CRITERIA FOR SEISMIC DESIGN OF UNDERGROUND STRUCTURES

These annexes are provided for information only. They have no contractual implication; as the title indicates, they provide general background for seismic design of underground structures. Because they are focused on the problem at hand, the derivations have been kept as simple as necessary to address the specific problems encountered. For more general derivations, references have been provided at the end of each annex.

Although an effort has been made to build one annex on the data from preceding annexes, it was not always possible to do so. As a result, the order follows primarily the needs for information developed during the preparation of the criteria themselves.

TABLE OF CONTENTS

LIST OF TABLES

LIST OF FIGURES

LIST OF FIGURES (CONTINUED)

LIST OF FIGURES (CONTINUED)

LIST OF FIGURES (CONTINUED)

ANNEX A

DERIVATION OF EQUATIONS AND EFFECTIVE SEISMIC VELOCITY

ANNEX A

DERIVATION OF EQUATIONS AND EFFECTIVE SEISMIC VELOCITY
(FOR SIMPLE STRESS WAVES PROPAGATING IN CONTINUOUS MEDIA)

For a Simple Wave Propagating in a Slender Rod

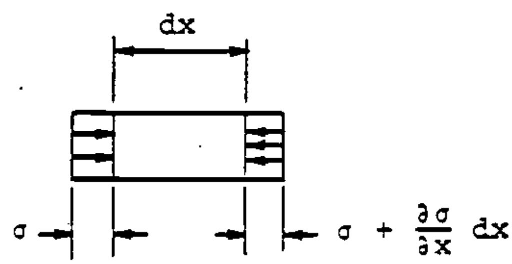

with:

ρ = mass density

A = cross sectional area

σ = stress

u = displacement in x-direction

$\ddot{u} = \dfrac{\partial^2 u}{\partial t^2}$ = acceleration in x-direction

Equilibrium requires:

$$\sigma + \rho \ddot{u} dx = (\sigma + \frac{\partial \sigma}{\partial x} dx), \text{ since A is common to all terms}$$

$$\rho \ddot{u} = \frac{\partial \sigma}{\partial x} \qquad \text{Eq. A}$$

and $$\varepsilon_x = \frac{\partial u}{\partial x}$$

For elastic conditions:

$$\sigma = E\varepsilon_x = E \frac{\partial u}{\partial x} \text{ and } \frac{\partial \sigma}{\partial x} = E \frac{\partial^2 u}{\partial x^2}$$

Thus: $\rho\ddot{u} = E\dfrac{\partial^2 u}{\partial x^2}$

Define $C^2 = \dfrac{E}{\rho}$ or $C = \sqrt{\dfrac{E}{\rho}}$, where C is the stress wave propagation velocity Eq. B

$$\therefore \ddot{u} = C^2 \frac{\partial^2 u}{\partial x^2}$$

The general solution is $u = f(x - Ct) + g(x + Ct)$

If consideration is restricted to waves propagating <u>only</u> in the positive x-direction:

$$u = f(x - Ct) \qquad \text{Eq. 1}$$

$$\varepsilon_x = \frac{\partial u}{\partial x} = f'(x - Ct) \qquad \text{Eq. 2}$$

$$\sigma_x = E\varepsilon_x = \rho C^2 \varepsilon_x = \rho C^2 f'(x - Ct) \qquad \text{Eq. 3}$$

$$\dot{u} = \text{velocity} = \frac{\partial u}{\partial t} = -Cf'(x - Ct) = -C\varepsilon_x \qquad \text{Eq. 4}$$

$$\ddot{u} = \frac{\partial^2 u}{\partial t^2} = C^2 f''(x - Ct) \qquad \text{Eq. 5}$$

$$\frac{\partial \varepsilon_x}{\partial x} = \frac{\partial^2 u}{\partial x^2} = f''(x - Ct) = \frac{1}{C^2}\ddot{u} \qquad \text{Eq. 6}$$

(from (3) and (4), $\sigma_x = -\rho C\dot{u}$)

<u>For a Concave Downward Stress-Strain Curve</u>

Equation A imposes no assumptions of stress-strain properties. If the condition is imposed that S = <u>instantaneous</u> slope of stress-strain curve,

$$S = \frac{\partial \sigma}{\partial \varepsilon_x}$$

From Equation A:

$$\rho\ddot{u} = \frac{\partial \sigma}{\partial x}$$

But: $\dfrac{\partial \sigma}{\partial x} = \dfrac{\partial \sigma}{\partial \varepsilon_x} \cdot \dfrac{\partial \varepsilon_x}{\partial x} = S\dfrac{\partial \varepsilon_x}{\partial x} \quad \therefore \quad \rho\ddot{u} = S\dfrac{\partial \varepsilon_x}{\partial x}$

But: $\varepsilon_x = \frac{\partial u}{\partial x} \therefore \rho\ddot{u} = S\frac{\partial^2 u}{\partial x^2}$

and the same solution as that given above results if we now define $\bar{C} = \sqrt{\frac{S}{\rho}}$ where S is the instantaneous slope of the concave downward stress-strain curve and substitute $\bar{C}$ for C. The results above can be generalized for a plane wave propagating in a continuum by use of the Lame relationships:

$$\sigma_x = \lambda e + 2G\varepsilon_x$$

$$\sigma_y = \lambda e + 2G\varepsilon_y$$

$$\sigma_z = \lambda e + 2G\varepsilon_z$$

with $e = \varepsilon_x + \varepsilon_y + \varepsilon_z$ and $\lambda = \frac{\upsilon E}{(1+\upsilon)(1-2\upsilon)}$

and $G = \frac{E}{2(1+\upsilon)}$

where: λ and G are Lame constants and E and υ are modulus of elasticity and Poisson's Ratio, respectively.

But for plane strain:

$$\varepsilon_y = \varepsilon_z = 0 \therefore e = \varepsilon_x \text{ and } \sigma_x = (\lambda + 2G)\varepsilon_x \qquad \text{Eq. 7}$$

$$\sigma_y = \lambda\varepsilon_x$$

$$\sigma_z = \lambda\varepsilon_x$$

$$\frac{\sigma_y}{\sigma_x} = \frac{\lambda\sigma_z}{\sigma_x} = \frac{\lambda}{\lambda + 2G} = \frac{\upsilon}{1-\upsilon}$$

From similarity of Equations 3 and 7, the solution in Equations 1 through 6 holds if we substitute C_p for C_s

where: $C_p = \sqrt{\frac{\lambda + 2G}{\rho}}$ Eq. 8

It can be shown that the governing equations are of the same form for a shear wave propagating in the x-direction with a (seismic) velocity

$$C_s = \sqrt{\frac{G}{\rho}} \text{ where G = modulus of rigidity.}$$

Thus, Equations 1 through 6 apply for a shear wave with appropriate changes in notation, such as γ_{xy} substituted for ε_x and τ_{xy} for σ_x. A more general derivation of all wave equations may be found in several references such as Ewing, et al (1957) and Kolsky (1963).

The value of the instantaneous slope, S, referred to above has been the subject of research for several years. An often used set of laboratory data for soils giving the effective shear-wave velocity as a function of shear strain is Seed and Idriss (1970). As shown in Grant and Brown (1981), either the laboratory or field data seem more appropriate for approximating the effective shear-wave velocity in the New Alluvium encountered in only limited segments of the routing for the Los Angeles Metro Rail Project, and even then only at relatively shallow depths. The field data are more appropriate for most of the alignment, since for Old Alluvium or rock the laboratory data give significantly lower effective shear-wave velocities than the in situ field data determined by in situ impulse tests.

Figures A.1 through A.4 are taken directly from Grant and Brown (1981) where they appear as Figures 5 through 8. Note that the feature distinguishing "Medium Stiff to Stiff Clay/Silt" from "Hard Clay/Silt" is shear-wave seismic velocity of 1000 fps. As noted by Grant and Brown (1981), the laboratory values for either material type are quite similar; however, the field values are significantly higher than the laboratory values for "Hard Clay/Silt." The notation "(S-I)" on Figures A.3 and A.4 are curves reported by Seed and Idriss (1970). In accord with the definitions given above, the moduli of rigidity in Figures A.3 and A.4 are derived from:

$$\frac{G}{G_{max}} = \frac{C_s^2}{C_{s_{max}}^2}$$

where:

G = Effective modulus of rigidity at the strain of interest.

G_{max} = Modulus of rigidity at small strain consistent with conventional methods of measuring seismic velocities.

C_s = Shear-wave velocity at the value of strain of interest.

$C_{s_{max}}$ = Conventional shear wave seismic velocity (at very low strains of about 10^{-6} (10^{-4} percent)).

Since the strain levels induced by the postulated earthquakes for Metro Rail are in the range of 0.001 (10^{-1} percent) and since most of the alignment is underlain by Old Alluvium or rock, the effective seismic velocities are approximately 80 to 90 percent of the measured seismic velocities and the effective moduli of rigidity are approximately 60 to 80 percent of those values implied by the measured seismic velocities. The higher numbers apply generally to ODE; lower values generally to MDE. These values are taken directly from Figures A.2 and A.4. It is recommended that the values within the ranges given above be used unless other data are available which allows refinement of the values recommended here.

FIGURE A.1

Shear-Wave Velocity Attenuation - Medium Stiff to Stiff Clay/Silt (from Grant and Brown, 1981)

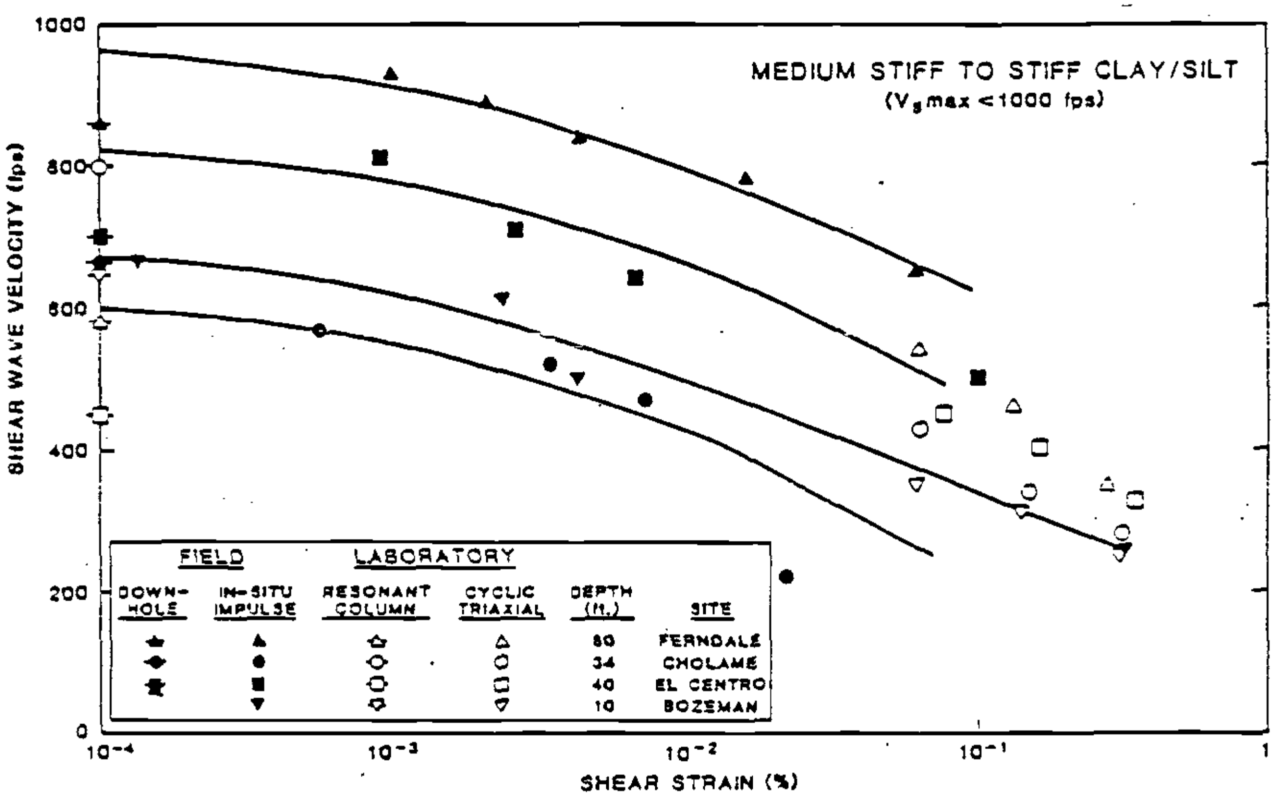

FIGURE A.2

Shear-Wave Velocity Attenuation -
Hard Clay/Silt
(from Grant and Brown, 1981)

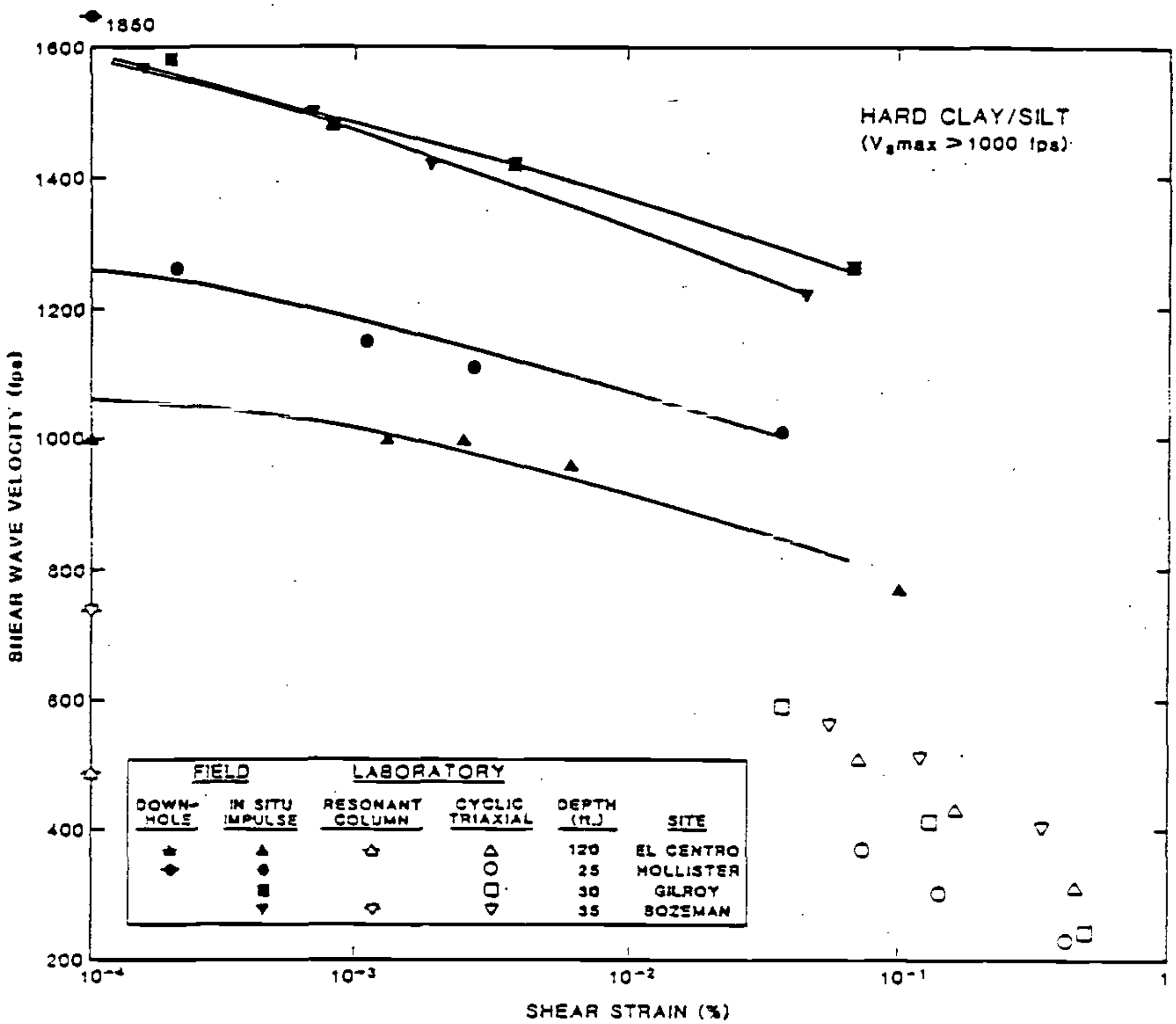

FIGURE A.3

Normalized Shear Moduli -
Medium Stiff to Stiff Clay/Silt
(from Grant and Brown, 1981)

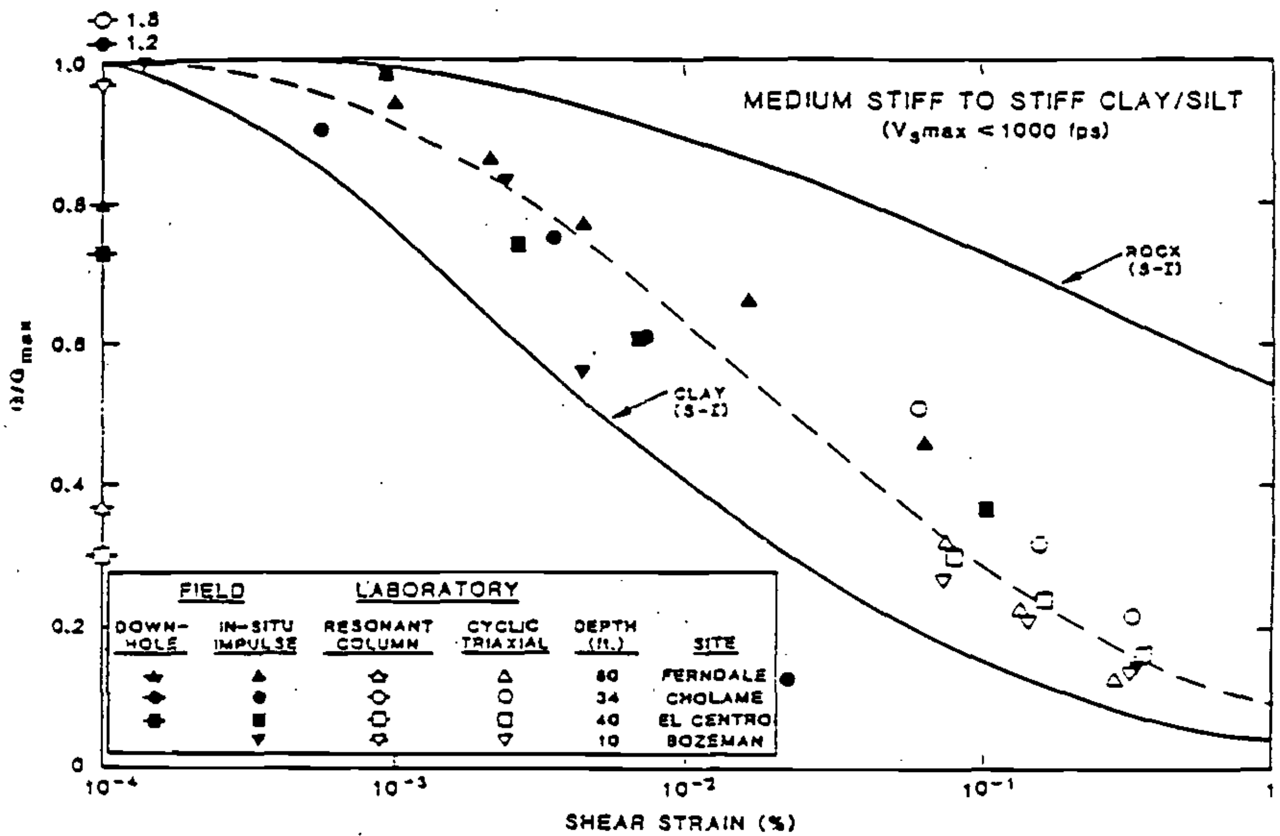

FIGURE A.4

Normalized Shear Moduli -
Hard Clay/Silt
(from Grant and Brown, 1981)

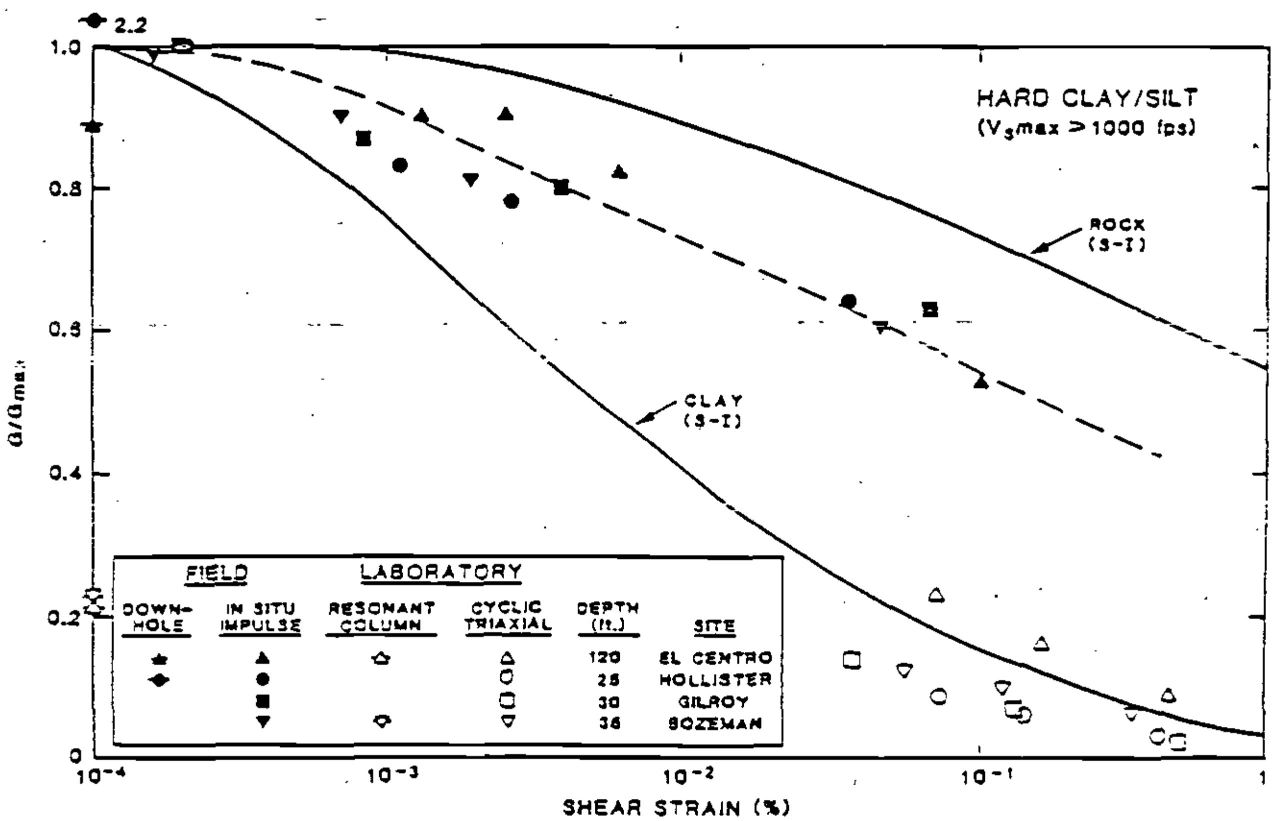

REFERENCES

A.1 Ewing, W.M., Jardetzky, W.S. and Press, F. (1957), Elastic Waves in Layered Media, McGraw Hill, New York.

A.2 Kolsky, H. (1963), Stress Waves in Solids, Dover, New York.

A.3 Seed, H.B. and Idriss, I.M. (1970), Soil Moduli and Damping Factors for Dynamic Response Analysis, EERC 70-10, University of California, Earthquake Engineering Research Center, Berkeley.

A.4 Grant, W.P. and Brown, F.R., Jr. (1981), "Dynamic Behavior of Soil from Field and Laboratory Tests," Proceedings, International Conference on Recent Advances in Geotechnical Earthquake Engineering and Soil Dynamics, University of Missouri, Rolla, pp. 591-596.

ANNEX B

DISTORTION REQUIREMENTS FOR RUNNING LINES

ANNEX B

DISTORTION REQUIREMENTS FOR RUNNING LINES

Shaking Motion

Following the procedures by Peck, et al (1972), the running lines are flexible relative to the media surrounding them; consequently, the shaking motion of these structures will be nearly identical to the shaking motion of the immediately surrounding soil or rock. In the following, therefore, only the motion in the ground (or in the volume of soil or rock displaced by the structure) is specifically considered. In this annex only the longitudinal and racking distortions are considered, the "shaking" distortion is discussed in Annex D.

If we define ε_k as the strain induced locally in the surrounding medium due only to curvature of the earthquake generated stress wave, we find from Newmark (1968) that the curvature is numerically equal to the acceleration divided by the square of seismic velocity. The associated strain is the product of this curvature and the radius of the cylinder of soil or rock displaced by the structure:

$$\varepsilon_k = R \frac{ag}{C^2} \qquad \text{Eq. B.1}$$

where:

ε_k = Strain induced by curvature of stress wave motion.

R	=	Internal radius of structure (or mean distance between geometric center of structure and point of maximum strain for a noncircular structure).
a	=	Component of local acceleration in g's.
g	=	Acceleration of gravity.
c	=	Propagation velocity for appropriate wave.

Also from Newmark (1968), the maximum value of local strain directly induced by a wave in the medium is:

$$\varepsilon = \frac{v}{c} \qquad \text{Eq. B.2}$$

where:

ε	=	directly induced component of strain
v	=	maximum local particle velocity
c	=	propagation velocity for appropriate wave

For a dilitational or P-wave, the strain is in the direction of propagation of the wave. For a shear or S-wave, the shear strains are in any one of a group of planes perpendicular to the plan of the wave front; in turn, these shear strains produce a linear strain at 45° to the direction of propagation and its magnitude is one-half the shear strain. Thus, for a shear wave:

$$\varepsilon = \frac{v}{2c_{se}} \qquad \text{Eq. B.2a}$$

where ε and v are as defined above and c_{se} (see Annex A) is the shear wave propagation velocity consistent with the amplitude of the wave (typically less than the small amplitude shear wave seismic velocity).

The values of a and v are the values of acceleration and particle velocity induced by a single wave, which in the general case impinges on the structure at some angle, θ, as shown in Figure B.1. As noted by Kuesel (1964 and 1969), Newmark (1968), Yeh (1974), ASCE (1983), and Nyman (1983), the maximum strain ε_{max} induced in the structure is likely to occur for angles of incidence other than parallel or perpendicular to the longitudinal axis of the structure.

To account for the effect of angle of incidence, the procedure initially suggested by Kuesel (1964) may be used. From the procedures derived by Yeh (1974), Equations B.1 and B.2 can be combined taking into account the geometry specified in Figure B.1.

As defined in Figure B.1, A is the peak amplitude of a wave regardless of its source, A $\sin\theta$ is the component along the axis of the structure, A $\cos\theta$ is the component perpendicular to the axis and $\frac{L}{\cos\theta}$ is the apparent length of the structure affect; thus $\frac{c}{\cos\theta}$ is the apparent wave velocity along the structure. In what follows, the peak amplitude, A, is treated for each wave (P or S) typically as either the maximum induced acceleration or the maximum induced particle velocity. Theoretically these maxima cannot occur at the same instant in time for any single wave, but the conservatism imposed by assuming that they are coincident in time may not be excessive; furthermore, the temporal spreading of these parameters is probably impossible to predict for any postulated future earthquake. The results of combining Equations B.1 and B.2 in accord with Figure B.1 and Yeh's solutions are shown in Table B.1. The rows of this table specify the single wave type assumed.

In each case it is also assumed for conservatism, even though it may be physically impossible, that the values of v_{max} and a_{max} are induced by this single wave type, and, as already noted, they occur simultaneously.

The second column of Table B.1 specifies the angle (θ) of direction of propagation of the assumed wave relative to the axis of the running line.

The third column gives the general formula used while the fourth column gives as a representative value, the strain for Old Alluvium and the maximum design earthquake (MDE). The effective shear wave seismic velocity c_{se} for Old Alluvium and MDE is assumed in the absence of better data to be 0.8 x 1200 fps = 960 fps (see Annex A). Similarly, for the operating design earthquake (ODE), the value is 0.9 x 1200 = 1080 fps. As noted in the footnote, the better approach for defining the effective seismic velocity for the P-wave in wet soil (c_p) is to define it from the S-wave velocity; the measured P-wave velocity in saturated soils is governed primarily by the wave propagating through the water in the interstices.

The recommeneded value, which is the same as the maximum for the S-wave at 45° angle of incidence, is shown in the last line of Table B.1. The result, even for the nearly worst case considered in Table B.1 (v_{max} = 3.2 fps and a_{max} = 0.6g for the MDE), produces values of strain for the Old Alluvium (c_s = 960 fps) which do not exceed the compressive strain capability of a reinforced concrete lining. The joints in the segmented lining will mitigate undue damage in the lining. However, if the effective seismic velocity is below 800 fps it may be necessary to consider placing soft spacers within the circumferential joints to accommodate the compressive strain.

For the operating design earthquake (ODE), the maximum particle velocity in alluvium is 1.4 fps and the maximum acceleration is 0.3 g. Use of the recommended value in Table B.1 gives a value of maximum strain in Old Alluvium (c_{se} = 1080 fps) of 0.00071 in./in. Such a value is well within the allowable range for compression in concrete. For such a strain in tension, of course, a solid lining would be cracked, but the joints in the segmented linings will mitigate this strain within the circumferential joints and the reinforcement will distribute any cracks which might develop between joints, so that servicability is maintained.

As noted at the outset in this annex, the structures are assumed to move with the surrounding soil during the shaking motion. As a result, no differential motion occurs and the shear which develops on the surfaces of the structure due to shaking are only those consistent with forcing the structural motion to conform to that in the soil. These effects of these shears are implicitly included in the strains considered above. Near bends in the structure, additional constraints generally will develop; however, the minimum radius of any curve must be large to accommodate the rolling stock. The effect of these constraints will be much less than the induced conditions produced by lateral relative displacements of the type considered by Kennedy, et al (1977).

The effects must also be considered of relative displacement and strain induced by a wave over a finite length of the structure, such as b in Figure B.1. As stated by Newmark (1968), the following relations apply if:

a_m	=	Maximum acceleration induced by a stress wave.
b	=	Distance between points 1 and 2.
c	=	<u>Apparent</u> seismic velocity along axis of tunnel.

u_{max2} = maximum displacement at point 2 along axis of structure.

u_{max1} = Maximum displacement at point 1 along axis of structure.

δb_{21} = Maximum change in distance between points 1 and 2 along axis of structure.

$u_{max1,2}$ = Maximum displacement of point 1 relative to point 2.

$u_{min2,1}$ = Minimum displacement of point 2 relative to point 1.

ε_{max} = Maximum strain at any point between points 1 and 2.

$v_{max2,1}$ = Maximum induced particle velocity of point 2 relative to point 1.

y_m = Maximum amplitude of displacement perpendicular to axis of tunnel.

$\ddot{y}_m$ = Maximum acceleration perpendicular to axis of tunnel.

Quoting directly from Newmark (1968) and changing only Equations 21 to 26 in the original to Equations B.3 to B.8 here, produces the following:

"Other relationships are of importance in the case where the motions are caused by more general disturbances than a wave of nearly constant shape transmitted in one direction. For example, it is apparent that the maximum change in the distance between points

1 and 2, δb_{21}, is related to the maximum displacements at points 2 and 1 in the following way:

$$\delta b_{21} \geq u_{max2} - u_{max1} \qquad \text{Eq. B.3}$$

In many instances, this relation may be trivial because the maximum displacements may be nearly equal, but since they do not occur at the same time, it is obvious that the maximum transient change in length must be greater than the difference in the maximum displacements. It is, however, true that the maximum change in length is less than the difference between the maximum displacement at either point 1 or point 2, less the minimum displacement, or the displacement in the opposite direction, at the other point. The minimum displacement would of course be zero, if the displacements do not reverse in direction. This relation is expressed as follows:

$$\delta b_{21} \leq u_{max1,2} - u_{min2,1} \qquad \text{Eq. B.4}$$

"Similarly, the maximum change in length between points 2 and 1 must be less than the maximum strain anywhere along the line connecting the two points, multiplied by the length, as given in the following relation:

$$\delta b_{21} \leq \varepsilon_{max} b \qquad \text{Eq. B.5a}$$

"For the special case where the maximum strain is related to the maximum velocity by Equation 18,* corresponding to a wave transmission situation, then one can derive from the preceding equation the following results:

$$\delta b_{21} \leq \frac{b}{c} v_{max2,1} \qquad \text{Eq. B.5b}$$

---

*

$$\varepsilon_{max} = \frac{v_{max}}{c}$$

"For the special case where the deflection transverse to the line is give by an arc of a sine curve, as in the relation

$$y = y_m \sin \pi x/b \qquad \text{Eq. B.6}$$

then the curvature is obtained by the second derivative of this relation as follows:

$$\text{curvature}\Big|_{max} = \frac{\partial^2 v}{\partial x^2}\Big|_{max} = -\frac{\pi^2}{b^2} y_m = \frac{\ddot{y}_m}{c^2} \qquad \text{Eq. B.7}$$

From this relation and Equation 19** one derives the following result:

$$y_m \cong -\frac{b^2}{\pi^2 c^2} a_m \qquad \text{Eq. B.8}$$

This is applicable, however, only for the special case considered."

From the equations above, it is obvious that if the displacements defined by u with various subscripts are axial in nature, the induced strain in the segment of lining are axial in nature and these strains are

$$\varepsilon = \pm \frac{\delta b_{21}}{b} \qquad \text{Eq. B.9}$$

with δb_{21} defined by Equation B.4 taking appropriate account of signs of the displacements.

**

$$\frac{\partial^2 v}{\partial x^2} = c^2 \frac{\partial^2 v}{\partial t^2} = c^2 a_m .$$ The approximate sign is needed since Equation B.6 does <u>not</u> assume a stress wave with peak acceleration of a_m.

If these axial displacements are accompanied by lateral displacements, y_m, Equations B.1, B.7, and B.9 give a maximum strain in a finite length b of

$$\varepsilon_{max} = \pm \frac{\delta b_{21}}{b} \pm R \frac{\ddot{y}_m g}{c^2}, \text{ or} \qquad \text{Eq. B.10a}$$

$$\varepsilon_{max} = \pm \frac{\delta b_{21}}{b} \mp R \frac{\pi^2}{b^2} y_m \qquad \text{Eq. B.10b}$$

If the displacements defined by u with various subscripts are lateral in nature, the maximum strain in a finite length b according to Equations B.1 and B.7 is

$$\varepsilon_{max} = R \frac{\pi^2}{b^2} y_m = R \frac{\pi^2}{b^2} \delta b_{21} \qquad \text{Eq. B.11}$$

As for the special case where $y_m = \delta b_{21}$ stated in Equation B.5a, all strains induced in a finite length are <u>less</u> than those recommended in Table B.1; it is proper to use the smaller value computed as defined above in Equations B.9 to B.11 if the length b is less than approximately 2,000 ft. The actual length depends on the effective shear-wave seismic velocity <u>and</u> the effective shear strength at the structure-medium interface. For distances less than this limit the structure must be capable of resisting the differential shears (frictional drag) which may develop along its length (see Example 1 in Appendix 1), or the reduced strain noted immediately above whichever is greater. For lengths greater than approximately 2,000 ft., Table B.1 prevails. (Soil drag is considered to produce an upper bound on axial strain as limited by interface friction or soil strength).

Racking Strain

Racking stain is defined for the purpose of these criteria as that distortion induced in planes of the running line perpendicular to the axis and caused by a shear wave. Shear acting on an element of soil or rock, treated as an elastic medium, is the equivalent of a compression in one-direction and an equal tension in a direction perpendicular to that of the compression, see Figure B.2. For this case, the maximum displacement of the circular hole, for conditions of plane strain along the axis of the tunnel, occurs as indicated in the figure B.2 and it is equal to:

$$u = \pm 4 \frac{SR}{E_m} (1 - \upsilon_m^2) \qquad \text{Eq. B.12}$$

where the notation is defined in Figure B.2. If ΔD is defined as the maximum change in diameter, D(=2a), then this last equation becomes:

$$\frac{\Delta D}{D} = \pm 4 \frac{S}{E_m} (1 - \upsilon_m^2) \qquad \text{Eq. B.13}$$

If the hole is lined by a structure which distorts an amount equal to $\Delta D/D$, the strain in the structure, except for the slight difference in outside to mean diameter, caused by the racking is:

$$\varepsilon_{\theta b} = \pm \frac{3}{2} \left(\frac{t}{R}\right) \left(\frac{\Delta D}{D}\right) \quad \text{or} \quad \varepsilon_{\theta b} = \pm 6 \left(\frac{t}{R}\right) \frac{S}{E_m} (1 - \upsilon_m^2) \qquad \text{Eq. B.14}$$

But: $$S = \frac{E_m v_s}{2(1+\upsilon_m) c_{se}} \text{ from Figure B.2}$$

Thus: $$\varepsilon_{\theta b} = \pm 3 \left(\frac{t}{R}\right) \left(\frac{v_s}{c_{se}}\right) \frac{(1-\upsilon_m^2)}{(1+\upsilon_m)}$$

Or: $$\varepsilon_{\theta b} = \pm 3 \left(\frac{t}{R}\right) \left(\frac{v_s}{c_{se}}\right) (1-\upsilon_m) \qquad \text{Eq. B.15}$$

If: $\upsilon_m = \frac{1}{3}$:

$$\varepsilon_{\theta b} = \pm 2 \left(\frac{t}{R}\right) \left(\frac{v_s}{c_{se}}\right)$$

This is the bending component of strain induced in the lining. The distortion will also produce thrust, or a uniform component of strain at least in compression. (Since only limited tensile strain can develop across the soil or rock surface to the outside of the structure, little or no added tension will develop). The added compressive strain induced in the structure, if the soil and structure column and soil columns above and below it (the soil columns in Figure B.2) have the same stiffness, is

$$\varepsilon_{\theta c} = \frac{SR}{2tE_\ell} \qquad \text{Eq. B.16}$$

where E_ℓ is the modulus of elasticity of the lining material. By superposition, the total maximum strain ε_{tot}, is

$$\varepsilon_{tot} = 2 \left(\frac{t}{R}\right) \left(\frac{v_s}{c_{se}}\right) + \left(\frac{E_m v_s}{4(1+\upsilon_m) c_{se}}\right) \left(\frac{R}{t}\right) \left(\frac{1}{E_\ell}\right)$$

Or: $$\varepsilon_{tot} = \left(\frac{v_s}{c_{se}}\right) \left[2 \left(\frac{t}{R}\right) + \frac{3}{16} \left(\frac{R}{t}\right) \left(\frac{E_m}{E_\ell}\right)\right] \qquad \text{Eq. B.17}$$

If: $\upsilon_m = 1/3$.

The maximum tensile strain is:

$$\bar{\varepsilon}_{tot} = -2 \left(\frac{t}{R}\right) \left(\frac{v_s}{c_{se}}\right) \qquad \text{Eq. B.18}$$

For: $\upsilon_m = 1/3$.

A single calculation was completed using an elastic, finite element code. The distortion shown in the upper figure in Figure B.2 was imposed with v_s = 3.4 fps and c_{se} = 1,000 fps. The structure used was an 8 in. thick concrete lining, 114 in. in radius. The maximum compressive strain calculated in the lining was 0.0009. Use of the same parameters in Equation B.17 and with $E_m = 50{,}000$ psi and $E_\ell = 4.6 \times 10^6$ psi as were also used in the finite element calculation, yields:

$$\varepsilon_{tot} = 0.0006$$

Certainly a single calculation cannot be used to qualify an approximate procedure; a series of calculations should be run, especially to measure the effect of relative stiffness of lining to medium. However, until such a set of calculations is completed, the approximation used in Equations B.17 and B.18 can be used directly, or if more conservative results are desired, the results of the equation can be multiplied by 1.5 (the ratio of the value from the single calculation to that given by the equation). Whether or not this amplification is used, the compressive strain is well below the allowable of 0.004. Even for very low values of effective shear wave velocity, c_{se}, it is unlikely that the compressive strain will cause serious problems for <u>flexible</u> linings. Of course, the racking strain must be added to strains caused by other loads, but even the combination does not appear to be severe (see example in Appendix) unless c_{se} is low. As already noted, spacers in the longitudinal and circumferential joints may be required when c_{se} is low.

The tensile strain due to racking will be generally larger than that which causes tension cracking. However, the strain will be generally significantly less than that normally allowed on the tension side of reinforced concrete beams (in the range of 0.001 even at design loads). The lining segments being doubly reinforced, the reinforcement is generally distributed across each face and in each direction. The reinforcement will adequately distribute any cracks which might develop. Furthermore, even though cracks caused by racking may generally extend through the thickness, the two layers of steel will maintain the flexural strength at essentially the original value; thus, the section will adequately resist any return loadings (dead, live and earthquake). In similar fashion, the bolts fastening the longitudinal joints may actually yield when subjected to the imposed racking but they will maintain their shear and flexural strength; thus no adverse situation should be expected from the tension.

Lateral Distortion

Some tendency toward abrupt lateral distortion may develop where the running line crosses clearly defined faults. Such a condition may develop at the Santa Monica Fault where the MDE fault displacement has been estimated as 6.6 ft. (Appendix A, Converse, 1983).

For force transfer between steel lining segments shown in Figure B.3 in the logitudinal direction, it is impractical to provide a sufficient number of bolts to develop the yield strength of the skin plate. For example, with 48 bolts (A325) in the circumferential joints and a minimum thickness of 3/8 in. in the skin plate the stress in the plate is approximately:

Bolt Diameter (in.)	Allow. Direct Tension on Bolt (kips)	Approx. Stress in 3/8" Plate for 48 A 325 Bolts (ksi)
3/4	17.7	1.3
1	31.4	2.3

With the gage (g) of 3.5* in. and the edge distance (e) 2.5* in. in Figure B.4 and the flange bent in double curvature, causing

* Assumed values.

compression over the edge distance e, a 1/2 in. flange thickness (t_w) will develop the forces in the 1 in. bolt indicated above at initial yielding of the flange. Although a smaller flange thickness could be used with 3/4 in. bolts, it seems desirable to transmit the higher force indicated since, as shown below, a large length of lining must be mobilized in accommodating the distortion.

For the dimensions shown in Figure B.4, the deflection (δ_ℓ), conservatively ignoring stretching of the bolt, is:

$$\delta_\ell = \frac{Tx^3}{3EI} + \frac{Tx^2}{2EI}(g - x) + \frac{T}{3EI}(g - x)^3 \qquad \text{Eq. B.19}$$

If x = kg:

$$\delta_\ell = \frac{Tg^3}{EI}\left[\frac{1}{3} - k - \frac{3k^2}{2} - \frac{k^3}{2}\right] \qquad \text{Eq. B.20}$$

The term in brackets is:

k	Bracketed Term
1/4	0.169
1/3	0.148
3/8	0.143
1/2	0.146
5/8	0.172
2/3	0.185
3/4	0.216

Since the smallest δ_ℓ is the conservative case, use

$$\delta_\ell = \frac{Tg^3}{7EI} \qquad \text{Eq. B.21}$$

(Although this deflection is less than half that in single curvature,

$$\frac{Tg^3}{3EI},$$

developing single curvature requires leaving the bolts loose; such a practice is hard to control to attain and maintain a specified looseness, but more importantly, it exacerbates any waterproofing problems.)

For the values of δ_ℓ in Equation B.21 and the geometry shown in Figures B.3 and B.4:

$$\frac{\delta_\ell}{\ell} = 2\,\frac{R}{L}\cdot\frac{\delta}{L} \text{ but} \leq 0.013 \text{ in./in.} \qquad \text{Eq. B.22}$$

for R = 114 in. and ρ = 750 ft. (to accommodate rolling stock).

With t_w = 1/2 in. and g = 3.5 in., δ_1 0.024 in. The tension in the skin plate to develop a 1 in., A325 bolt with the flange in double curvature is 1.2 k/in. (The bolt force is 2.1 k/in. while the total compressive force on the edge distance e is 0.9 k/in. assuming a linearly distributed bearing force ranging from zero at the center of the bolt to a maximum at the tip of the flange). Obviously δ_ℓ/ℓ for any practical value of ℓ is less than the limit (0.013 in./in.) required to maintain the required minimum radius of curve.

<u>If</u> freedom to slip <u>along the axis of the tunnel</u> can somehow be provided to allow mobilizing the number of steel segments needed to develop the curvature shown in Figure B.3, the length of tunnel required is:

ℓ (ft.)	δ_ℓ/ℓ (in./in.)	L (ft.) for R = 114 in. & δ = 6.6 ft.
2	0.0010	350
2 1/2	0.00081	390
3	0.00068	430
3 1/2	0.00058	460
4	0.0005	500

The forces developed by such slip must remain significantly below the 2.1 k/in. (of circumference) in the bolt since the axial tension is governed by the net force, allowing for compression of the toe. As indicated above this net force is 1.2 k/in. but if the bolts should loosen for any reason the force could reach the full capacity of the bolt of 2.1 k/in. Thus, shear failure in the interface must occur below 1.2 k/in. even though the force capability of the lining may be as high as 2.1 k/in.

The analysis given above is appropriate for the bolted standard steel lining. The approach given by Kennedy et at. (1977) and refined by Nyman (1983) is not considered appropriate for the current case since this last method was developed for relatively small diameter uniform thickness pipe with fully (full penetration) welded joints.

TABLE B-1

SELECTED PRINCIPAL EFFECTS OF EARTHQUAKE-GENERATED WAVES ON FLEXIBLE UNDERGROUND STRUCTURES

Wave Type	Propagation Direction Relative to Tunnel Axis (θ)	Effect of Combined Waves: Axial Strains Induced in Medium — General Formula[a]	Effect of Combined Waves: Axial Strains Induced in Medium — Representative Numerical Value for Old Alluvium (in/in)	Remarks (See Annex B)
Dilational (P-) Wave	0°	$\epsilon_p \cong \pm \frac{v_{max}}{c_{pe}}$	± 0.0017 [b,c]	No curvature is induced for (0° incidence)
Shear (S-) Wave	45°	$\epsilon_s \cong \pm \frac{v_{max}}{2c_{se}} \pm 0.7\ R\ \frac{a_{max}g}{c_{se}^2}$	± 0.0018 [b]	R = 10' (assumed)[d]
Recommended Value	Shear Wave at 45°	$\overline{\epsilon}_l = \pm \frac{v_{max}}{2c_{se}} \pm 0.7\ R\ \frac{a_{max}g}{c_{se}^2}$	± 0.0018 [b]	R = 10' (assumed)[d]

[a] Assumes a_{max} and v_{max} are produced only by the wave considered and they occur simultaneously which is physically impossible but an acceptable conservative approximation.

[b] For Old Alluvium and MDE; c_s = 1200 fps and C_{se} = 0.8 x 1200 = 960 fps (See Annex A)

[c] $c_p = 2c_s$ for $\nu = 1/3$; this is a better approach for deriving strain in the soil than a measured valued in saturated or nearly saturated soil for which c_p approaches that for the water in the interstices. For dry soils $c_p \cong 2c_s$

[d] Coefficient includes required trigonometric terms for angle of incidence.

FIGURE B.1

Geometrical Parameters for Wave Intersecting
A Structure at an Angle

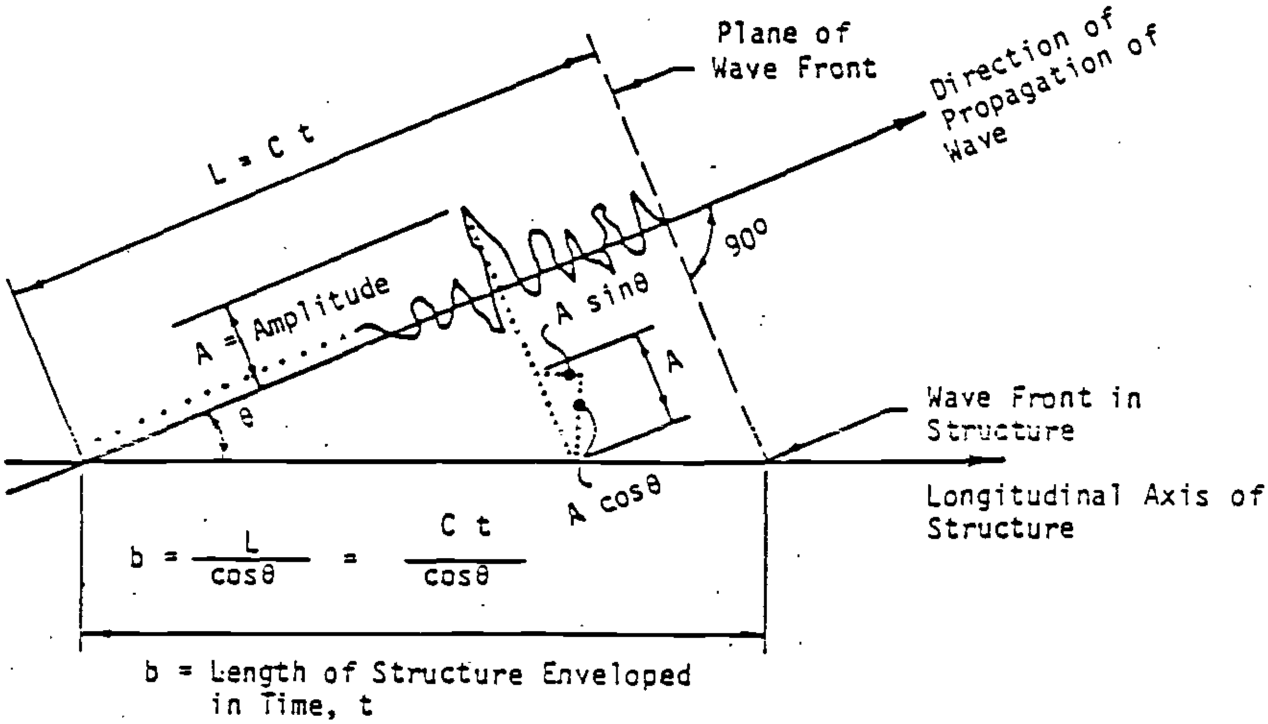

FIGURE B.2

Shear Stress and Equivalent Direct Stresses On an Elastic Element with a Hole (Exaggerated Distortion Shown Dashed)

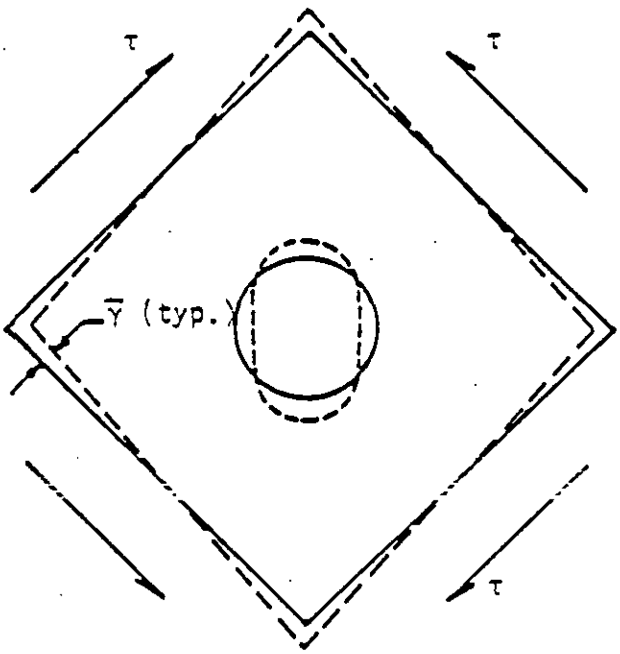

$$\tau = G\bar{\gamma}$$

$$\bar{\gamma} = \frac{v_s}{c_{se}}$$

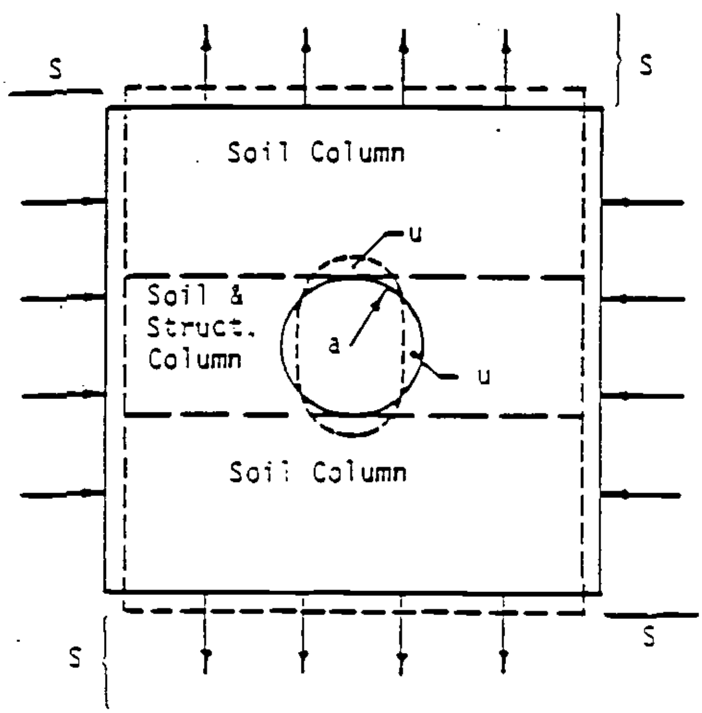

$$S = \tau$$

$$S = \frac{G_m v_s}{c_{se}}$$

$$S = \frac{E_m v_s}{2(1+\nu_m) c_{se}}$$

FIGURE B.3

Distortion of Running Line
From Fault Offset

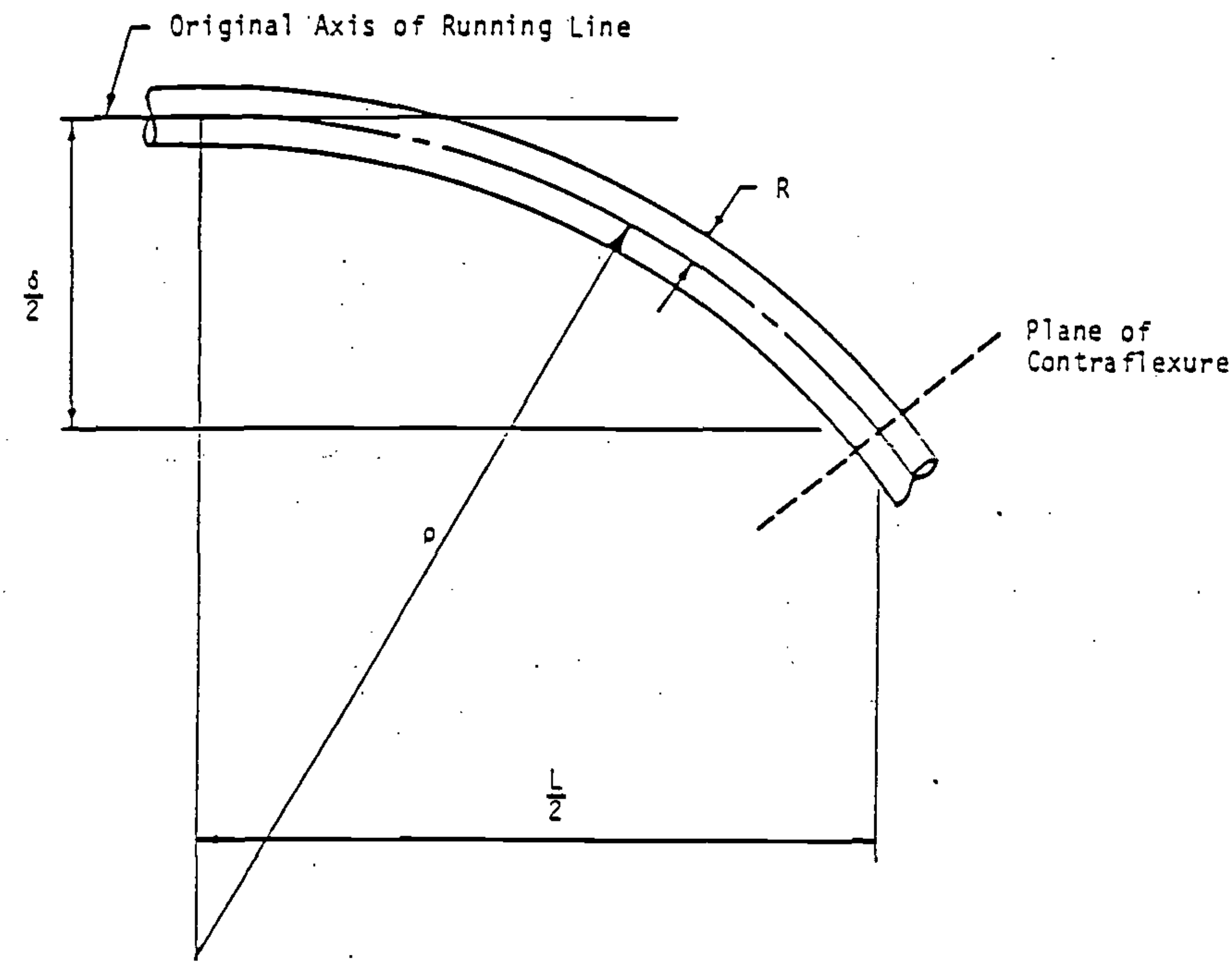

FIGURE B.4

Critical Dimensions of Standard
Steel Lining Segments

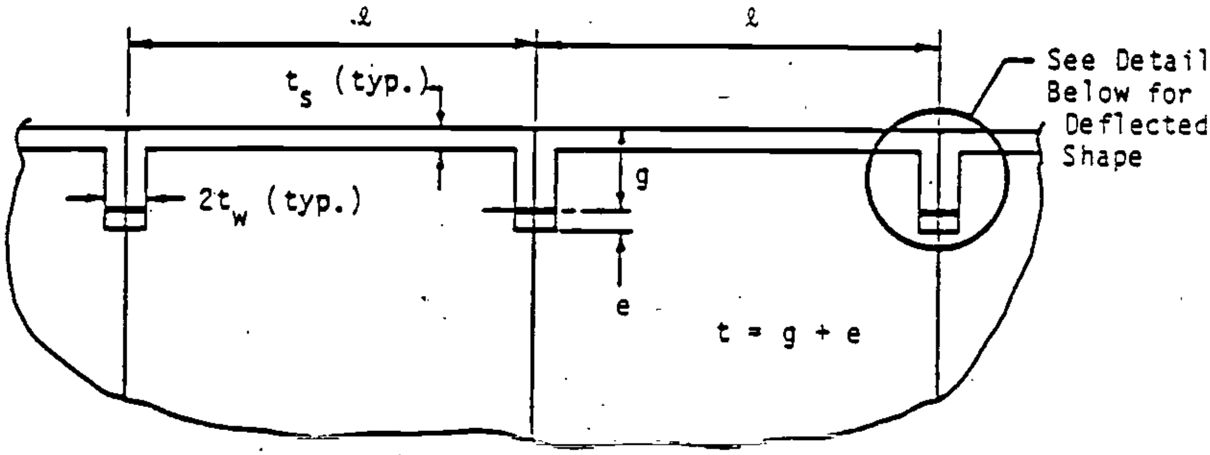

Longitudinal Wall Section

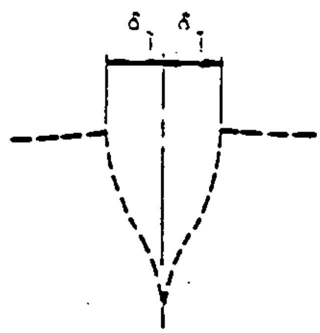

REFERENCES

B.1 Kuesel, T.R. (1964), "Earthquake Design Criteria for Subways," Article 1906 of Design Criteria for Bay Area Rapid Transit (BART) System, San Francisco.

B.2 Newmark, N.M. (1968), "Problems in Wave Propagation in Soil and Rock," Proceedings, International Symposium: Wave Propagation and Dynamic Properties of Earth Materials, Albuquerque.

B.3 Kuesel, T.R. (1969), "Earthquake Design Criteria for Subways," Journal of Structural Division, Proceedings, ASCE, 95: ST6, New York (with Discussions by A.H. Hadjian (96: ST1) and A.A. Eremin (96: ST3).

B.4 Peck, R.B., Hendron, Jr., A.J. and Mohraz, B. (1972), "State of the Art of Soft-Ground Tunneling," First North American Rapid Excavation and Tunneling Conference, ASCE-AIME, Chicago.

B.5 Yeh, Gordon C.K. (1974), "Seismic Analysis of Slender Buried Beams," Bulletin, Seismological Society of America, 64: 5, Oakland.

B.6 Kennedy, R.P. Chow, A.W. and Williamson, R.A., (1977), "Fault Effects on Buried Oil Pipeline," Transportation Engineering Journal, ASCE, New York.

B.7 ASCE Committee on Seismic Analysis, Structural Division Committee on Nuclear Structures and Materials (1983), "Seismic Response of Pipes and Structural Components," New York.

B.8 Nyman, D.J. (1983), Private Communication.

ANNEX C

EFFECTS OF TEMPORAL CHARACTERISTICS OF EARTHQUAKE-GENERATED WAVES ON UNDERGROUND STRUCTURES

ANNEX C

EFFECTS OF TEMPORAL CHARACTERISTICS OF EARTHQUAKE-GENRATED WAVES ON UNDERGROUND STRUCTURES

Because earthquake shaking is a dynamic effect, it is often tempting to consider the detailed time-varying characteristics of the waves. Such consideration is proper for above-ground structures, especially when non-linear response is allowed. Dynamic response is also appro-priate for elements mounted on the interior of structures, regardless of their location relative to the ground surface. For the basic underground structural response, however, it appears that the time variations are not important. This annex briefly summarizes the fundamental analyses which support the conclusion that time variations of the shaking motion are not important in the basic design of underground structures.

Numerous writers, each in many papers prepared over several years, such as, in alphabetical order, Barton, Blume, Fung, Housner, Mohraz, Newmark, Rosenblueth, Shah, Tung, and Veletsos, have considered the effects of temporal characteristics of earthquake motions, especially on shapes of response spectra. However, the random nature of these motions and complex paths over which they propagate for shock isolation have made generalizations difficult; they have been especially difficult when non-linear response is included with or without relatively higher percentages of critical damping. Most of these studies have considered ranges of periods of structures from short to long. More importantly most have implicitly or explicitly addressed the response of above ground structures or shock isolation of equipment in underground structures.

For the basic underground structures (running line or stations) encountered in subway systems, fundamental periods of response are short compared to those for typical above ground structures. For example, the fundamental period for the running line is of the order of 5 msec. (see Merritt and Newmark (1964); period is approximately radius divided by 1800 fps). The fundamental period for the station is in the range 0.1 to 0.4 sec. (see Merritt and Newmark (1964);

period in seconds is at least $\frac{L^2}{(3,000 \text{ fps})\ d\sqrt{\phi}}$ with L and d in ft. and ϕ, the reinforcing ratio, in percent).

Figures C.1 to C.3 show earthquake records with amplitudes in the range of interest or even exceeding it. As already noted, earthquakes produce motions which tend to be random in nature. Nevertheless, certain conditions of interest can be deduced from counting zero crossings of the typical accelerogram. These crossings may reflect, in selected instances, points of inflexion in the velocity record; even then they reflect higher frequencies of response. The number of zero crossings in the accelerogram reflect very nearly twice the frequency of the velocity pulse. As seen in the figures, the number of crossings is in the approximate range of 10 to 20 per second. Thus, the inherent frequencies[1] of velocity, which is proportional to strain and stress, are in the range of 5 to 10 hertz or the periods are 0.1 to 0.2 sec. The rise time of these disturbances is in the range of one-fourth to one-half the period; thus, the rise times of the velocities or

[1]Although a standard seismograph is limited in the frequencies it can respond to, it will be shown later that even the highest frequencies cause only minor overshoot of the dynamic response over the static response.

strains are in the range of 25 to 100 msec. (It should be noted also that the durations of these pulses are comparable to the rise times.) For the running line, the ratio of rise time to period is in the range of 5 to 20 times the fundamental natural period; for the stations, one-fourth to one times the fundamental natural period. (The durations of the individual spikes of velocity or strain are approximately double the values just given.)

Figures C.4 to C.6 are copies directly from Merritt and Newmark (1964). Although they were generated for blast loads, they apply to individual spikes of stress or strain for earthquakes when the temporal characteristics are defined in terms of period as noted above.[2]

The effect of rise-time of loading, as reflected by the velocity, is perhaps most clearly indicated by solutions for response of a simple oscillator.[3] Figure C.4 illustrates the dynamic amplification of the displacement of a simple oscillator when subjected to step pulses of infinite duration (the worst case for a single pulse) with rise time measured in relation to the natural period of vibration. For a zero rise time, the ratio of the maximum deflection (Y_m) to the static deflection ($Y_s = P_m/K$ where P_m is the amplitude of the load and K is the stiffness of the oscill-

---

[2]Velocity pulses generated by earthquakes produce a continuous series of waves while in blast waves there is only a single pulse of primary concern; however, earthquake motions tend to be random, thus, resonance or near resonance with associated enhancement of response by the string of waves is minimal.

[3]Note that for elastic structures, modal response techniques allow consideration of response of several simple oscillators and adding these separate modal responses to define the total response of multi-degree of freedom systems.

ator) is 2. The amplification factor is identically unity for all rise times which are integer multiples of the period. For all rise times greater than one times the period, the peak amplification factor is progressively smaller with the largest value of approximately 1.2 occurring for $t_r/T = 1.5$; thus the maximum overshoot of the dynamic over static deflection is approximately 20 percent for an elastic oscillator subjected to a pulse of infinite duration. Since for the running lines, the ration of t_r to T is at least 5, Figure C.4 implies essentially no dynamic amplification. For the stations, the amplification could be as high as 1.4 ($t_r/T = 3/4$) according to Figure C.4, but the duration is much less than that assumed in this figure and some non-linear response is acceptable for at least the Maximum Design Earthquake (MDE).

For inelastic oscillators (Y_m greater than Y_y, the deflection at yielding), and/or for finite durations of loading, the results in Figures C.5 and C.6 apply. In these figures, the ordinate is now the ductility factor (ratio of maximum deflection to <u>yield</u> deflection) and <u>not</u> the amplification factor. When response is measured in terms of ductility factor, this parameter can be quite large for a step pulse of infinite duration as illustrated by the top curve in Figure C.5. Note, however, that this figure is constructed for a ratio of peak applied load (P_m) to the yield resistance (R_y) of 1.0. Figure C.6 addresses the question parametrically in values of P_m/R_y while holding the ratio of pulse duration (t_d) to period (T) constant at 2 (the value for the lowest curve in Figure C.5). Since the duration of earthquake loads relative to the period of the running line is at least 2, the maximum ductility factor required would be at the most 3 (Figure C.5 or C.6) with a zero rise time, but the rise time is at least 5 times the period; thus, the required ductility factor is one and the running line remains elastic. Also from these figures, the maximum ductility factor required for t_r/T equal to or greater than about 0.9 is 1.4 for any static design for $t_d/T \leq 2$ (i.e., a design for which the peak load is set equal to the yield resistance). Since the maximum ratio of t_d to T is ≤ 2 for the stations, the maximum ductility factor required is 1.4 to allow a static design; since this is the worst case for a single pulse, little non-linear response can be expected even for the MDE.

From the above, it is clear that the maximum overshoot is 1.2 (the dynamic response is 20 percent higher than the static response) for all elastic cases where the period of the mode of response being considered is less than the rise time of the spike of motion of primary concern in the earthquake shaking. Similarly for all inelastic cases, allowing a ductility factor of 1.4 (a maximum deflection of 1.4 times the yield deflection) will allow static designs for all modes with natural periods less than the rise time of the spike of motion of concern. More importantly, it is necessary to note that the "spike of motion of concern" is a postulated quantity and the associated time variation is also postulated; thus, the amount of overshoot or required ductility are probably better known quantities than the principal parameter on which their definition must be based!

As noted by the footnote above, it is probable that standard seismographs may filter out frequencies of motion above 20 to 30 hertz as a result of their mechanical characteristics. As a result, it is desirable to investigate how buried structures inherently filter out higher frequencies of response. Behavior of lined and unlined tunnels in elastic media was considered by Paul (1963), Yoshihara (1963), Ali-Akbarian (1967); inelastic response was considered by Belytschko (1978). The first three writers specifically addressed the stresses (and by implication the strains) induced around lined or unlined tunnels subjected to either side-on loads (traveling perpendicular to the longitudinal axis) or end-on loads (traveling parallel to the longitudinal axis) (see Figure C.7). The fourth writer made a complete review of the blast-loading problem, and it was concluded that blast loads (primarily loads with a single[4] important spike) may be treated as quasi-static; i.e., although there is a minor potential for dynamic amplification of response, its magnitude, if present, has a smaller effect than the uncertainty in temporal and amplitude characteristics of the associated loading.

FIGURE C.7

Geometry and Parameters Used by Paul (1963)

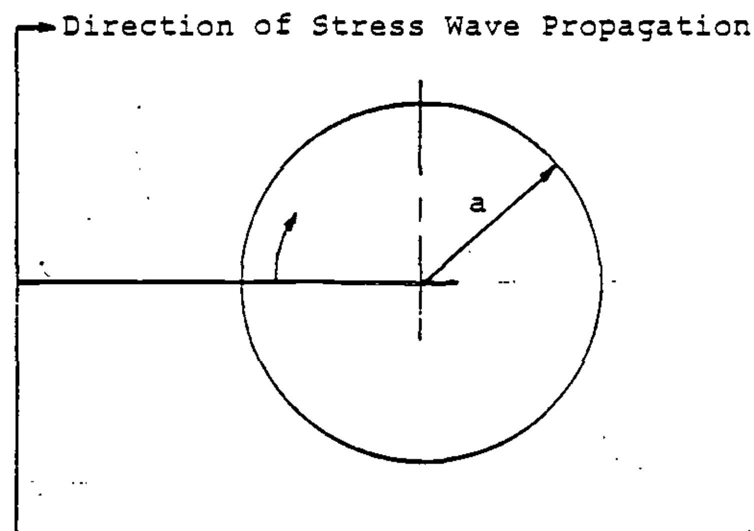

Circular Tunnel

(Note: a in above Figure is the radius, denoted by R elsewhere in these criteria.)

[4]As already noted, the random nature of the string of pulses in an earthquake minimizes the tendency toward resonance and associated major enhancement of response.

σ = peak amplitude of stress wave; in all cases tension is positive

n = mode number

t = time measures from time of first arrival at tunnel

c_1 = velocity of wave propagation of P-Wave

c_2 = velocity of wave propagation for S-Wave

$\sigma_{\theta\theta}$ = circumferentail stress at tunnel boundary

$\bar{\nu} = \dfrac{\nu}{1 - \nu}$ = "plane strain" lateral stress coefficient in elastic medium

"Static Value" = Value defined for static conditions

To place this last assertion into context it is only necessary to refer to Figures C.8, C.9, C.10, C.11 and C.12 taken directly from Paul (1963) (originally Figures 6.1, 6.2, 6.12, 6.10 and 6.11 of the reference). The first figure shows the maximum stress produced for side-on conditions, with $\theta = 0°$ the point of initial incidence of the wave. The wave is a step-pulse of infinite duration. The solution assumes only elastic materials. The maximum overshoot over the static value occurs at 0°, and it is 29 percent. The next larger overshoot occurs at $\theta = 90°$ and it is 11 percent. Similar results are shown for a different Poisson's ratio in Figure C.9, and for a pure shear wave in Figure C.10. The effect of an exponential decay (k is the coefficient of time as illustrated in the inset to Figure C.11) of the incident pulse is compared with the result for a step pulse in Figures C.11 and C.12. Although the increase in tensile stress (values above the origin) in Figure C.11 may be startling for the decaying pulse (or Figure C.10 for the shear wave), it must be remembered that these are theoretical stresses around an unlined tunnel in an elastic medium, and the proposed tunnels will be lined. At the same time, the lining will probably not be strongly bonded to the surrounding medium, and most important of all, the lining will be articulated. All of these last conditions ameliorate the effect of the tension in the surrounding medium, and for the joints in the segmented linings, the effects of any tension may be accommodated. Thus, the result in Figure C.12 is the important one. It is seen there that a decay coefficient (as defined by Paul, 1983) of less than 100 will eliminate the 10 percent overshoot of the peak stress compared to the static value for the step-pulse of infinite duration in Figure C.9 which is the solid curve in Figure C.12.

The above discussion indicates that a static treatment of the strain pulse, which is proportional to the stress or velocity pulse, will provide a solution which is entirely consistent with the degree of knowledge of the temporal characteristics of the postulated earthquake.

FIGURE C.1

Ground Acceleration, Velocity, and Displacement,
El Centro, CA, Earthquake of May 18, 1940
N-S Component
(from Blume et al, 1961)

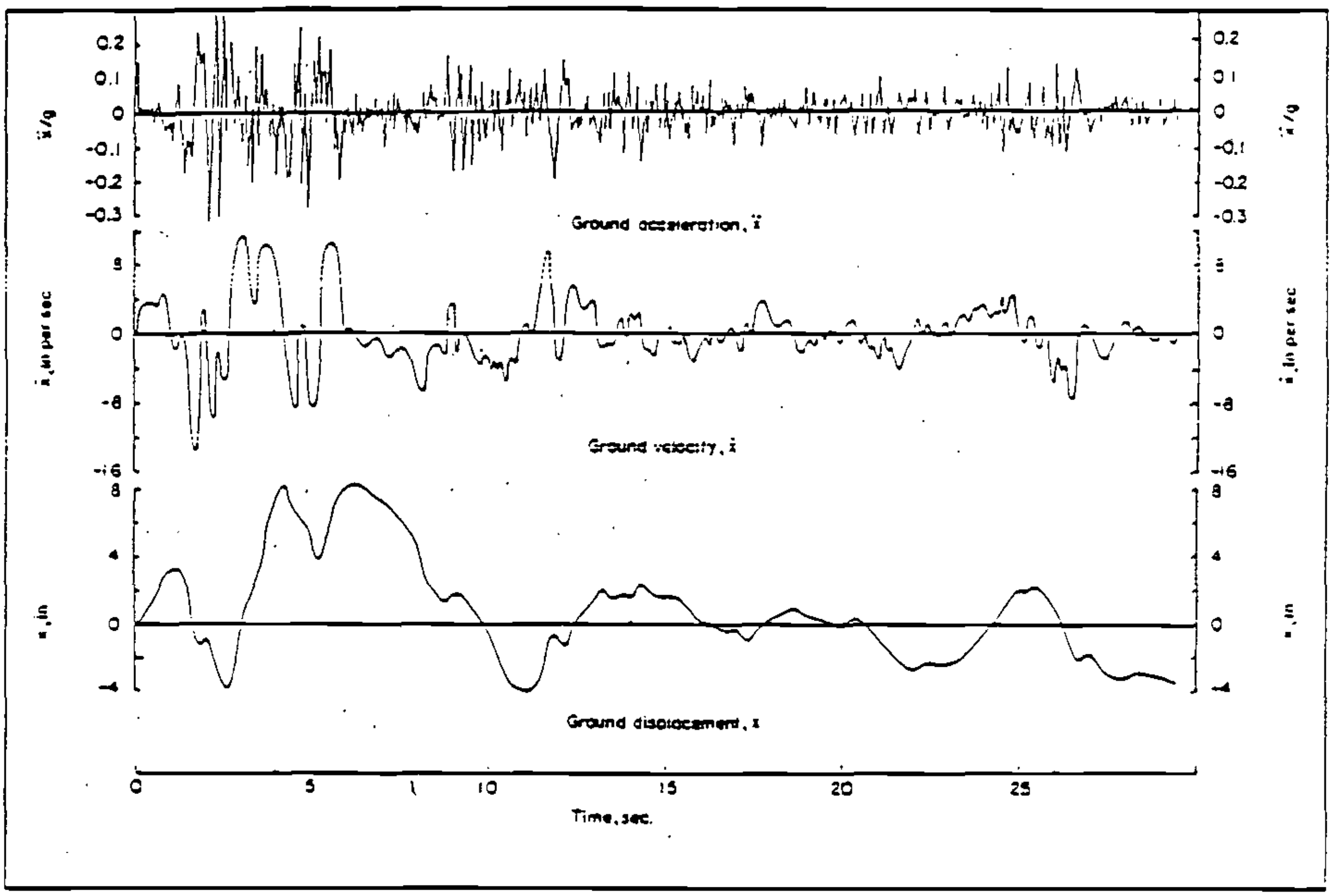

FIGURE C.2

Plot of Digitized Acccelerograms
Recorded at Pacoima Dam
(from NOAA, 1973)

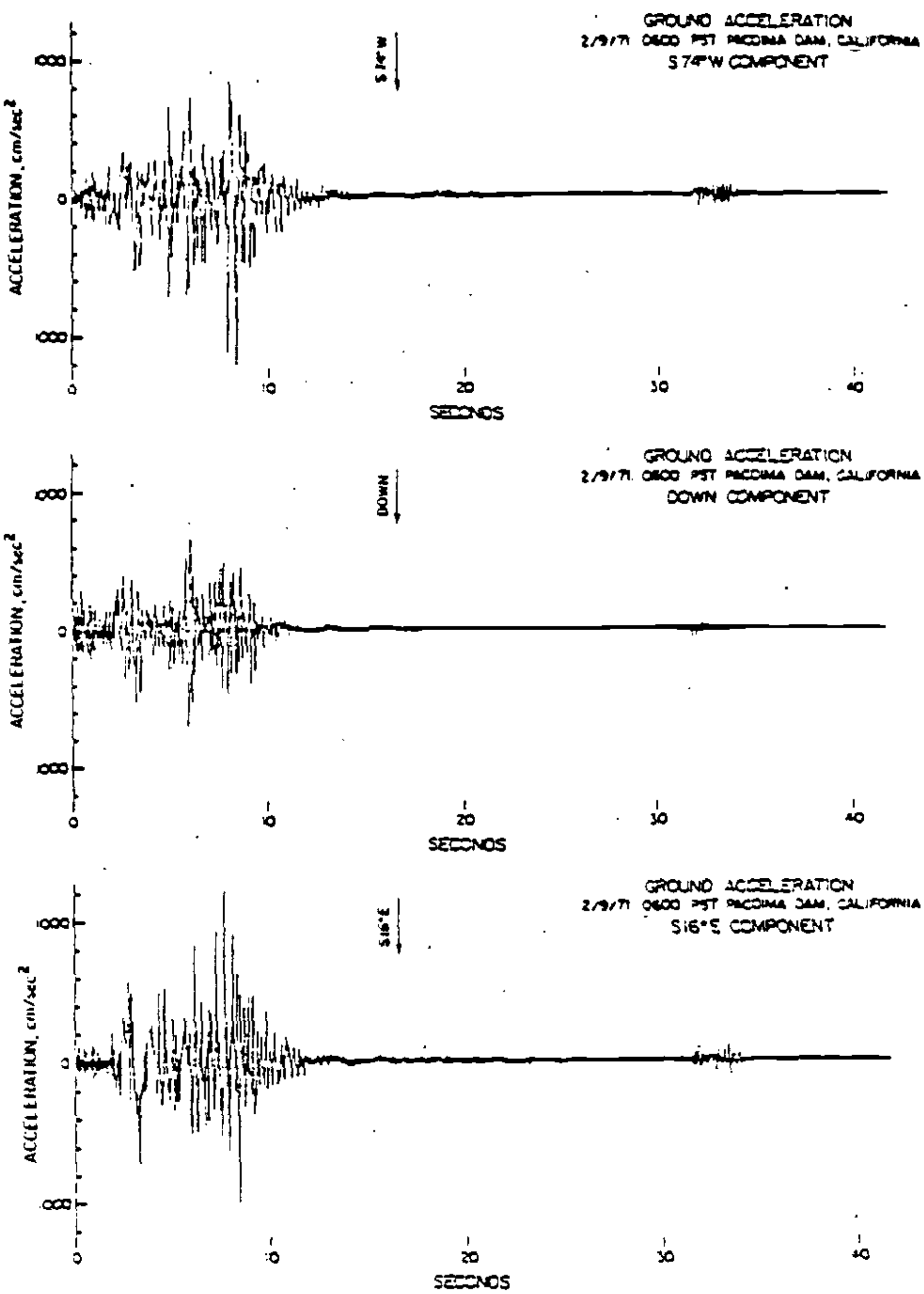

FIGURE C.3

USGS Accelerograms

USGS Accelerograms From Stations Within 30 km of Fault Rupture of 1979 Earthquake Showing Peak Accelerations. Solid Horizontal Lines are Zero Reference Traces. Poor Quality of Some Data Traces is due to High-Frequency High-Amplitude Motion Recorded on Photo-Optical Accelerographs (from USGS, 1982).

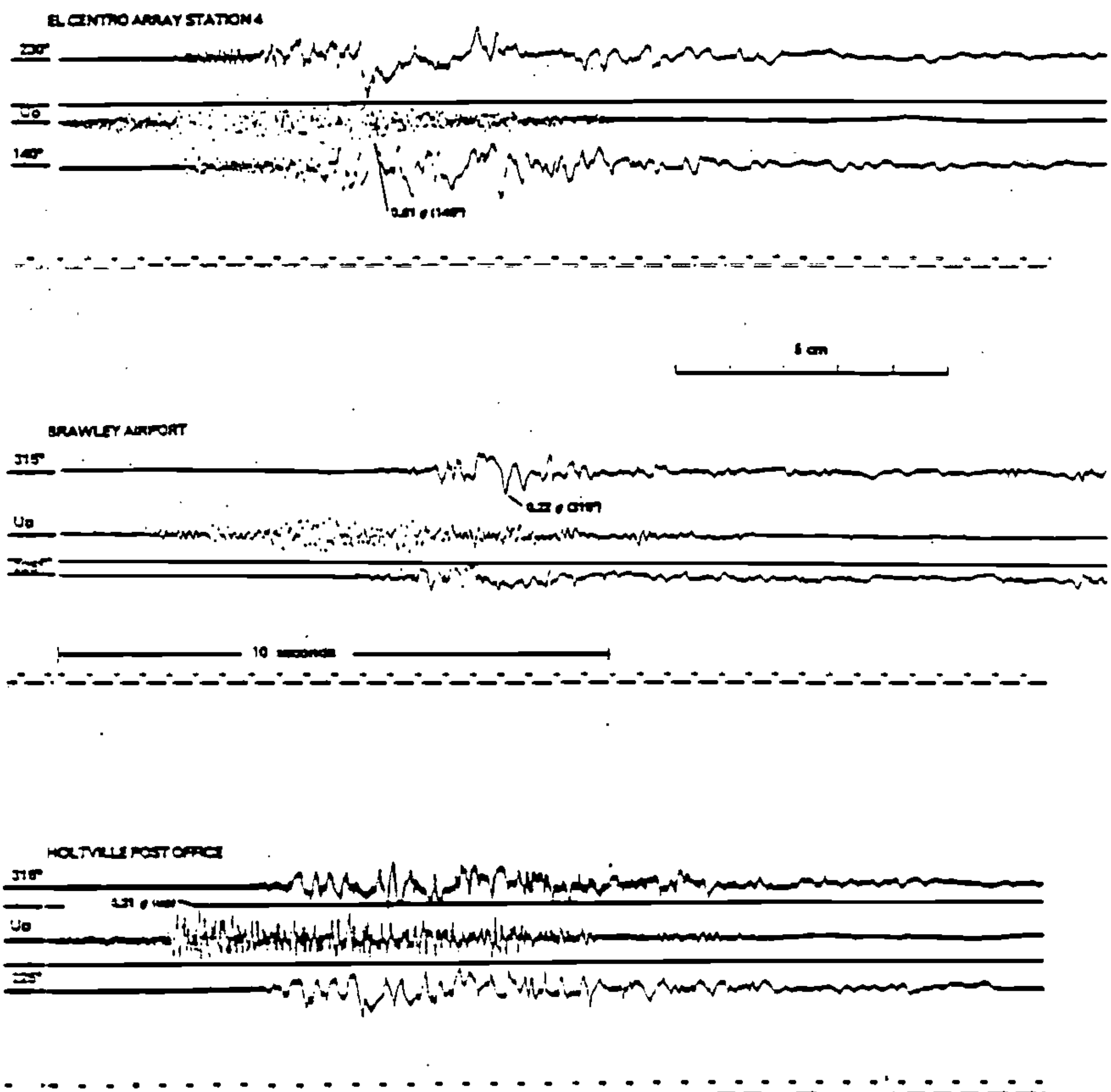

FIGURE C.4

Effect of Rise Time of Load Pulse on
Response of Simple Elastic Oscillator

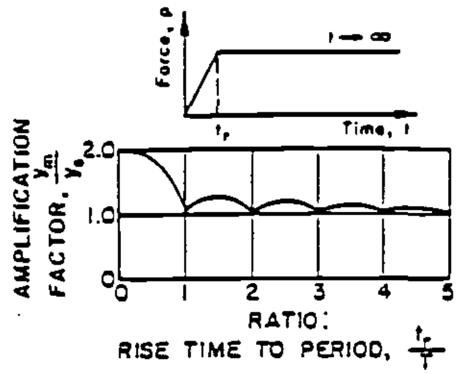

FIGURE C.5

Approximate Effect of Rise Time on Response of Simple Oscillator for a Damage-Pressure Level (P_m/R_y) of 1.0; Loads of Long Duration

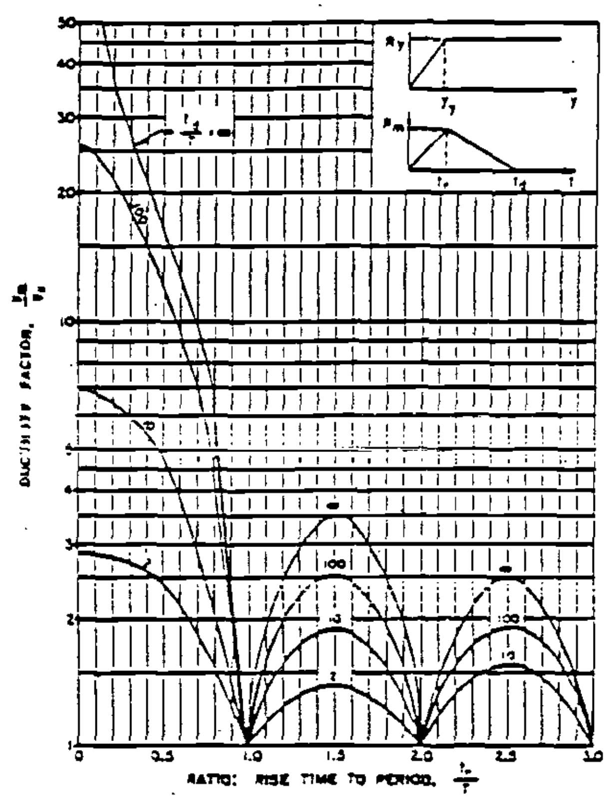

FIGURE C.6

Approximate Effect of Rise Time on Response of
Simple Oscillator for a Ratio of Pulse Duration to Period of 2

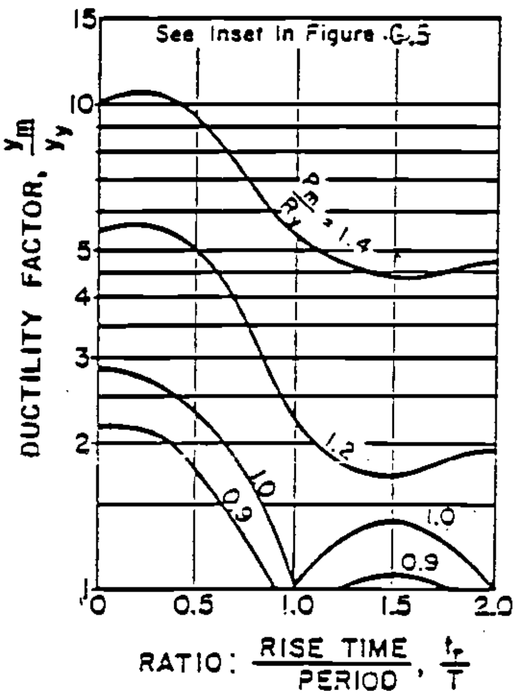

FIGURE C.8

Hoop Stress at the Boundary due to an Incident Wave of Dilation Using n = 0, 1, 2 ($\bar{\nu}$ = 0) (from Paul, 1963)

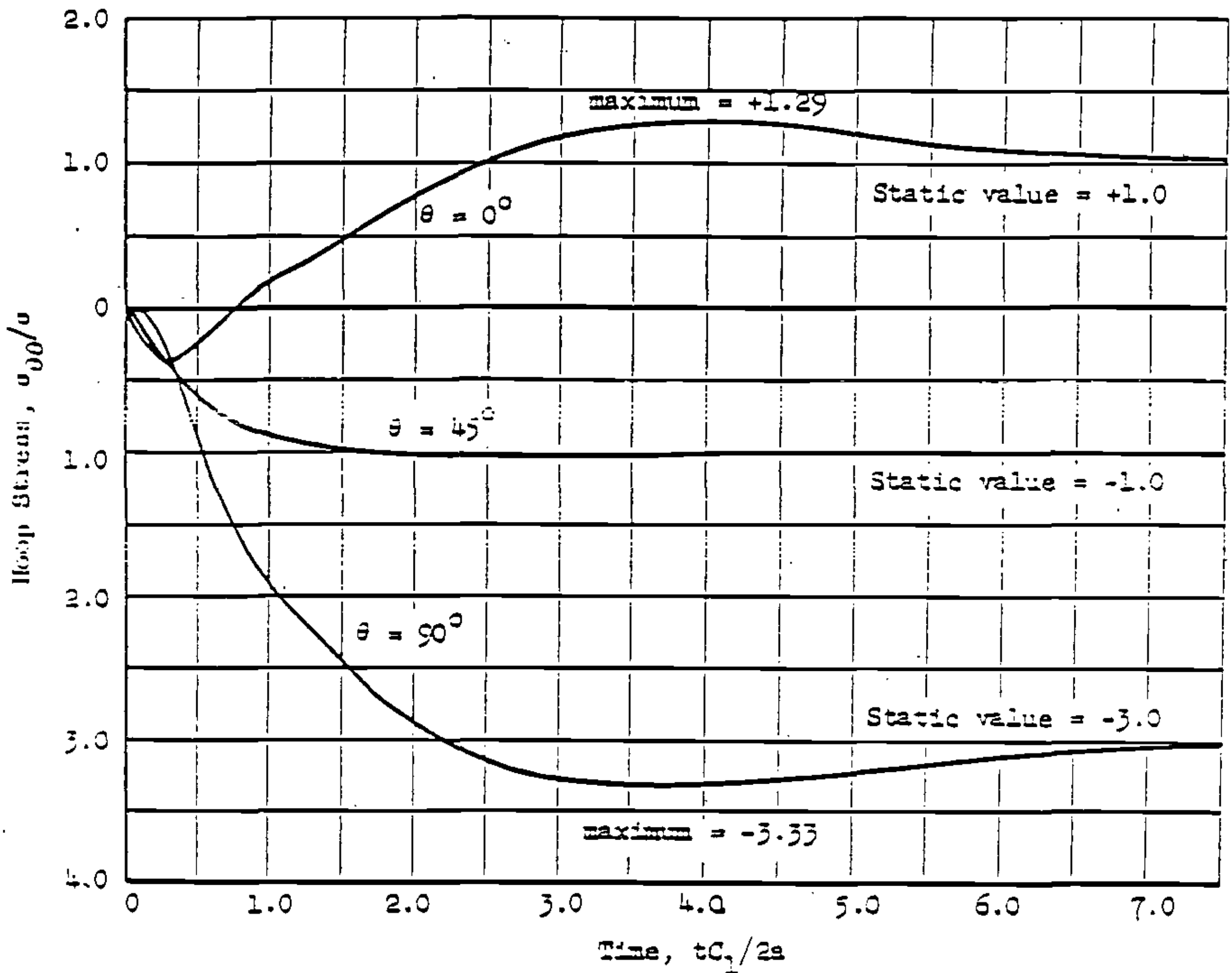

FIGURE C.9

Hoop Stress at the Boundary due to an Incident Wave of Dilation Using n = 0, 1, 2 ($\bar{\nu}$ = 1/3)
(from Paul, 1963)

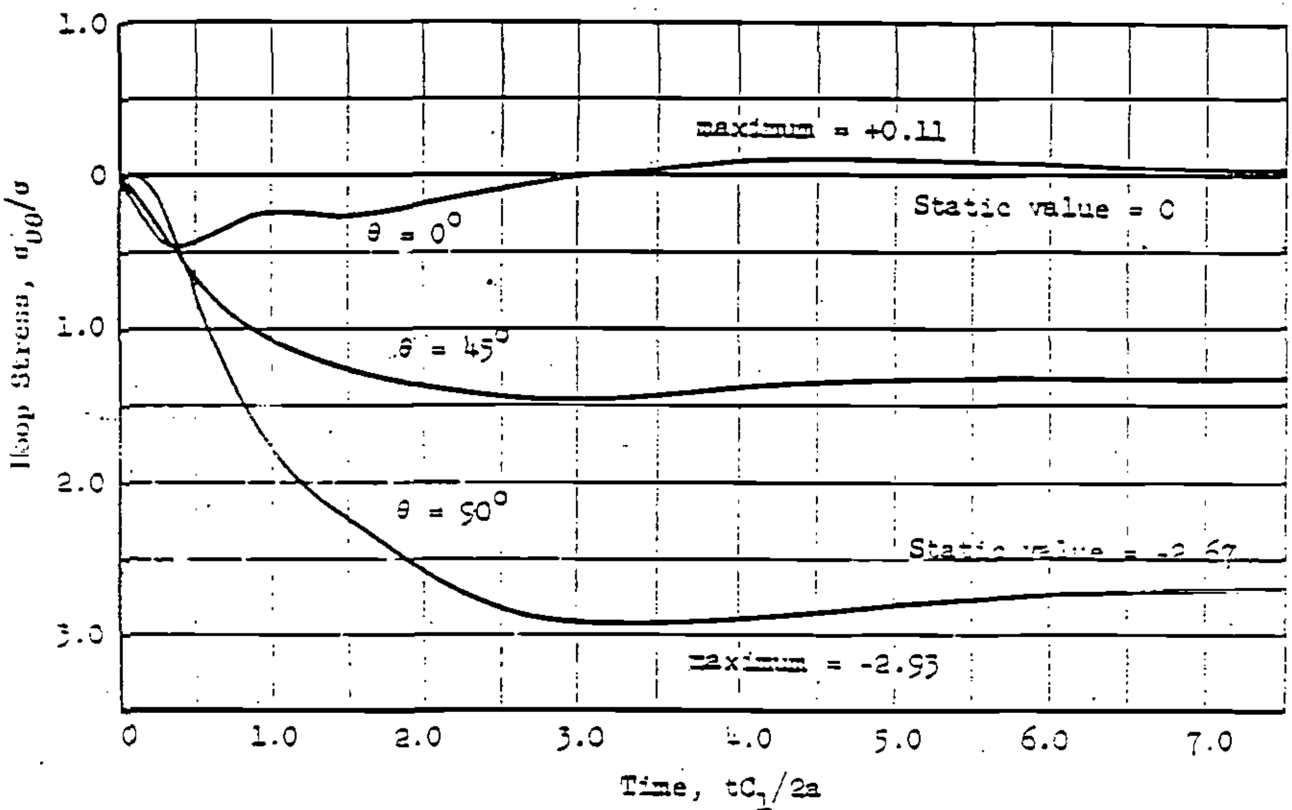

FIGURE C.10

Hoop Stress at the Boundary due to an Incident Shear Wave
Using n = 0, 1, 2 ($\bar{\nu}$ = 0)
(from Paul, 1963)

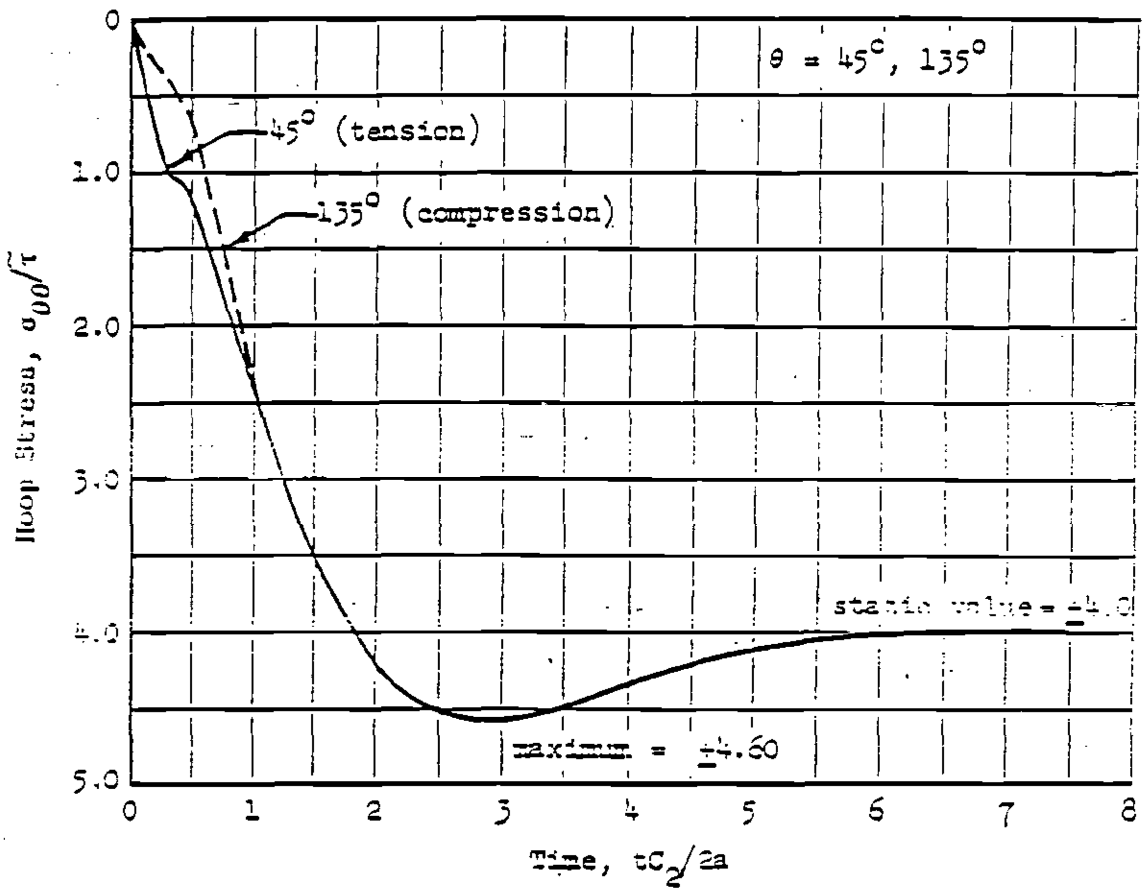

FIGURE C.11

Hoop Stress at the Boundary vs. Time due to an Incident Wave of Dilation with 4,000 psi at the Front and Various Rates of Decay Behind the Front ($\bar{\nu} = 1/3$, $\theta = 0°$)

(from Paul, 1963)

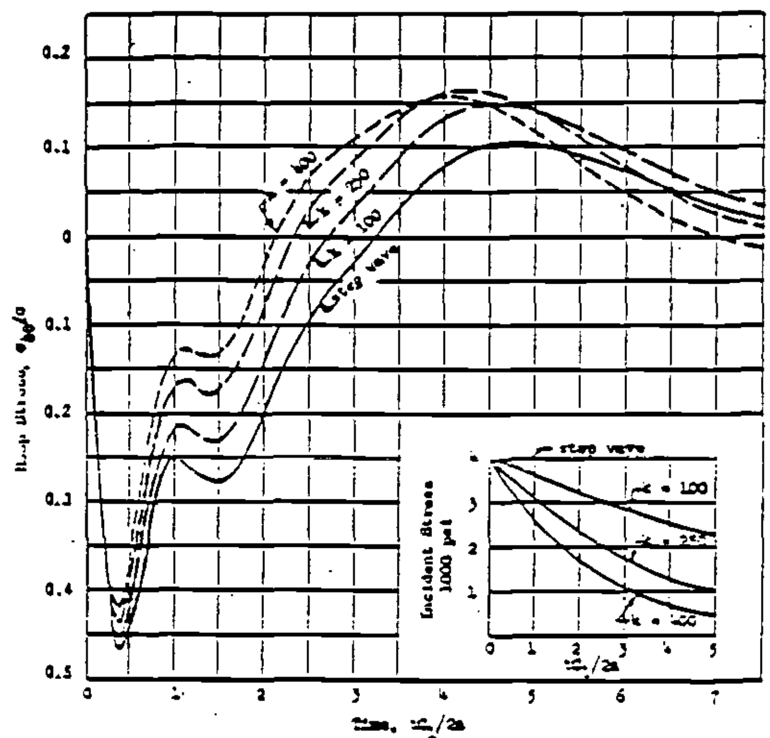

(Note: Ordinate normalized by peak amplitude of incident stress for direct comparison with Figure C.9 for $\theta = 0°$; in original document ordinate was in absolute value of stress.)

FIGURE C.12

Hoop Stress at the Boundary vs. Time due to an Incident Wave of Dilation with 4,000 psi at the Front and Various Rates of Decay Behind the Front ($\bar{\nu} = 1/3$, $\theta = 90°$)

(from Paul, 1963)

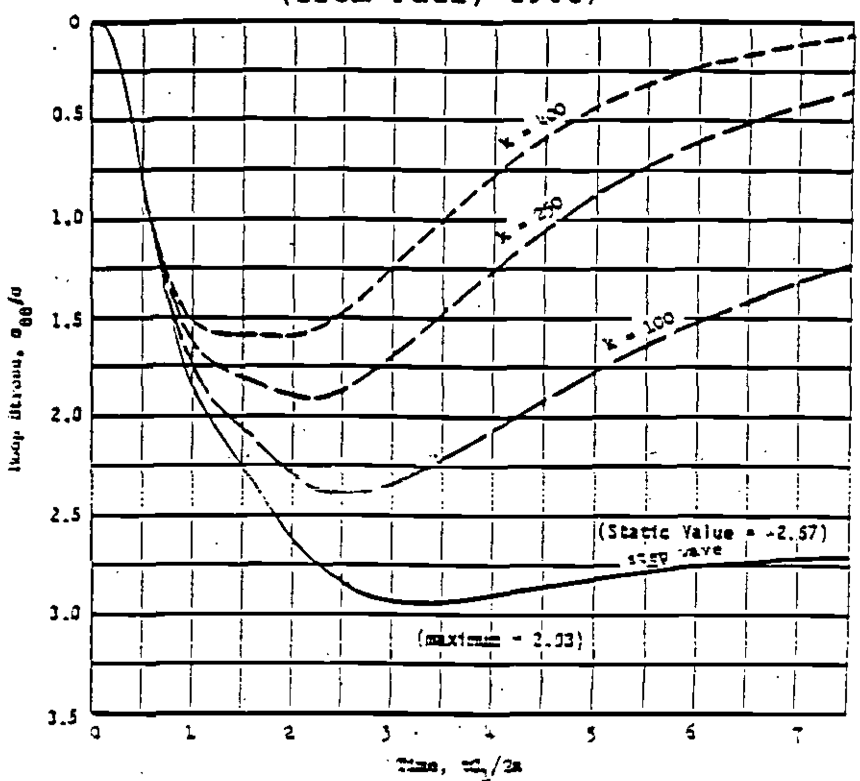

(Note: Ordinate normalized by peak amplitude of incident stress for direct comparison with Figure C.9 for $\theta = 90°$; in original document ordinate was in absolute value of stress.)

REFERENCES

C.1 Bluem, J.A., Newmark, N.M. and Corning, L.H. (1961), Design of Multistory Reinforced Concrete Buildings for Earthquake Motions, PCA, Skokie.

C.2 Paul, L.S. (1963), "Interaction of Plane Elastic Waves with a Cylindrical Cavity," Ph.D. Thesis, University of Illinois at Urbana-Champaign.

C.3 Yoshihara, T. (1963), "Interaction of Plane Elastic Waves with an Elastic Cylindrical Shell," Ph.D. Thesis, University of Illinois at Urbana-Champaign.

C.4 Merritt, J.L. and Newmark, N.M. (1964), Nuclear Geoplosics, Part V, "Effects on Underground Structures and Equipment," Report DASA1285(V), Washington.

C.5 Ali-Akbarian, M. (1967), "Oblique Incidence of Plane Stress Waves on a Circular Tunnel," Ph.D. Thesis, University of Illinois at Urbana-Champaign.

C.6 Belytschko, T. (1978), Private Communication.

C.7 NOAA (1973), San Francisco Earthquake of February 9, 1971, Vol III, Washington.

C.8 USGS (1982), The Imperial Valley, California, Earthquake of October 15, 1979, Prof. Paper No. 1254, Washington.

ANNEX D

STIFFNESS OF UNDERGROUND STRUCTURES

ANNEX D

STIFFNESS OF UNDERGROUND STRUCTURES

Tunnel Lining

The general approach taken in assessing either the static or dynamic behavior of a lined tunnel depends on the relative stiffness of the liner/soil system is conveniently considered as being divided into two separate and distinct types. The first is extensional stiffness, which is a measure of the equal all-around uniform pressure necessary to cause a unit diametral strain of the liner with no change in shape. A measure of the extensional stiffness of the medium relative to that of the liner is given by the compressibility ratio C (Peck, et al, 1972):

$$C = \frac{E_m(1 - \upsilon_\ell^2)\ R}{E_\ell\ t_\ell(1 + \upsilon_m)(1 - 2\upsilon_m)} \qquad \text{Eq. D.1}$$

where:
- E_m = modulus of elasticity of medium
- E_ℓ = modulus of elasticity of liner
- R = radius of liner
- υ_m = Poisson's ratio of medium
- υ_ℓ = Poisson's ratio of liner
- t_ℓ = average thickness of liner per unit length.

Since the earthquake loadings involve shear waves which primarily change the shape of elements in the ground mass without significantly changing the average principal stress, the compressibility ratio of the tunnel has very little effect on the behavior of the tunnel.

The second measure of stiffness is <u>flexural stiffness</u>, which is a measure of the magnitude of the nonuniform pressures necessary to cause a unit diametral change in shape or an ovalling of the liner.

The <u>flexibility ratio</u> is a measure of the flexural stiffness of the medium relative to that of the lining. The flexural stiffnesses of both the medium and the liner, as defined here, are essentially measures of the resistance of each to a change in shape under a state of pure shear. The flexibility ratio, F, is given by the following equation (Peck, et al, 1972):

$$F = \frac{E_m(1 - \upsilon_l^2)\ R^3}{6E_\ell I_\ell\ (1 + \upsilon_m)} \qquad \text{Eq. D.2}$$

where: I_ℓ = Moment of inertia of the liner cross-section per unit length along the axis of the tunnel.

Calculations of liner-medium interaction for various loading conditions, (Peck, et al, 1972, and Mohraz, et al, 1973) show that a liner will behave essentially as a perfectly flexible structure if the flexibility ratio is larger than 20. That is, the liner will conform to the distortions imposed upon it by the medium and, therefore, the distortions experienced by the liner can be estimated by calculating the distortions for the free field. For the Metro Rail Project, it is reasonable to assume that the most unfavorable soil conditions are in the alluvium where a representative (low) seismic velocity is 900 fps. The following material properties are then obtained for an 8 in. thick lining with a mean radius of 109 in. and an ultimate concrete strength of 6,500 psi.

$$G_{seismic} = \rho v_s^2 = \frac{120\ \text{pcf}}{32.2\ \text{ft./sec.}^2} \times \frac{(900)^2\text{ft.}^2}{\text{sec.}^2}$$

$$= 3.20 \times 10^6\ \text{psf} = 21{,}000\ \text{psi}$$

$$G_{effective} = (0.6 \text{ to } 0.8)\ G_{seismic} = 12{,}600 \text{ to } 16{,}800 \text{ psi}$$

$$E_{m\ effective} = 2(1 + \upsilon)G_{effective} = 2.6\ G_{effective}$$

$$= 32{,}750 \text{ to } 43{,}700 \text{ psi}$$

$$R = 109 \text{ in.}$$

$$E_{\ell} = 57{,}000 \sqrt{f'c} = 57{,}000 \sqrt{6{,}500}$$

$$= 4.6 \times 10^{6} \text{ psi}$$

$$I = \frac{(8)^3}{12} \text{ per inch of length}$$

Therefore, the flexibility ratio for the precast concrete lining is calculated to be

$$F = \frac{(32{,}750 \text{ to } 43{,}700) \quad (1 - 0.2^2)\ (109)^3}{6(4.6 \times 10^6) \quad \frac{(8)^3}{12} \quad (1 + 0.15)} = 30 \text{ to } 40$$

Thus since the flexibility ratio for the articulated liner under consideration is even larger than that indicated above, it is certainly above the 20 imposed by Peck, and the liner will behave as a flexible liner; as discussed above, the liner will conform to the distortions imposed by the medium.

<u>Snaking Mode for Tunnel Linings and Stations</u>

Flexibility of the subway structure in plan view, where the structure appears as a long narrow tube or "snake" subjected to the earthquake ground wave motion, has not been defined mathematically in the literature. However, it is recommended that the structure be investigated by imposing on the structure the strains produced in the ground by the earthquake (derived in Annex B) as a design bound. This recommendation is based on the following considerations:

a. If the structure exhibits the same flexibility as the ground replaced, then assuming the structure strains are equal to the strains in the ground is the exact solution.

b. If the structure is more flexible than the ground (as preliminary calculations indicate), the structure will certainly follow exactly the ground motions so that once again assuming the structure strains equal to the strains in the ground is the exact solution.

c. If the structure is less flexible than the ground, it will attempt to move less than the ground moves in the free field. By moving less than the ground, the structure necessarily is strained less than the ground. Therefore the strains in the ground are an upper bound to the strains in the structure and imposing the strains in the ground on the structure is conservative.

Thus, for all cases of structural flexibility (less than, equal to, or greater than the replaced ground) the strain in the ground is either equal to or a bound of the strain in the structure, and imposing the strain in the ground on the structure is a conservative assumption.

<u>Racking Mode for Stations</u>

Preliminary calculations indicate that the station may be less flexible than the ground under racking motion. As discussed above, however, it is conservative to assume that the motion of the station structure is the same as that of the surrounding ground. Even with the conservative assumption it is expected that the earthquake conditions will impose only minor, if any, modifications to the static design (see Appendix 1).

ANNEX E

TUNNEL ANALYSES FOR LOOSENING LOAD

ANNEX E

TUNNEL ANALYSES FOR LOOSENING LOAD

I. Introduction

The basic design of the precast concrete segments has been performed by MRTC following the "Guidelines for Tunnel Lining Design" (O'Rourke, 1984). It is recognized, however, that those guidelines are general in nature and address, for the most part, only static loading conditions. Under the dynamic loading conditions induced by a earthquake, the tunnel will be subjected to:

- o Distortions which have been discussed elsewhere in these Annexes, and

- o Vertical accelerations. If, during construction, loosening of earth materials above the tunnel has been permitted, these vertical accelerations will increase the impact of this loosened load on the tunnel. This problem has not been addressed fully in the literature.

Available information indicates the impact of this loosened load is extremely sensitive to methods of construction and to assumptions regarding the properties and condition of the tunnel lining and surrounding materials. With the recognition of this sensitivity, a preliminary investigation of the SCRTD tunnel liner section was performed to provide estimates of the adequacy of the section to resist "gravity loading" resulting from the weight of a zone of loosened material above the tunnel. The results are presented in terms of normalized thrust and bending moment distributions around the tunnel cross-section. A parametric approach was adopted to determine the sensitivity of peak bending moments to variation of key variables. The problem was analyzed in a static, plane strain configuration with a vertical axis of symmetry. The SATURN program (Sweet, 1979) was used with the existing grid shown in Figure E.1. As discussed below, a grid with a shallower tunnel was later used and the results agreed to the third significant figure. The liner was modeled as a continuous concrete cylinder containing 20 elements surrounded by a medium herein referred to as "rock" or "soil" and composed of 280 elements. Both materials were modeled as linearly elastic. The boundary conditions used are as shown in Figure E.1.

Table E.1 summarizes the 11 problems analyzed to show the parameters investigated. Symbols used in Table E.1 are defined in Table E.2. Section II discusses the problems chosen for analysis and discusses the rationale for varying each parameter. Section III discusses the processing models used and the method of computing moments and thrust. Section IV summarizes the results and draws conclusions therefrom. Section V offers recommendations for more study. Section VI provides the detailed data from the calculations.

II. Assumptions for Problems Analyzed

Figure E.2 illustrates the general configuration of all problems analyzed. The uniform load shown in (a) was used for Run 1 only; all other runs used the triangular load shown in (b). All loads were applied over the top 90° segment as shown, and the uniform and triangular load magnitudes were selected to result in the same <u>total</u> applied load for all runs. Boundary conditions for the remaining 270° were varied as described below. The total applied load was the weight of a triangular "loosened" zone of rock $\sqrt{2}$ R in width and h high, as shown in Figure E.3. The unit weight of rock was taken as 120 lb./ft.^{3}. The ratio, h/R was taken as one. Table E.6 shows peak moments at other h/R ratios for all runs.

All runs except Run 11 were modeled with a 140-ft. depth of burial to the tunnel springline.

The material properties used for the analysis were obtained from representative data used to approximate the layered geology anticipated for the tunnel system. These data are shown in Table E.3 and are those used for the new SHAKE computer runs reflected in Figures III-1 and III-2.

Runs 1 and 5 used identical material properties, differing only in the load shape which was uniform in Run 1 and triangular in Run 5. For these runs, the soil was considered representative of a soil below the water table at approximately 100 ft. with a shear-wave velocity of 1,500 ft./sec. and a P-wave velocity of 5,000 ft./sec.[a] The "loosened zone" above the tunnel section had elastic properties of one-tenth the insitu material. These reduced values essentially reduced the load carrying capacity of this zone to better represent the actual behavior. The strength of the concrete was assumed as 8,000 psi in Runs 1 and 5.

The second series of runs varied the soil/liner stiffness characteristics. The properties of Run 9 represent a dry soil with a shear-wave velocity of 1,200 ft./sec. and a P-wave velocity of 2,400 ft./sec. A wet soil with a similar shear strength was used for comparison (V_s = 1,200 ft./sec.; V_p = 5,000 ft./sec.). For these two runs a lower concrete strength was used (f_c' = 4,000 psi). In addition, the stiffness of the loosened zone was set to zero, thus eliminating any transfer of stress into this material. Run 11 was a repeat of Run 9 except the depth of burial was reduced to 65 ft. (Figure E.4).

---

[a] Despite the recommendation in Appendix B that v_p be taken equal to twice v_s, it was necessary to use v_p for the water in saturated cases in this annex because SATURN, the computer program used, has appropriately considered the effective stress in a saturated soil; it properly transfers the stresses between soil and water.

Runs 13 through 18 used a common set of soil and liner properties throughout but included slight variations in the loosened zone properties. These properties represent a dry soil near the surface and above the water table (V_s = 830 ft./sec.; V_p = 1,660 ft./sec.). Also, material properties of the elements adjacent to the liner were varied as a means of approximating a slip condition or slip layer. The concrete strength was increased to the actual design value of 6,500 psi. Figure E.5 shows the materials within the grid.

Run 13, the control run, used properties of the slip layer the same as the surrounding soil in order to assess the effect of the new soil and concrete properties when compared to previous runs. Loosened zone stiffness was again zero, the same as Runs 9 to 11.

Run 14 differed from Run 13 in that a "slip layer" was approximated by reducing the shear modulus to one-tenth that of the surrounding medium. In Run 15, the slip layer shear modulus was reduced further, to zero.

In both Runs 17 and 18, the slip layer was made the same as for Run 14, i.e., one-tenth the shear modulus of the surrounding medium. The loosened zone in Run 17 was given one-tenth the elastic properties of the in situ material.

Run 18 again used zero stiffness in the loosened zone, but employed two layers of "slip" elements in the slip layer with a 90 percent reduction in shear modulus.

III. Solution Method

The initial solution step was to define and set up the problem, including the element grid geometry and the applied loading. The grids used have been previously described; symmetry about the vertical tunnel axis was employed for computational efficiency.

Figure E.3 details the load geometry resulting from a triangular loosened zone above the tunnel. For $a = 9.5$ ft. and $h = a$, the net area is found to be 56.8 ft². With a unit weight of soil of 120 lb./ft.³ this gives a load of 6,810 lb. per foot of tunnel. The same total load was applied in the uniform loading (Run 1) though the shape was different.

SATURN is a generalized three-dimensional finite element computer code with dynamic and nonlinear capability. All runs for these analyses were made with static loadings and linearly elastic materials. All grid elements were quadrilateral continuum elements in plane strain.

The nodal displacements obtained from SATURN were used to compute circumferential strains at the interior and exterior surface of each liner element. Figure E.6 details the strain calculation procedure which was used. Axial and flexural strains were computed from:

$$\text{Axial strain} = \varepsilon_c = \frac{\varepsilon_o + \varepsilon_i}{2} \qquad \text{Eq. E.1}$$

$$\text{Flexural strain} = \varepsilon_f = \frac{\varepsilon_o - \varepsilon_i}{2} \qquad \text{Eq. E.2}$$

in which ε_i and ε_o are the interior and exterior circumferential strains respectively. Thrust and moment were then computed assuming an elastic ring of uniform thickness:

$$\text{Thrust} = T = Et\varepsilon_c \qquad \text{Eq. E.3}$$

$$\text{Moment} = F = \frac{Et^2\varepsilon_f}{6} \qquad \text{Eq. E.4}$$

where E is the modulus of Elasticity and t is the liner thickness for a unit length.

Ranken et al (1978) provide solutions to various related problems which are useful for comparison. Since those solutions are normalized by the factors Pa for thrust and Pa^2 for moment, these factors must be computed for the present analysis. P is the equivalent uniform load magnitude per unit tunnel length; that is, the total applied load divided by the loaded span. The tunnel radius is a.

For the present problem a is 114 in. giving a load span of a $\sqrt{2}$ = 161 in. The total load was computed earlier as 6,810 lb./ft. so that P is (1/12)(6,810)/161 = 3.520 lb./in². Pa is then 400 per inch of tunnel length and Pa^2 is 45,750 per inch.

Pa was also used as a normalized factor for thrust computed from SATURN. Moments computed from SATURN were normalized with respect to ultimate moment capacity in view of the fact that moment controls the design. This ultimate moment capacity was computed from $M_u = 0.9\ A_s f_y d$. A_s is 1/2 percent, f_y is 40,000 psi and d is taken as 7 in. Using A_s 0.005 d gives $M_u = 0.0045\ f_y d^2$ = 8,820 in.-lb./in.

The values of C and F listed in Table E.4 can be used to enter plots of coefficients for the terms in Equations E.7 and E.8 and Equations 7.1 and 7.2 of Ranken to obtain normalized thrusts and moments for comparison purposes. These results are tabulated in Table E.4.

IV. Results

The complete results of the finite element calculations are presented in Section VI. These results are given in terms of thrust and moment as a function of angular position around the circumference of the liner. In this section influences of the various parameters are discussed. Peak moments are summarized for all runs expressed in terms of a percentage of the ultimate moment capacity of the section. These moment values, presented in Table E.6, are given for several values of h/r, where h is the height of the triangular "loosened" zone above the tunnel. The calculations were performed with an $h/r = 1$. Other values were scaled in proportion to the change in weight of the loosened zone as a function of h. The last three columns in Table E.6 related to values of maximum moment from Ranken for a tunnel and medium with the same flexibility and compressibility factors. A comparison of these values will be discussed later.

Runs 1 and 5 investigated the effect of a uniform vs. a triangular load distribution on the liner. Results of these two calculations are presented in Figures E.10 and E.11 in terms of normalized thrust and moment around the liner. These normalizing factors are discussed in Section III. The two figures show that the triangular load distribution generates higher moments and less thrust than the uniform case. The peak moments are 2.75 times greater for the triangular load.

The next series of runs looked at the variation in stiffness of the medium. In addition, a zero stiffness was assumed for the "loosened-zone" as a worst case assumption. Run 9, using a "dry" material with V_s = 1,200 ft.sec. and V_p = 2,400 ft./sec., resulted in higher moments and thrust than the previous runs as shown in Figure E.12. Figure E.13, a similar run (Run 10) with a wet material (V_s = 1,200 ft./sec.; V_p = 5,000 ft./sec.) produced very little change. The difference between these two runs and Run 5 are attributed to the reduced shear stiffness of the medium (63,700 psi vs. 38,900 psi) and the zero stiffness of the loosened zone. Results of Run 11 showed the calculations to be relatively insensitive to burial depth (material properties held constant from Run 9).

The final series of calculations was concerned primarily with the effect of slip between the concrete liner and the surrounding medium. Run 13 was a repeat of Run 9 with near surface soil and the design strength concrete. Results indicate a 38 percent increase in maximum bending moment for the weaker soil (no slip). By incorporating a layer of elements with lower shear stiffness (slip layer) the calculated peak moment increased significantly to 62 percent of ultimate section capacity (Run 14). By decreasing the shear stiffness to zero (Run 15) a full slip condition was approximated and the peak moment increased to 75 percent of ultimate. It should be noted that for these runs, the elastic properties of the "loosened" zone are zero; thus, there are no forces acting between the loosened zone and the surrounding medium.

To assess the relative importance of "loosened" zone properties, Run 17 was performed with elastic properties of this zone at one tenth their in situ values. Comparing this run with Run 14 one sees a 33 percent reduction in peak moment in going from 0 to one-tenth the elastic properties. The last calculation (Run 18) was a repeat of Run 14 only with 2 slip layers. This resulted in a slight increase in maximum moment of approximately 8 percent.

From the above calculations it is evident that the worst-case conditions are a zero stiffness (E = G = K = 0) "loosened" zone combined with a full-slip condition (Run 15). It appears that some slip resistance as well as some soil resistance in the "loosened" zone may be a more realistic assumption. Nevertheless, the worst-case (Run 15) assumptions result in a maximum bending resistance of only 72 percent of the ultimate section capacity. By assuming some small amount of slip resistance between the liner and soil (Run 14), a maximum moment of 62 percent of ultimate is reached. Finally, by allowing some stress capability in the loosened zone (Run 17) the peak moment is reduced to only 42 percent of ultimate. Of these three calculations, the second case (Run 14) provides a reasonably conservative estimate of section capacity. The last case (Run 17) may overestimate the stress capability of the loosened zone by allowing some tensile stresses to develop.

The last three columns in Table E.6 provide a means of comparison between the method of analysis of "gravity loading" presented in Ranken and the preceding calculations. The first of these columns are for a uniform load with the same total weight of the assumed "loosened" zone distributed over a 90° arc of the lining. Both slip and liner separation from the "loosened" zone are allowed. These values should be compared to the h/r = 1 column. In the second of these columns, the peak moments are multiplied by a factor of 2 reflecting the difference between the peak load of the triangular distribution versus the uniform distribution. The last column represents the peak moment of the first column multiplied by the ratio of the peak moment of Run 5 (triangular) and Run 1 (uniform). This approximates the difference between the uniform load assumption of Ranken and the triangular load used for the present calculations. If one assumes this ratio (2.75), the peak moment given by Ranken is in good agreement with the worst case value in Run 15. (This case is also the problem configuration most like that of Ranken.

V. Recommendation

Based on the preceding results, the assumed uniform ring appears adequate to resists the assumed "gravity loading." More research is required to determine the behavior of actual liners.

The problems reflected in Table E.6 and Section VI have gaps; they certainly do not represent a complete parametric study. Nevertheless, as already noted, the approximate results indicate that the "loosening load" by itself is relatively benign. In fact it is perhaps so benign that even when combined with the racking distortion, which most likely would occur after any strain due to loosening load has developed, gives a total distortion which is not going to create any condition which approaches collapse unless the effective shear-wave velocity in the surrounding soil is low. Because in New Alluvium this velocity may be low enough to create difficulty, the following approximate procedure is suggested.

The approximate procedure is generally based on the plots in Figure E.14. The open circles represent, for modulus of the loosened zone of 0 and 5,000 psi, Runs 13, 14, 15, and 17, from Table E.6. The two open circles at a modulus of 16,700 psi are from new runs just completed. The curves drawn are best slopes interpolated or extrapolated from the data available. The square solid point represents a result using an entirely different finite element model, but otherwise using parameters essentially the same as for the run immediately above it. The models are so different that the results cannot be considered comparable; the comparison merely shows the results of two independent model formulations. (However, it is probably not entirely coincidental that the ratio of the ordinate for the square and the circle immediately above it is nearly equal to the ratio of the total loads; the square assumes approximately a sinusoidal loading while the circle assumes approximately a triangular loading, each acting over one-fourth the circumference.)

Since the results described in detail in this Annex are more conservative than earlier work (Ranken) they may be used for the current design efforts. To be reasonably sure that refinements are not going to produce results which are worse (higher strains than those implied here) than those deduced from the following procedure, the data from Run 14 (stiffness of loosened zone 5,000 psi) are used to define conditions for using Ranken as the basis for accounting for variations in lining stiffness.

The stiffness of the linings used in the preceding calculations is defined as that for an uncracked, homogeneous concrete ring with modulus of elasticity of 4.6×10^6 psi. The segmented linings, on the other hand, have a stiffness more consistent with a cracked section. Since the moment coefficient is only 68 percent of ultimate and since the yield moment is essentially numerically equal to the ultimate moment, the strain in the steel is approximately 69 percent of that corresponding to initial yielding of the steel. At this level of strain in the steel, the concrete is still in its nearly linear range of behavior. Thus even for the case recommended, essentially elastic conditions are maintained. Since the solution used in this annex and that used by Ranken are for elastic conditions, it is an acceptable approximation to use the comparison between uniform load and triangular load in Table E.6 (Runs 1 and 5) to define, on a consistent basis, the ratio of moments at the crown produced by a triangular and a uniform load distribution. As already noted, this ratio is 2.75. At the same time it is noteworthy that Run 15 comes as close as possible to that used by Ranken. The detailed results for this run are consistent with those of the model used by Ranken as generally indicated by the comparison in Table E.6.

Before this coefficient was applied, however, other data had to be developed from Ranken to provide data for a range of relative flexibilities for the lining/medium combinations. As noted earlier, Ranken developed an approximate equation to represent his computer-generated data for various distributions of uniformly distributed loosening loads (distributions from 60° - 180° of included angle). These are given above as Equations E.7 and E.8. Additionally, some derivations were required. These are given below. As already noted, the curvature (α) induced by bending in a uniform elastic ring is:

$$\alpha = -3 \left(\frac{\Delta D}{D}\right) \left(\frac{1}{a}\right) \qquad \text{Eq. E.10}$$

$$\text{But } \alpha = -\frac{M}{E_l I_l} \text{ or } M = 3 \left(\frac{\Delta D}{D}\right) \left(\frac{E_l I_l}{a}\right)$$

If M is scaled by Pa^2 as done by Ranken:

$$\frac{M}{Pa^2} = 3 \left(\frac{\Delta D}{D}\right) \left(\frac{E_l}{P}\right) \left(\frac{I_l}{a^3}\right)$$

But Ranken also scales $\frac{\Delta D}{D}$ by $\frac{P}{E_m}$, therefore:

$$\frac{M}{Pa^2} = 3\left(\frac{\Delta D/D}{P/E_m}\right)\left(\frac{E_\ell P}{PE_m}\right)\left(\frac{I_\ell}{a^3}\right) \text{ or } \frac{M}{Pa^2} = 3\left(\frac{\Delta D/D}{P/E_m}\right)\left(\frac{E_\ell}{E_m}\right)\left(\frac{I_\ell}{a^3}\right)$$

and $\frac{\Delta D/D}{P/E_m} = \frac{1}{3}\left(\frac{M}{Pa^2}\right)\left(\frac{E_m}{E_\ell}\right)\left(\frac{a^3}{I_\ell}\right)$

but F (Peck, et al, 1972) is:

$$F = \frac{E_m}{E_\ell}\,\frac{a^3}{6I_\ell}\,\frac{1-\nu_\ell^2}{1+\nu_m}$$

Therefore:

$$\frac{\Delta D/D}{P/E_m} = 2F\left(\frac{M}{Pa^2}\right)\left(\frac{1+\nu_m}{1-\nu_\ell^2}\right) \qquad \text{Eq. E.11}$$

Equation E.11 obviously can be used to plot the left hand term as a function of F if values of M/Pa^2 are know. They are know approximately from Equation E.7 and E.8. The results are plotted in Figure E.15 as an approximation to the diameter change (downward in the vertical direction and outward in the horizontal) for the loosening load.

Finally we address the significance of the 2.75 mentioned prior to the above derivation: To investigate the implications of the approximation in Figure E.15, and attempt was made to derive Figure 7.9 ($\frac{\Delta D/D}{P/E_m}$ vs. F) of Ranken from Figure 7.8 (M/Pa^2 vs. F). This comparison is shown in Figure E.16. To make the computations, a correction had to be included for the differences in load distribution between the computations given in this annex (triangular or sinusoidally distributed loads) and those in Ranken (uniform). (Incidentally, a sinusoidal distribution is inherent in Equation

E.10; also Equation E.10 can be derived assuming a circle is deformed into an ellipse.) The 2.75 factor from Table E.6 was used for this adjustment. The adjusted values agree approximately with Ranken over the range from F = 4 to 500. A somewhat better fit would be given by:

$$\frac{\Delta D/D}{P/E_m} = 0.5F \left(\frac{M}{Pa^2} \right) + 1$$

Although there is theoretical justification for a fit of this form, it required assuming a cracked section to define moment of inertia, (I_ℓ) and area (A_ℓ), rather than an uncracked section. Since an uncracked section was apparently assumed by Peck and carried forward to Ranken, there appears to be no current justification to use a cracked section to interpolate Ranken's data.

VI. SATURN Calculations;-Data

Table E.1 is repeated on page E-14 to summarize the 10 SATURN runs which were made. In subsequent pages, liner strains and forces are tabulated for all 20 liner elements of each run. The columns tabulated are described in Table E.7.

TABLE E.1

Run Summary Matrix

Run No.	Load Shape	V_s soil ft./sec.	V_p soil ft./sec.	E soil psi	ν soil psi	K soil psi	G soil psi	E "loosened" zone-psi	G "interface"-psi	f'_c - psi
1	Uniform	1,500	5,000	184,700	0.45	622,300	63,700	18,500	63,700	8,000
5	Triangular	1,500	5,000	184,700	0.45	622,300	63,700	18,500	63,700	8,000
9	Triangular	1,200	2,400	103,600	0.33	103,500	38,900	0.0	38,900	4,000
10	Triangular	1,200	5,000	114,200	0.47	621,800	38,900	0.0	38,900	4,000
11[a]	Triangular	1,200	2,400	103,600	0.33	103,500	38,900	0.0	38,900	4,000
13	Triangular	830	1,670	50,000	0.33	50,000	18,700	0.0	18,700	6,500
14	Triangular	830	1,670	50,000	0.33[b]	50,000	18,700	0.0	1,870	6,500
15	Triangular	830	1,670	50,000	0.33[c]	50,000	18,700	0.0	0.0	6,500
17	Triangular	830	1,670	50,000	0.33	50,000	18,700	5,000	1,870	6,500
18[d]	Triangular	830	1,670	50,000	0.33	50,000	18,700	0.0	1,870	6,500

a Depth of Burial = 65 ft. in this case only, otherwise 140 ft.

b At interface = 0.48

c At interface = 0.50

d Two rings of interface elements

TABLE E.2

Definition of Symbols

E	-	Modulus of esasticity (soil mass, loosened soil, or concrete)
ν	-	Poisson's ration (soil mass, loosened soil, or concrete)
K	-	Bulk Modulus $= \dfrac{E}{3(1-2\nu)}$
G	-	Shear modulus $= \dfrac{E}{2(1+\nu)}$
f_c'	-	Concrete compressive strength (28-day)
V_s	-	Shear-wave velocity
V_p	-	P-wave velocity

TABLE E.3

Shear Wave Velocities from SHAKE Computer Runs (ft./sec.)

Depth \ SHAKE Run No.	1	2	3	4	5
0	800	1200	1200	1200	1200
25	990*	1200*	1900*	1200	1200
50	1120	1900	1900	1900	1900
75	1300	1900	1900	1900	1900
100	1500	1900	2500	1900*	1900
130	2000	1900	1500	1900	1900
200	3000	4000	4000	4000	4000*

$V_p = 2V_s$ above water table ; i.e., $\nu = 1/3$

V_p = 5,000 ft./sec. below water table

---

* water table

TABLE E.4

Peak Moments and Thrusts Approximated from Ranken, et al., (1978) Equations

Run No.	C	F	$\frac{T}{Pa}$	$\frac{M}{Pa^2}$	$\frac{M}{M_{ult}}$ -%	$\frac{2M^a}{M_{ult}}$ -%
1	3.297	124.7	0.644	0.0326	16.9	33.8
5	3.297	124.7	0.644	0.0326	16.9	33.8
9	0.855	107.8	0.663	0.0309	16.0	32.0
10	4.671	176.6	0.646	0.0266	13.8	27.6
11	4.671	176.6	0.646	0.0266	13.8	27.6
13	0.323	40.7	0.538	0.0551	28.6	57.2
14	0.323	40.7	0.538	0.0551	28.6	57.2
15	0.323	40.7	0.538	0.0551	28.6	57.2
17	0.323	40.7	0.538	0.0551	28.6	57.2
18	0.323	40.7	0.538	0.0551	28.6	57.2

C - Compressibility ratio $= \frac{E_m}{E_l} \left(\frac{a}{t}\right)\left[\frac{(1-\nu_l^2)}{(1+\nu_m)(1-2\nu_m)}\right]$ (E.5)

F - Flexibility ratio $= \frac{E_m}{E_l} \left(\frac{a}{t}\right)^3 \left[\frac{2(1-\nu_l^2)}{(1+\nu_m)}\right]$ (E.6)

$\frac{T}{Pa} = (B_t)_{i,j} \ (F_t')_{i,j} - M_i \ C^{1.11}$ (Ranken, et al., 1978, eq. 7.1)[b,c] (E.7)

$\frac{M}{Pa^2} = (M_f)_{i,j} + (3.53 \ C^{1.11}) \ (M_{cf})_{i,j}$ (Ranken, et al., 1978, eq. 7.2)[b,c] (E.8)

$\frac{M}{M_{ult}} = \frac{M}{Pa^2} \cdot \frac{Pa^2}{M_{ult}} = \frac{M}{Pa^2} \ \frac{45,750}{8,820}$ (E.9)

In C and F definitions above (Peck, et al. 1972), "a" is the tunnel radius and "t" is the liner thickness. The subscripts "m" and "l" refer to the medium (soil) and the liner respectively.

---

[a] Factor of 2 used to adjust results from Ranken, et al. (1978) to give the same <u>total</u> applied load.

[b] See Table E.5 which is Table 7.2 from Ranken for $\alpha=90^\circ$; i=3 and m=0.028 from Table 7.1 of Ranken.

[c] See Figures E.7a and b, E.8a and b and E.9a and b which are Figures 7.12a and b, 7.16 a and b, and 7.20 a and b from Ranken.

TABLE E.5

Base Values of the Thrust Coefficient for use in Equation 7.1

j	$(B_t)_{1,j}$ $\alpha = 180°$	$(B_t)_{2,j}$ $\alpha = 120°$	$(B_t)_{3,j}$ $\alpha = 90°$	$(B_t)_{4,j}$ $\alpha = 60°$
1	.540	.540	.520	.440
2	.582	.582	.563	.483
3	.712	.712	.700	.621
4	.872	.872	.849	.671
5	1.015	.997	.873	.653
6	1.068	.989	.833	.653
7	1.084	.964	.817	.619
8	1.083	.960	.815	.615
9	1.080	.957	.814	.614
10	1.079	.957	.813	.613
11	1.078	.957	.812	.613
12	1.077	.957	.811	.613
13	1.076	.957	.810	.613

(From Ranken et al (1978))

TABLE E.6

Results Summary

h/R RUN NO	0.2	0.4	0.6	0.8	1.0	1.5	2.0	2.5	3.0	Ref 2 1.0	2 x Ref 2 1.0	2.75 x Ref 2 1.0
	MAXIMUM MOMENT FOR VARIOUS h/R VALUES (%)											
1	.64	2.07	3.53	4.94	6.37	9.95	13.53	16.83	20.70	16.90	33.80	46.48
5	1.76	5.70	9.69	13.58	17.52	27.36	37.21	46.26	56.90	16.90	33.80	46.48
9	3.44	11.12	18.90	26.48	34.16	53.36	72.56	90.22	110.95	16.00	32.00	44.00
10	3.34	10.81	18.37	25.73	33.20	51.85	70.51	87.67	107.82	13.80	27.60	37.95
11	3.42	11.07	18.82	26.36	34.00	53.11	72.22	89.80	110.44	13.80	27.60	37.95
13	4.76	15.39	26.15	36.63	47.26	73.81	100.37	124.80	153.49	28.60	57.20	78.65
14	6.22	20.13	34.21	47.92	61.81	96.55	131.29	163.25	200.77	28.60	57.20	78.65
15	7.25	23.44	39.84	55.81	72.00	112.46	152.92	190.14	233.34	28.60	57.20	78.65
17	4.20	13.57	23.06	32.30	41.67	65.08	88.50	110.04	135.33	28.60	57.20	78.65
18	6.74	21.80	37.04	51.89	66.94	104.56	142.18	176.79	217.42	28.60	57.20	78.65

TABLE E.7

Definition of Parameters

ELEM - Element number, 1 at crown, 20 at invert

E_o - Exterior element strain - microstrain, + compression

E_i - Interior element strain - microstrain, + compression

E_c - Axial element strain - microstrain, + compression

E_f - Flexural element strain - microstrain, + tension on inside fiber

Thrust - Axial force, K in Kips/in., T_f normalized to Pa.

Moment - Flexural force, K in in.-Kips/in., M_f, fraction of ultimate moment capacity of 8,820 in.-kips/in.

Definition of Parameters

RUN NUMBER: 1

ELEM	Eo	Ei	Ec	Ef	K -THRUST-	Tf	K -MOMENT-	Mf
1	17.3	-3.4	7.0	10.3	0.284	0.710	0.562	0.064
2	15.4	-0.7	7.3	8.0	0.299	0.748	0.438	0.050
3	11.9	4.7	8.3	3.6	0.337	0.843	0.195	0.022
4	9.2	12.1	10.6	-1.4	0.433	1.084	-0.078	-0.009
5	4.0	17.9	11.0	-6.9	0.448	1.119	-0.377	-0.043
6	0.9	19.6	10.2	-9.3	0.417	1.043	-0.508	-0.058
7	3.1	16.9	10.0	-6.9	0.408	1.020	-0.376	-0.043
8	5.9	11.6	8.7	-2.9	0.356	0.891	-0.157	-0.018
9	4.7	7.8	6.2	-1.5	0.254	0.636	-0.083	-0.009
10	5.4	7.7	6.5	-1.1	0.266	0.665	-0.062	-0.007
11	5.2	6.6	5.9	-0.7	0.239	0.599	-0.037	-0.004
12	0.7	0.9	0.8	-0.1	0.033	0.084	-0.006	-0.001
13	2.5	2.9	2.7	-0.2	0.111	0.277	-0.011	-0.001
14	4.6	4.2	4.4	0.2	0.181	0.451	0.010	0.001
15	0.6	0.6	0.6	0.0	0.025	0.062	0.000	0.000
16	3.7	1.5	2.6	1.1	0.105	0.262	0.059	0.007
17	-0.3	-1.7	-1.0	0.7	-0.042	-0.105	0.037	0.004
18	0.4	-1.5	-0.5	1.0	-0.022	-0.055	0.052	0.006
19	-0.6	-2.5	-1.6	0.9	-0.063	-0.159	0.050	0.006
20	2.2	0.2	1.2	1.0	0.049	0.122	0.056	0.006

RUN NUMBER: 5

ELEM	Eo	Ei	Ec	Ef	K -THRUST-	Tf	K -MOMENT-	Mf
1	37.6	-19.2	9.2	28.4	0.374	0.935	1.545	0.175
2	24.1	-3.9	10.1	14.0	0.413	1.032	0.763	0.087
3	7.6	15.4	11.5	-3.9	0.468	1.170	-0.212	-0.024
4	-2.3	29.8	13.7	-16.1	0.560	1.401	-0.874	-0.099
5	-2.8	29.1	13.2	-16.0	0.537	1.343	-0.869	-0.099
6	1.1	18.3	9.7	-8.6	0.396	0.991	-0.469	-0.053
7	6.9	13.5	10.2	-3.3	0.416	1.040	-0.179	-0.020
8	6.8	10.6	8.7	-1.9	0.356	0.889	-0.104	-0.012
9	4.9	7.0	5.9	-1.0	0.243	0.607	-0.057	-0.006
10	5.4	7.2	6.3	-0.9	0.257	0.642	-0.050	-0.006
11	5.0	5.9	5.4	-0.4	0.222	0.555	-0.024	-0.003
12	0.5	0.6	0.6	-0.0	0.023	0.057	-0.002	-0.000
13	2.6	2.7	2.7	-0.0	0.108	0.271	-0.002	-0.000
14	4.5	3.7	4.1	0.4	0.167	0.419	0.023	0.003
15	1.3	-0.4	0.4	0.8	0.018	0.045	0.045	0.005
16	2.4	1.7	2.1	0.4	0.084	0.210	0.019	0.002
17	-0.6	-2.0	-1.3	0.7	-0.054	-0.136	0.038	0.004
18	0.0	-1.5	-0.7	0.8	-0.030	-0.074	0.042	0.005
19	-0.6	-2.9	-1.6	1.1	-0.072	-0.181	0.062	0.007
20	1.3	-0.3	0.7	1.0	0.030	0.075	0.055	0.006

TABLE E.7 (CONTINUED)

Definition of Parameters

RUN NUMBER: 9

ELEM	Eo	Ei	Ec	Ef	K -THRUST-	Tf	K -MOMENT-	Mf
1	100.5	-56.4	22.1	78.5	0.636	1.590	3.013	0.342
2	68.4	-20.5	23.9	44.5	0.690	1.724	1.709	0.194
3	25.0	28.5	26.7	-1.7	0.770	1.925	-0.067	-0.008
4	-10.5	69.9	29.7	-40.2	0.855	2.138	-1.545	-0.175
5	-18.3	80.4	31.1	-49.3	0.895	2.237	-1.894	-0.215
6	-5.3	59.8	27.2	-32.5	0.785	1.961	-1.249	-0.142
7	9.9	40.1	25.0	-15.1	0.719	1.797	-0.580	-0.066
8	14.0	28.6	21.3	-7.3	0.614	1.535	-0.279	-0.032
9	12.6	20.1	16.4	-3.7	0.471	1.178	-0.144	-0.016
10	12.2	16.4	14.3	-2.1	0.412	1.029	-0.079	-0.009
11	10.5	12.6	11.6	-1.0	0.333	0.833	-0.040	-0.005
12	4.6	4.9	4.8	-0.1	0.137	0.342	-0.006	-0.001
13	5.3	4.0	4.6	0.6	0.134	0.335	0.024	0.003
14	6.2	3.9	5.1	1.2	0.146	0.365	0.045	0.005
15	2.0	-1.9	0.1	2.0	0.002	0.004	0.076	0.009
16	2.7	-2.3	0.2	2.5	0.006	0.016	0.095	0.011
17	-1.5	-6.9	-4.2	2.7	-0.121	-0.301	0.104	0.012
18	-0.6	-7.8	-4.2	3.6	-0.121	-0.302	0.137	0.016
19	-2.7	-9.2	-6.0	3.2	-0.172	-0.429	0.124	0.014
20	0.0	-7.0	-3.5	3.5	-0.100	-0.251	0.135	0.015

RUN NUMBER: 10

ELEM	Eo	Ei	Ec	Ef	K -THRUST-	Tf	K -MOMENT-	Mf
1	99.8	-52.7	23.5	76.3	0.678	1.694	2.928	0.332
2	60.4	-17.5	21.5	39.0	0.619	1.547	1.496	0.170
3	23.4	30.5	26.9	-3.5	0.775	1.938	-0.136	-0.015
4	-9.9	70.4	30.2	-40.1	0.871	2.178	-1.540	-0.175
5	-15.6	78.3	31.4	-46.9	0.903	2.257	-1.802	-0.204
6	-3.7	56.5	26.4	-30.1	0.760	1.901	-1.155	-0.131
7	9.2	38.1	23.6	-14.4	0.680	1.701	-0.555	-0.063
8	13.8	25.0	19.4	-5.6	0.557	1.394	-0.215	-0.024
9	11.7	17.0	14.3	-2.7	0.413	1.033	-0.103	-0.012
10	11.5	13.8	12.6	-1.2	0.364	0.911	-0.045	-0.005
11	9.9	10.6	10.2	-0.4	0.295	0.737	-0.015	-0.002
12	4.1	3.5	3.8	0.3	0.110	0.274	0.013	0.001
13	4.7	3.0	3.9	0.8	0.111	0.278	0.032	0.004
14	6.6	2.9	4.3	1.8	0.137	0.343	0.071	0.008
15	1.7	-1.7	-0.0	1.7	-0.001	-0.002	0.065	0.007
16	2.4	-1.6	0.4	2.0	0.012	0.030	0.077	0.009
17	-0.8	-5.8	-3.3	2.5	-0.095	-0.238	0.095	0.011
18	-0.8	-5.7	-3.2	2.4	-0.094	-0.234	0.093	0.011
19	-1.8	-7.4	-4.6	2.3	-0.133	-0.332	0.109	0.012
20	0.6	-5.0	-2.2	2.8	-0.063	-0.159	0.108	0.012

TABLE E.7 (CONTINUED)

RUN NUMBER: 11 Definition of Parameters

ELEM	Eo	Ei	Ec	Ef	K -THRUST- Tf		K -MOMENT- Mf	
1	100.1	-56.1	22.0	78.1	0.632	1.581	2.999	0.340
2	63.4	-20.5	23.9	44.5	0.690	1.724	1.709	0.194
3	24.5	29.0	26.8	-2.3	0.771	1.928	-0.087	-0.010
4	-10.0	69.7	29.9	-39.8	0.860	2.150	-1.529	-0.173
5	-18.2	80.2	31.0	-49.2	0.893	2.232	-1.888	-0.214
6	-4.8	58.8	27.0	-31.8	0.777	1.943	-1.221	-0.138
7	10.1	40.8	25.5	-15.3	0.734	1.835	-0.589	-0.067
8	14.2	28.4	21.3	-7.1	0.614	1.534	-0.271	-0.031
9	12.9	20.5	16.7	-3.8	0.482	1.204	-0.147	-0.017
10	12.5	17.2	14.9	-2.4	0.429	1.071	-0.091	-0.010
11	10.9	13.3	12.1	-1.2	0.348	0.870	-0.046	-0.005
12	5.0	5.3	5.2	-0.2	0.149	0.372	-0.007	-0.001
13	5.7	4.8	5.2	0.4	0.150	0.376	0.017	0.002
14	7.0	3.8	5.4	1.6	0.155	0.389	0.061	0.007
15	1.6	-1.9	-0.2	1.7	-0.005	-0.013	0.067	0.008
16	2.6	-1.6	0.5	2.1	0.015	0.036	0.081	0.009
17	-1.0	-6.9	-3.9	2.9	-0.114	-0.284	0.113	0.013
18	-0.7	-7.6	-4.1	3.4	-0.119	-0.298	0.131	0.015
19	-2.2	-9.2	-5.7	3.5	-0.165	-0.412	0.134	0.015
20	0.2	-7.0	-3.4	3.6	-0.097	-0.244	0.139	0.016

RUN NUMBER: 13

ELEM	Eo	Ei	Ec	Ef	K -THRUST- Tf		K -MOMENT- Mf	
1	98.6	-71.2	13.7	84.9	0.504	1.260	4.168	0.473
2	70.9	-40.4	15.3	55.7	0.562	1.404	2.731	0.310
3	30.1	5.6	17.9	12.3	0.657	1.642	0.603	0.068
4	-7.3	48.9	20.8	-28.1	0.765	1.912	-1.379	-0.156
5	-28.1	72.0	22.0	-50.0	0.809	2.021	-2.455	-0.273
6	-27.7	68.0	20.2	-47.9	0.743	1.856	-2.348	-0.266
7	-13.4	53.7	20.2	-33.6	0.742	1.855	-1.646	-0.187
8	-2.2	36.3	17.1	-19.2	0.628	1.571	-0.944	-0.107
9	3.0	23.3	13.1	-10.2	0.484	1.210	-0.498	-0.056
10	6.5	17.4	11.9	-5.4	0.439	1.098	-0.266	-0.030
11	7.7	12.4	10.0	-2.4	0.369	0.923	-0.116	-0.013
12	3.5	3.6	3.5	-0.1	0.130	0.324	-0.003	-0.000
13	5.4	3.4	4.4	1.0	0.161	0.402	0.049	0.006
14	7.6	2.1	4.9	2.7	0.179	0.447	0.133	0.015
15	3.9	-3.4	0.3	3.7	0.011	0.027	0.179	0.020
16	5.8	-3.5	1.1	4.6	0.042	0.105	0.226	0.026
17	1.5	-8.4	-3.5	5.0	-0.128	-0.320	0.243	0.028
18	3.2	-9.2	-3.0	6.2	-0.111	-0.277	0.304	0.034
19	1.7	-10.9	-4.6	6.3	-0.169	-0.423	0.307	0.035
20	4.3	-8.7	-2.2	6.5	-0.080	-0.199	0.318	0.036

Definition of Parameters

RUN NUMBER: 14

ELEM	Eo	Ei	Ec	Ef	K -THRUST-	Tf	K -MOMENT-	Mf
1	121.0	-101.2	9.9	111.1	0.364	0.911	5.452	0.618
2	90.3	-66.3	12.0	78.3	0.443	1.107	3.843	0.436
3	42.2	-13.3	14.5	27.8	0.533	1.332	1.362	0.154
4	-6.7	42.6	17.9	-24.7	0.660	1.650	-1.210	-0.137
5	-44.0	84.1	20.1	-64.1	0.739	1.847	-3.143	-0.356
6	-52.7	92.3	19.8	-72.5	0.728	1.819	-3.558	-0.403
7	-46.1	81.9	17.9	-64.0	0.660	1.649	-3.140	-0.356
8	-22.7	54.3	15.8	-38.5	0.580	1.451	-1.889	-0.214
9	-5.5	29.7	12.1	-17.6	0.445	1.114	-0.863	-0.098
10	7.7	17.4	12.5	-4.8	0.460	1.151	-0.238	-0.027
11	13.6	10.5	12.0	1.5	0.443	1.108	0.075	0.008
12	11.2	3.1	7.2	4.0	0.264	0.659	0.197	0.022
13	14.0	4.4	9.2	4.8	0.338	0.846	0.238	0.027
14	15.9	5.7	10.8	5.1	0.398	0.995	0.252	0.029
15	13.5	2.1	7.8	5.7	0.287	0.718	0.278	0.032
16	15.8	2.6	9.2	6.6	0.338	0.844	0.323	0.037
17	12.4	-1.6	5.4	7.0	0.199	0.498	0.344	0.039
18	14.4	-0.8	6.8	7.6	0.250	0.625	0.374	0.042
19	13.6	-2.7	5.4	8.1	0.200	0.500	0.399	0.045
20	16.3	-0.5	7.9	8.4	0.291	0.728	0.413	0.047

RUN NUMBER: 15

ELEM	Eo	Ei	Ec	Ef	K -THRUST-	Tf	K -MOMENT-	Mf
1	136.6	-122.3	7.1	129.4	0.263	0.657	6.350	0.720
2	103.0	-84.1	9.4	93.6	0.347	0.869	4.592	0.521
3	50.0	-25.2	12.4	37.6	0.456	1.140	1.843	0.209
4	-7.1	39.7	16.3	-23.4	0.600	1.500	-1.149	-0.130
5	-57.1	93.9	18.4	-75.5	0.677	1.693	-3.706	-0.420
6	-69.8	110.0	20.1	-89.9	0.740	1.850	-4.411	-0.500
7	-63.3	99.7	18.2	-81.5	0.669	1.672	-3.998	-0.453
8	-34.5	65.5	15.5	-50.0	0.570	1.424	-2.455	-0.278
9	-9.0	34.8	12.9	-21.9	0.474	1.185	-1.074	-0.122
10	9.2	18.2	13.7	-4.5	0.505	1.261	-0.222	-0.025
11	17.9	10.5	14.2	3.7	0.524	1.310	0.182	0.021
12	16.9	3.6	10.2	6.7	0.377	0.942	0.327	0.037
13	20.2	5.6	12.9	7.3	0.475	1.187	0.360	0.041
14	22.0	8.5	15.2	6.7	0.561	1.402	0.329	0.037
15	19.7	5.3	12.5	7.2	0.460	1.150	0.351	0.040
16	22.2	6.8	14.5	7.7	0.534	1.335	0.379	0.043
17	19.5	3.5	11.5	8.0	0.422	1.055	0.393	0.045
18	21.5	4.0	12.7	8.7	0.469	1.173	0.428	0.049
19	20.9	2.6	11.7	9.2	0.432	1.081	0.449	0.051
20	23.8	5.0	14.4	9.4	0.529	1.324	0.460	0.052

TABLE E.7 (CONTINUED)

RUN NUMBER: 17

Definition of Parameters

ELEM	Eo	Ei	Ec	Ef	K -THRUST-	Tf	K -MOMENT-	Mf
1	80.5	-69.3	5.6	74.9	0.208	0.519	3.675	0.417
2	57.6	-43.1	7.2	50.4	0.266	0.664	2.471	0.280
3	24.1	-5.2	9.5	14.7	0.348	0.870	0.721	0.082
4	-7.9	32.6	12.3	-20.2	0.454	1.136	-0.992	-0.112
5	-28.9	55.7	13.4	-42.3	0.493	1.232	-2.076	-0.235
6	-34.3	58.0	11.9	-46.1	0.437	1.093	-2.264	-0.257
7	-24.4	48.9	12.2	-36.7	0.449	1.123	-1.799	-0.204
8	-10.9	32.2	10.7	-21.6	0.392	0.980	-1.059	-0.120
9	-2.7	18.2	7.8	-10.5	0.285	0.714	-0.514	-0.058
10	5.0	12.8	8.9	-3.9	0.328	0.820	-0.192	-0.022
11	8.2	9.1	8.7	-0.4	0.319	0.797	-0.021	-0.002
12	5.5	3.1	4.3	1.2	0.158	0.396	0.057	0.006
13	8.1	4.2	6.2	1.9	0.228	0.569	0.096	0.011
14	11.3	5.6	8.4	2.9	0.310	0.775	0.140	0.016
15	8.3	2.4	5.3	3.0	0.197	0.492	0.146	0.017
16	11.1	2.8	6.9	4.1	0.256	0.639	0.203	0.023
17	8.7	-1.2	3.8	4.9	0.139	0.347	0.242	0.027
18	9.5	-0.8	4.3	5.1	0.159	0.398	0.253	0.029
19	9.3	-2.2	3.6	5.7	0.131	0.328	0.280	0.032
20	12.3	0.3	6.3	6.0	0.232	0.580	0.296	0.034

RUN NUMBER: 18

ELEM	Eo	Ei	Ec	Ef	K -THRUST-	Tf	K -MOMENT-	Mf
1	129.5	-111.1	9.2	120.3	0.338	0.845	5.904	0.669
2	98.3	-76.1	11.1	87.2	0.408	1.020	4.277	0.485
3	50.2	-22.2	14.0	36.2	0.516	1.290	1.777	0.202
4	0.6	34.1	17.4	-16.7	0.639	1.597	-0.822	-0.093
5	-36.9	76.1	19.6	-56.5	0.721	1.801	-2.773	-0.314
6	-56.7	93.2	18.2	-75.0	0.670	1.675	-3.678	-0.417
7	-54.8	92.4	18.8	-73.6	0.691	1.728	-3.612	-0.410
8	-40.4	73.9	16.8	-57.1	0.617	1.542	-2.803	-0.318
9	-24.6	50.4	12.9	-37.5	0.474	1.186	-1.841	-0.209
10	-6.4	31.6	12.6	-19.0	0.462	1.156	-0.932	-0.106
11	6.4	16.5	11.4	-5.0	0.421	1.053	-0.247	-0.028
12	11.0	2.1	6.6	4.4	0.242	0.605	0.217	0.025
13	17.1	-2.0	7.5	9.6	0.277	0.692	0.469	0.053
14	22.1	-1.4	10.4	11.8	0.382	0.955	0.577	0.065
15	18.6	-5.6	6.5	12.1	0.240	0.600	0.593	0.067
16	19.9	-2.8	8.6	11.4	0.315	0.788	0.558	0.063
17	15.3	-5.5	4.9	10.4	0.181	0.452	0.509	0.058
18	15.8	-3.0	6.4	9.4	0.234	0.585	0.461	0.052
19	14.4	-3.9	5.3	9.2	0.193	0.483	0.450	0.051
20	16.8	-0.7	8.0	8.3	0.296	0.740	0.430	0.049

FIGURE E.2

Geometry and Loadings

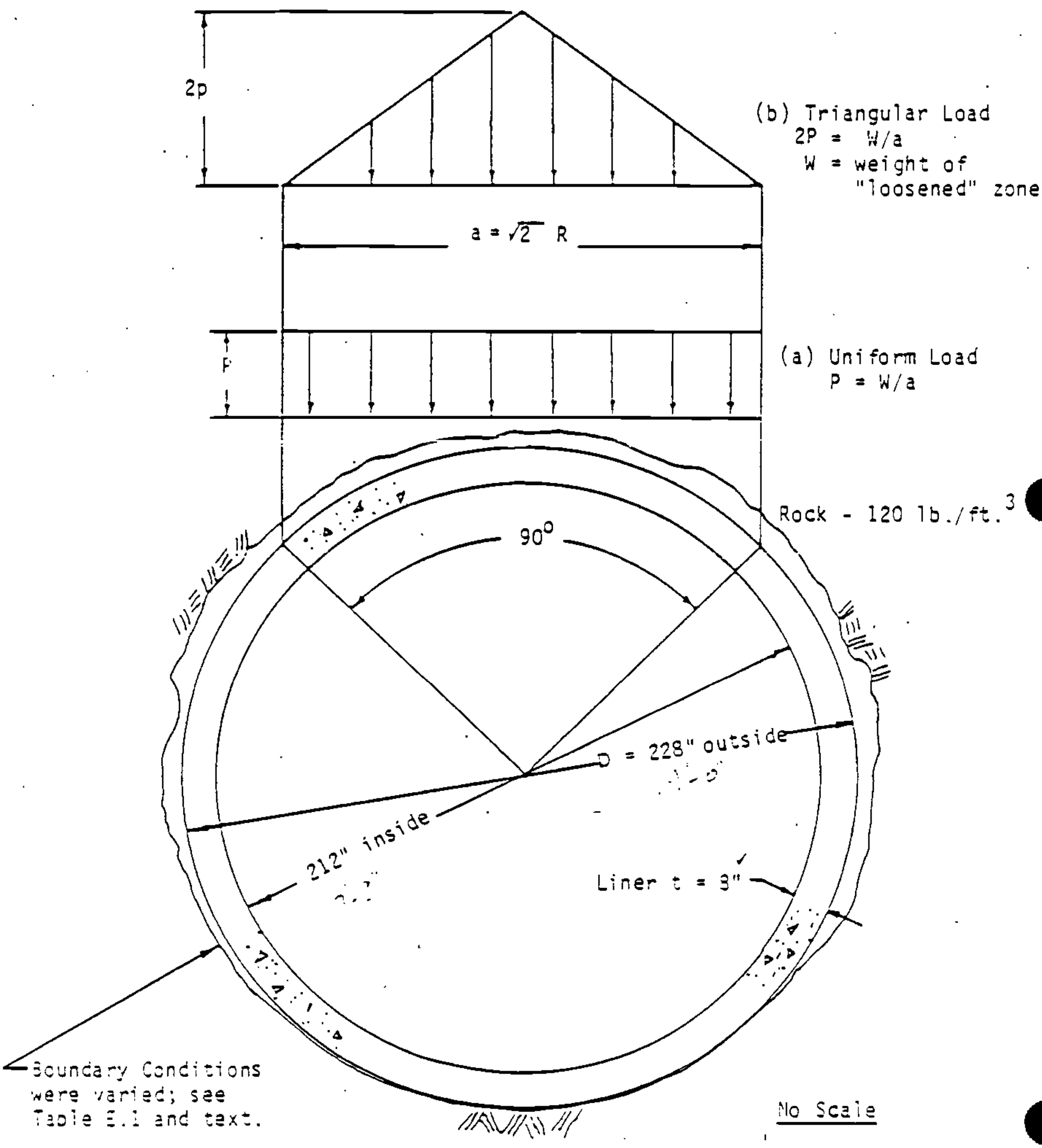

FIGURE E.3

Net Area Used To Compute Weight of the "Loosened" Zone

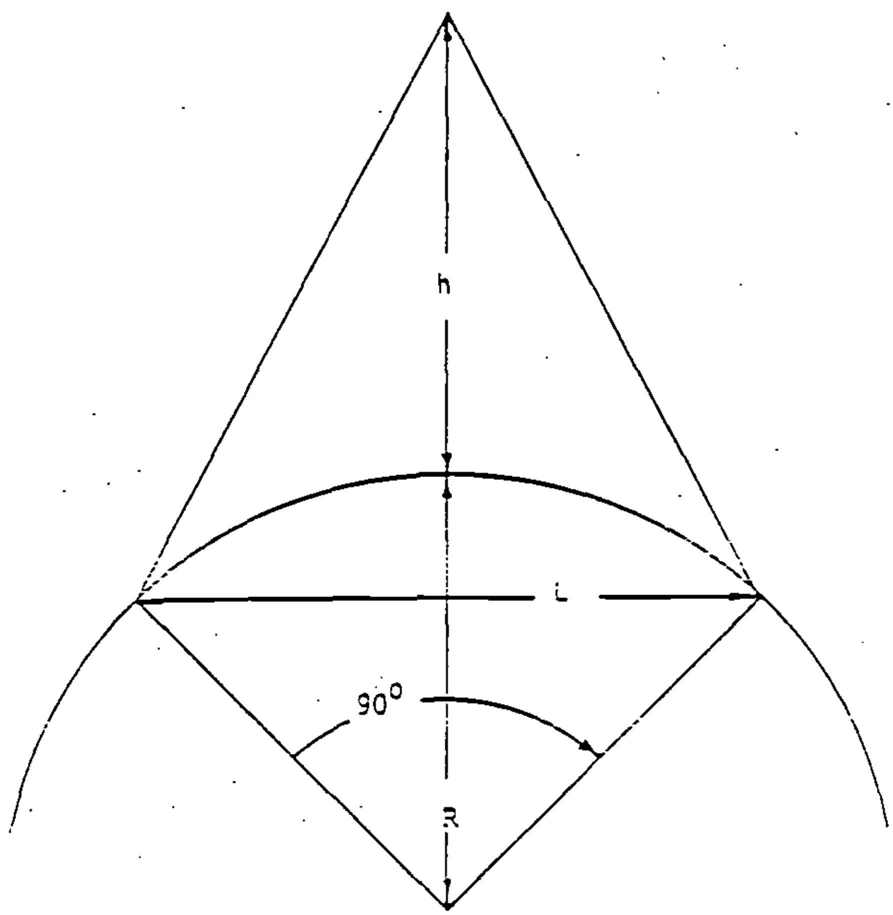

$$\text{Gross Area} = 1/2L\ (h + R)$$

$$\text{Sector Area} = \frac{90}{360}\pi R^2 = \frac{\pi R^2}{4}$$

$$L = R\sqrt{2}$$

$$\text{Net Area} = \frac{R\sqrt{2}}{2}(h + R) - \frac{\pi R^2}{4}$$

$$\text{for } h = R,\ \text{Net Area} = \left(\sqrt{2} - \frac{\pi}{4}\right) R^2$$

FIGURE E.4

Grid for 65-ft. Depth of Burial

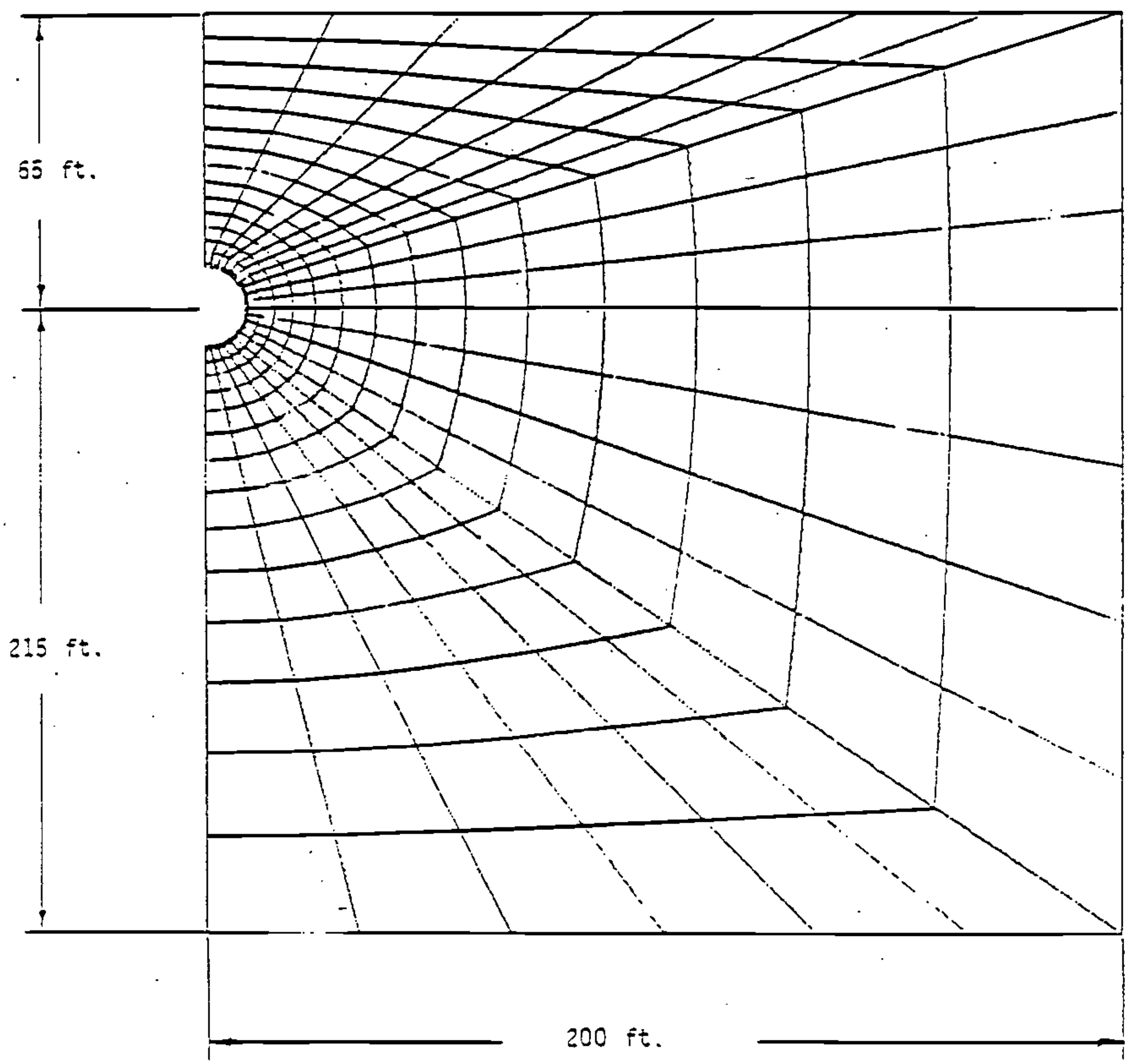

FIGURE E.5

Material Zones

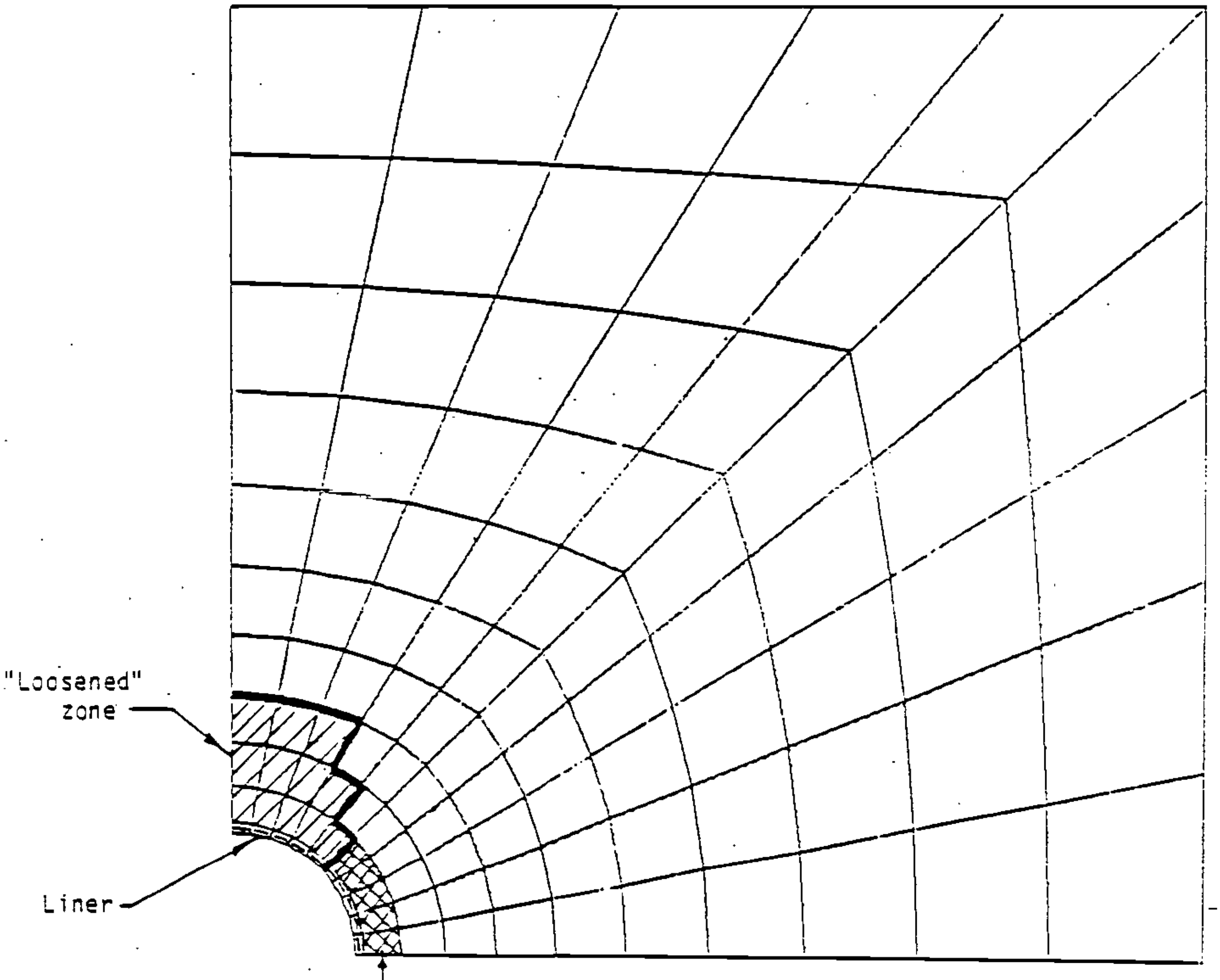

FIGURE E.6

Strain Determination

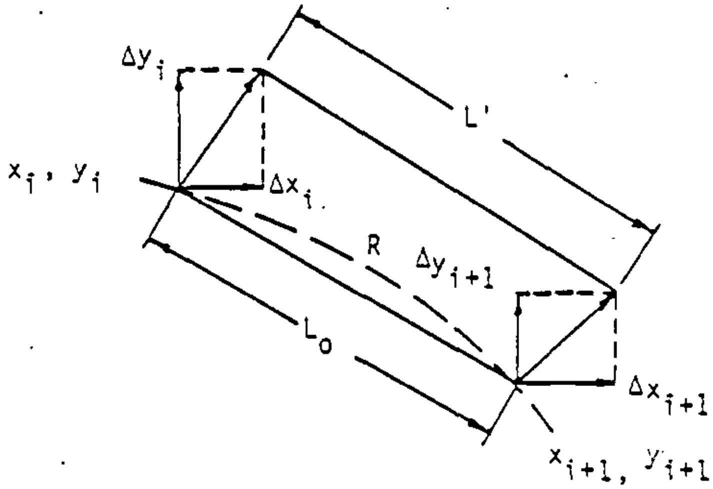

$$L_o = \sqrt{(x_{i+1} - x_i)^2 + (y_{i+1} - y_i)^2}$$

$$L' = \sqrt{(x_{i+1} + \Delta x_{i+1} - x_i - \Delta x_i) + (y_{i+1} + \Delta y_{i+1} - y_i - \Delta y_i)}$$

$\varepsilon_\theta = \dfrac{L' - L^o}{R\theta}$ where θ is the central angle in radians between X_i, y_i and x_{i+1}, y_{i+1}.

FIGURE E.7a

F'_t Versus Flexibility Ratio for $\alpha = 90°$ ($j = 1 - 5$)
(From Ranken et al 1978)

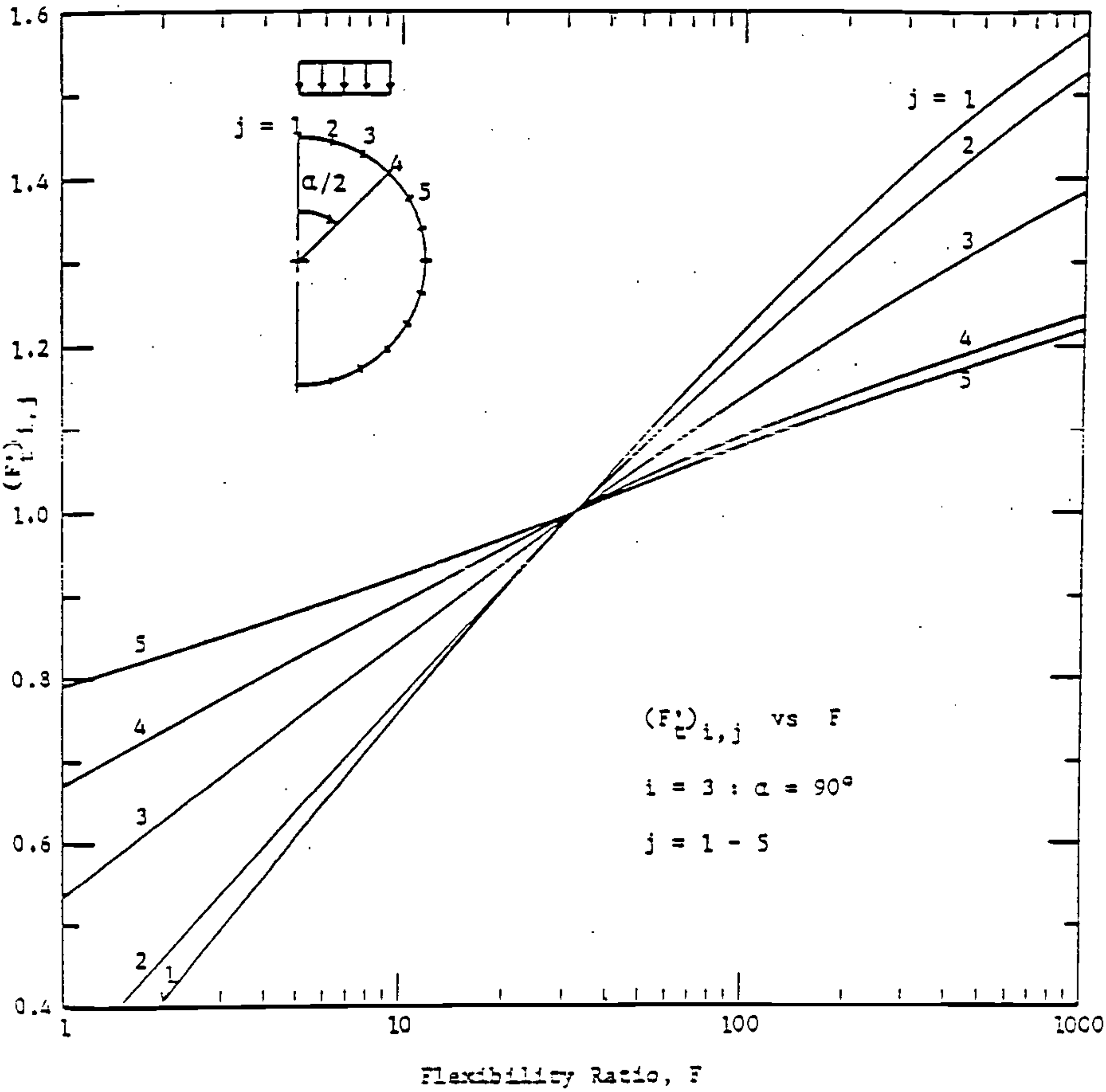

FIGURE E.7b

F'_t Versus Flexibility Ratio for α = 90° (j = 6 - 13)
(From Ranken et al 1978)

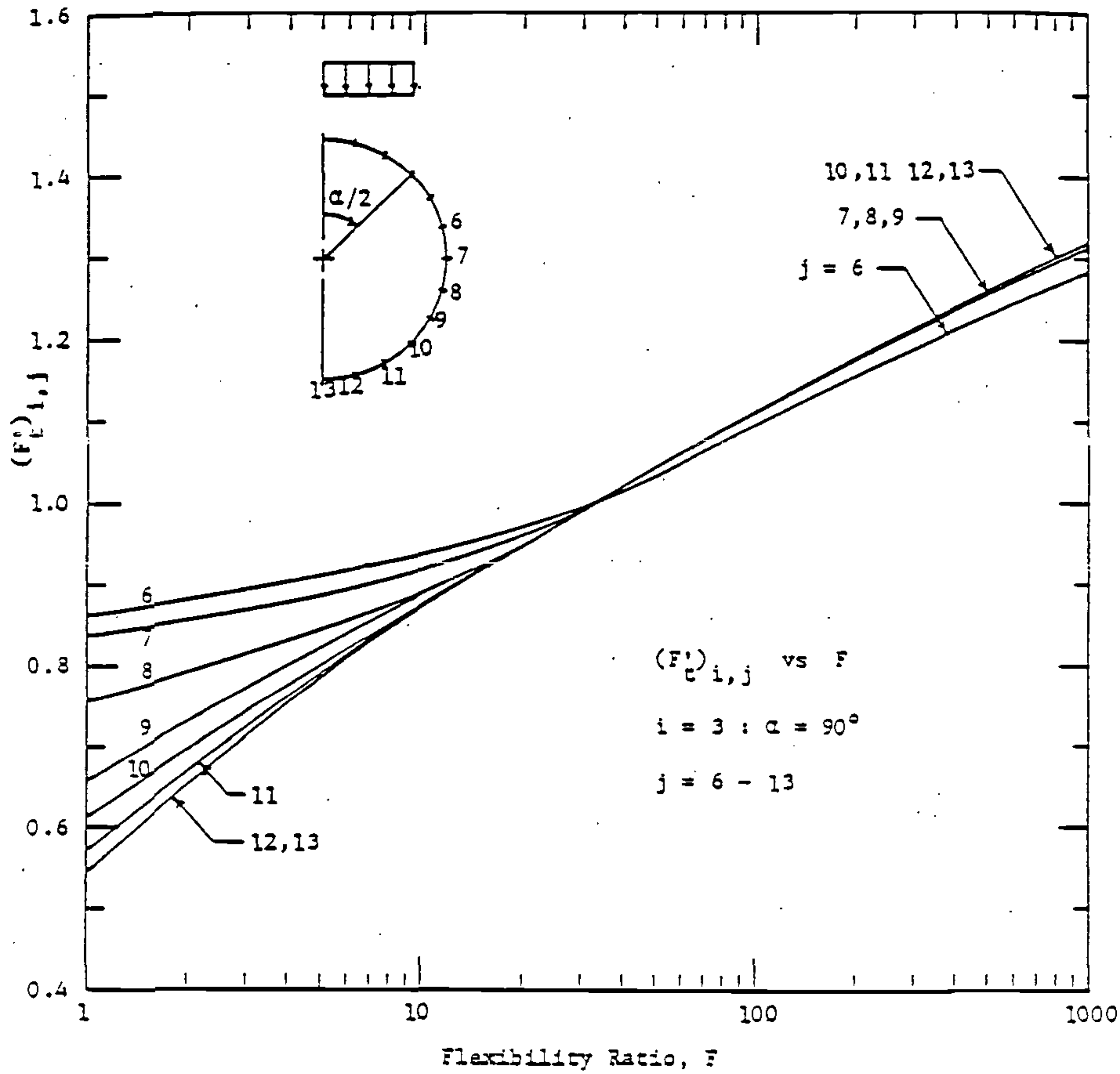

FIGURE E.8b

M_f Versus Flexibility Ratio for $\alpha = 90°$ (j = 4 - 9)
(From Ranken et al 1978)

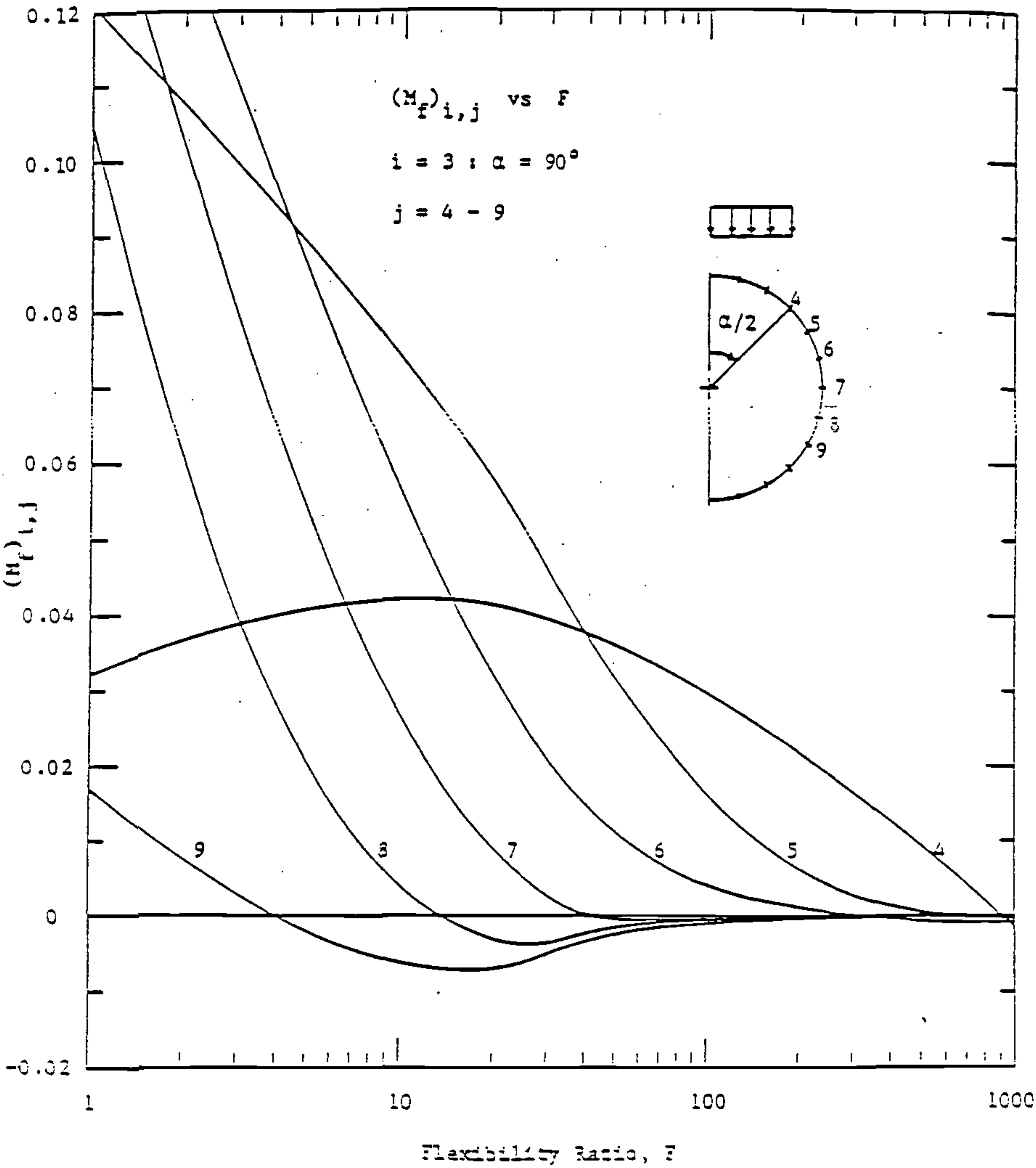

FIGURE E.9a

M_{cf} Versus Flexibility Ratio for α = 90° (j = 1 - 6)
(From Ranken et al. 1978)

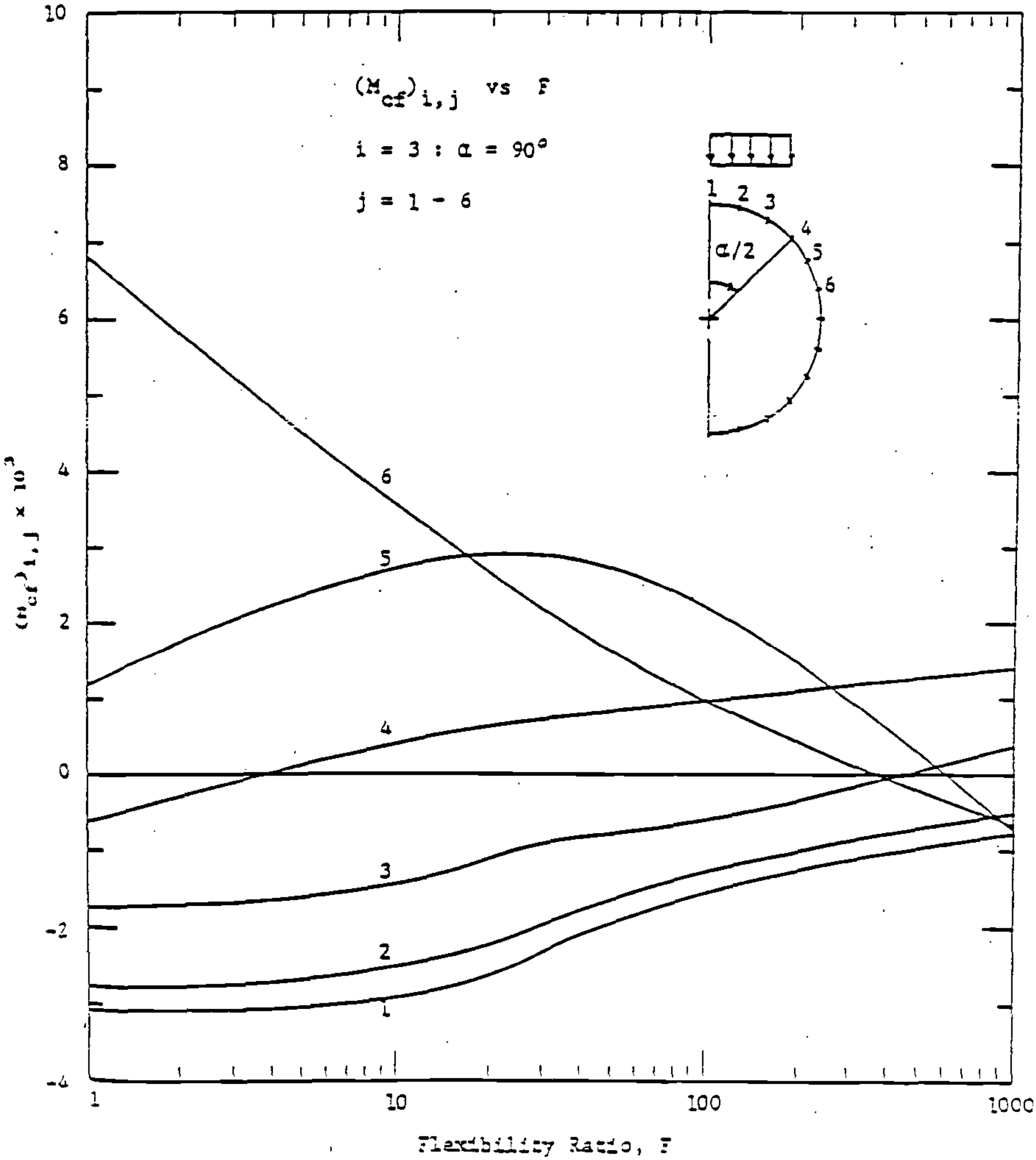

FIGURE E.9b

M_{cf} Versus Flexibility Ratio for α = 90° (j = 7 - 13)
(From Ranken et al 1978)

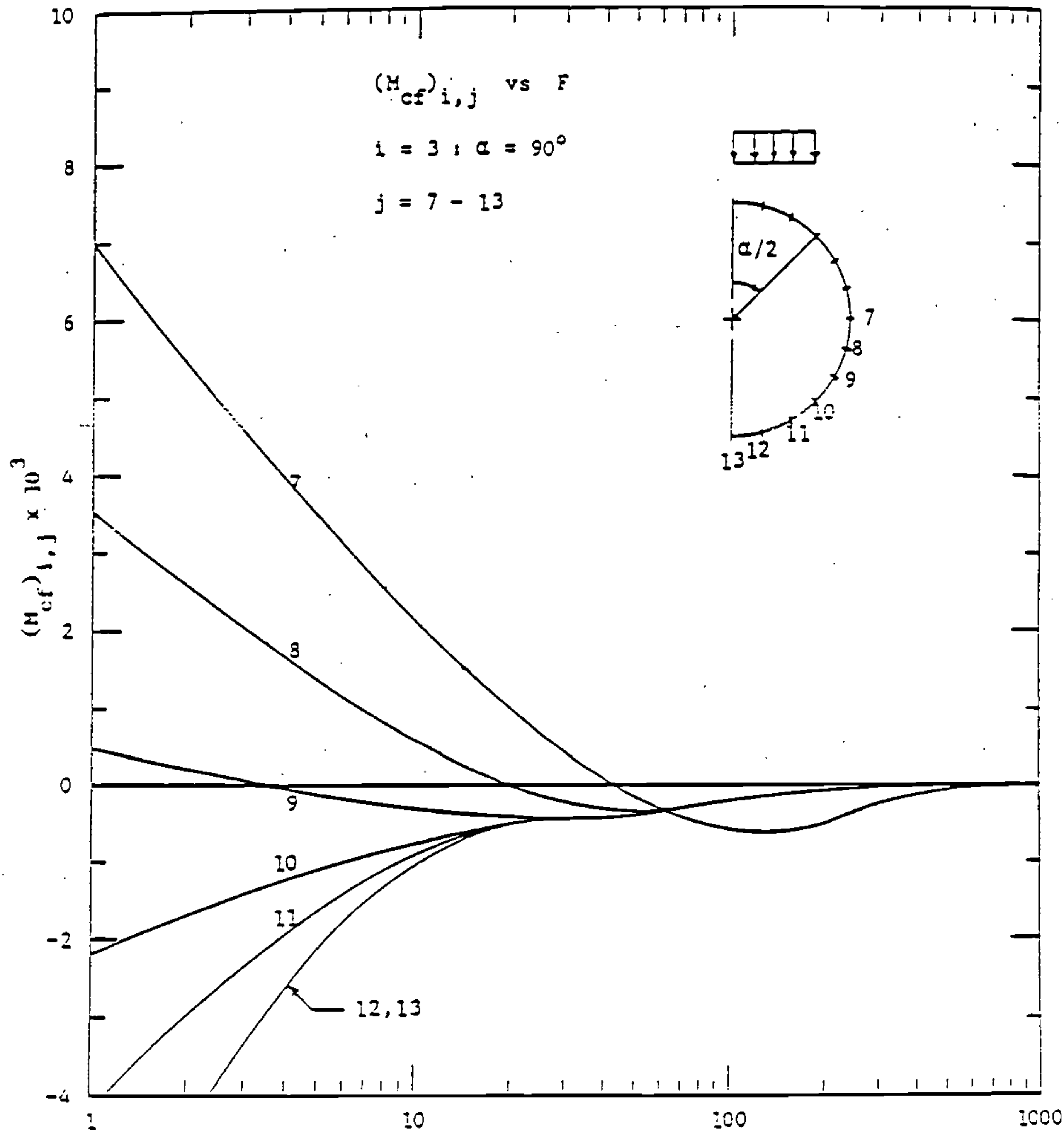

FIGURE E.10

Normalized Thrust and Moments from Run 1 (Uniform Load)

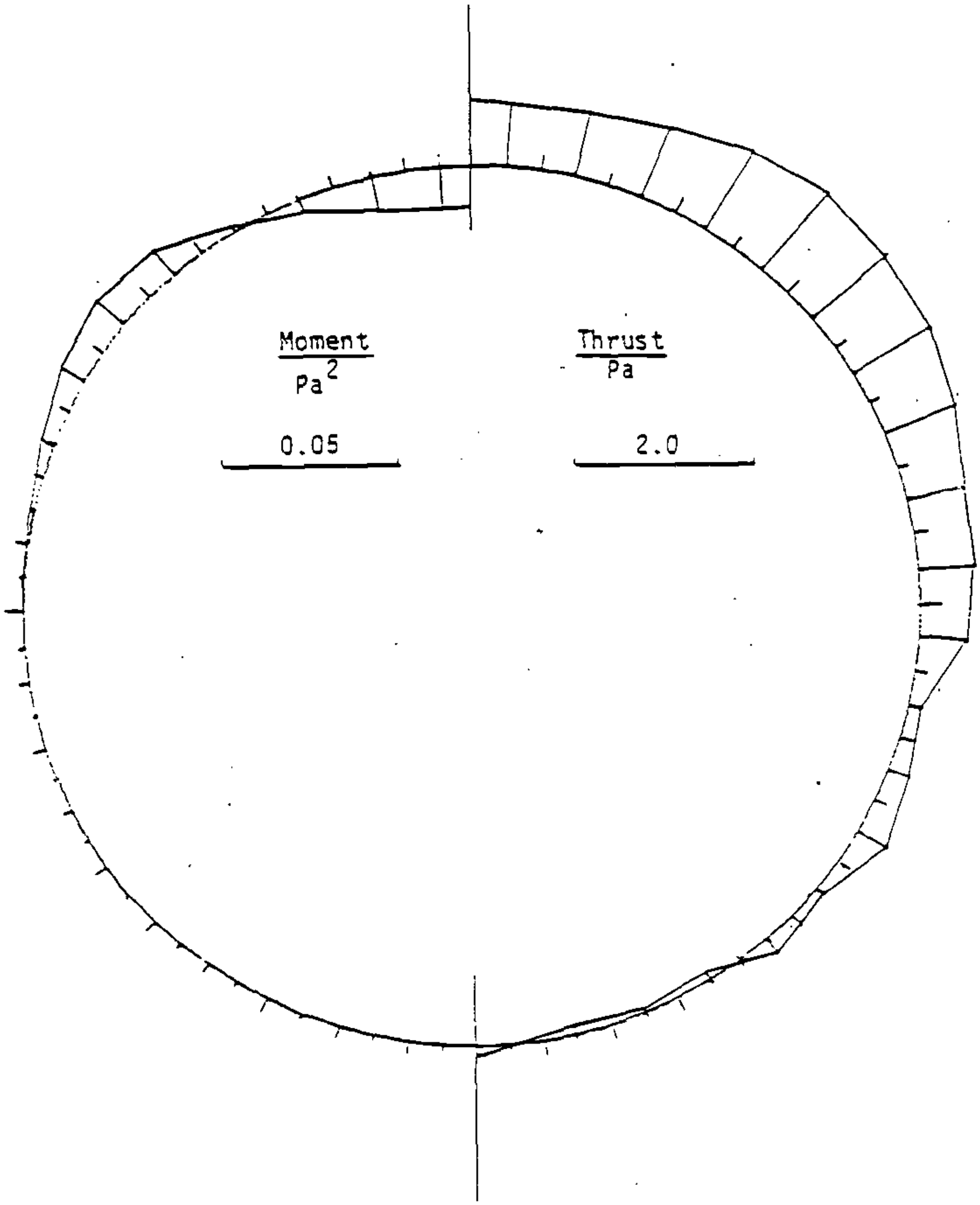

FIGURE E.11

Normalized Thrust and Moment from Run 5 (Triangular Load)

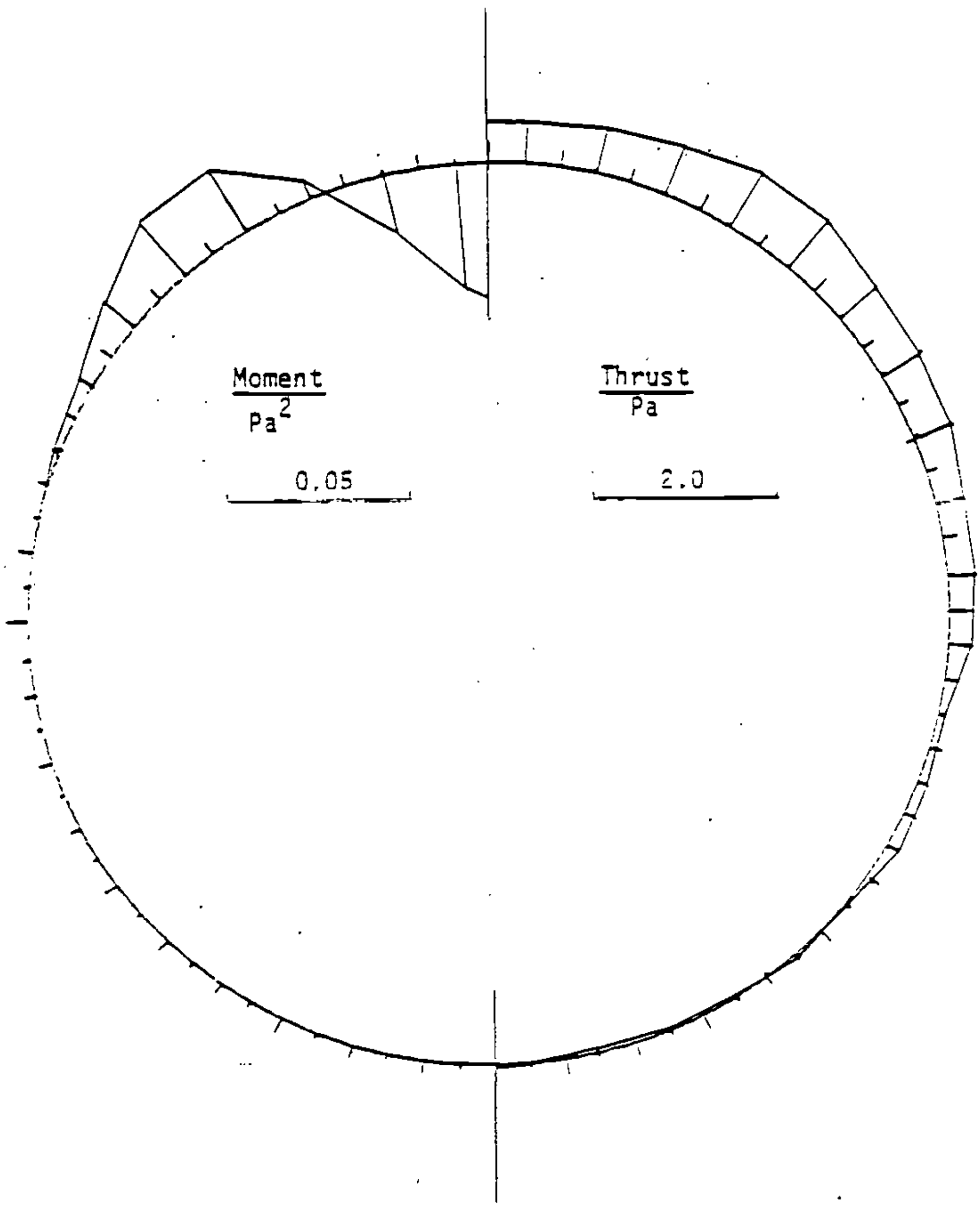

FIGURE E.12

Normalized Thrust amd Moment from Run 9(V_p = 2,400 ft./sec.)

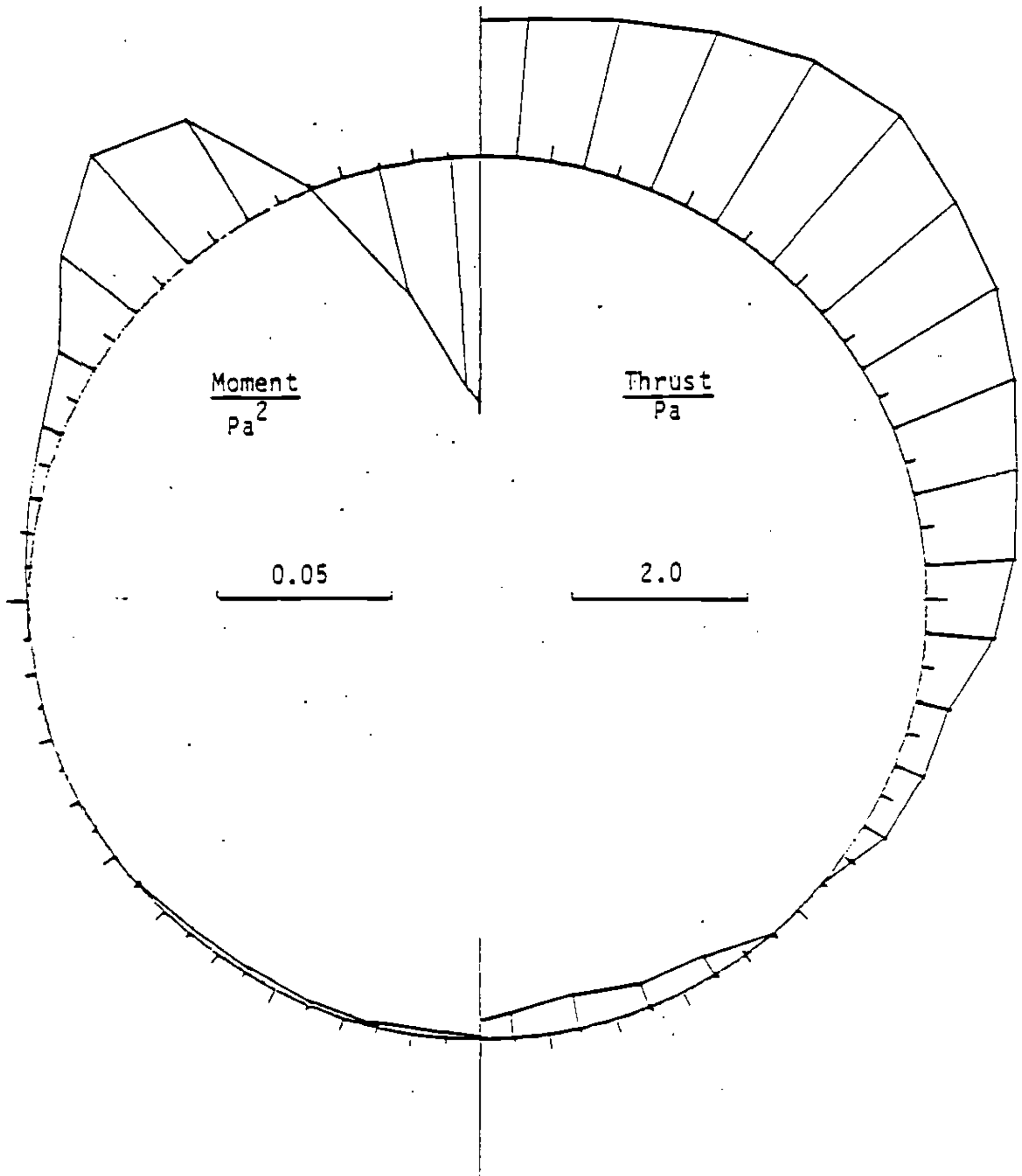

FIGURE E.13

Normalized Thrust and Moment from Run 10 (V_p = 5,000 ft./sec.)

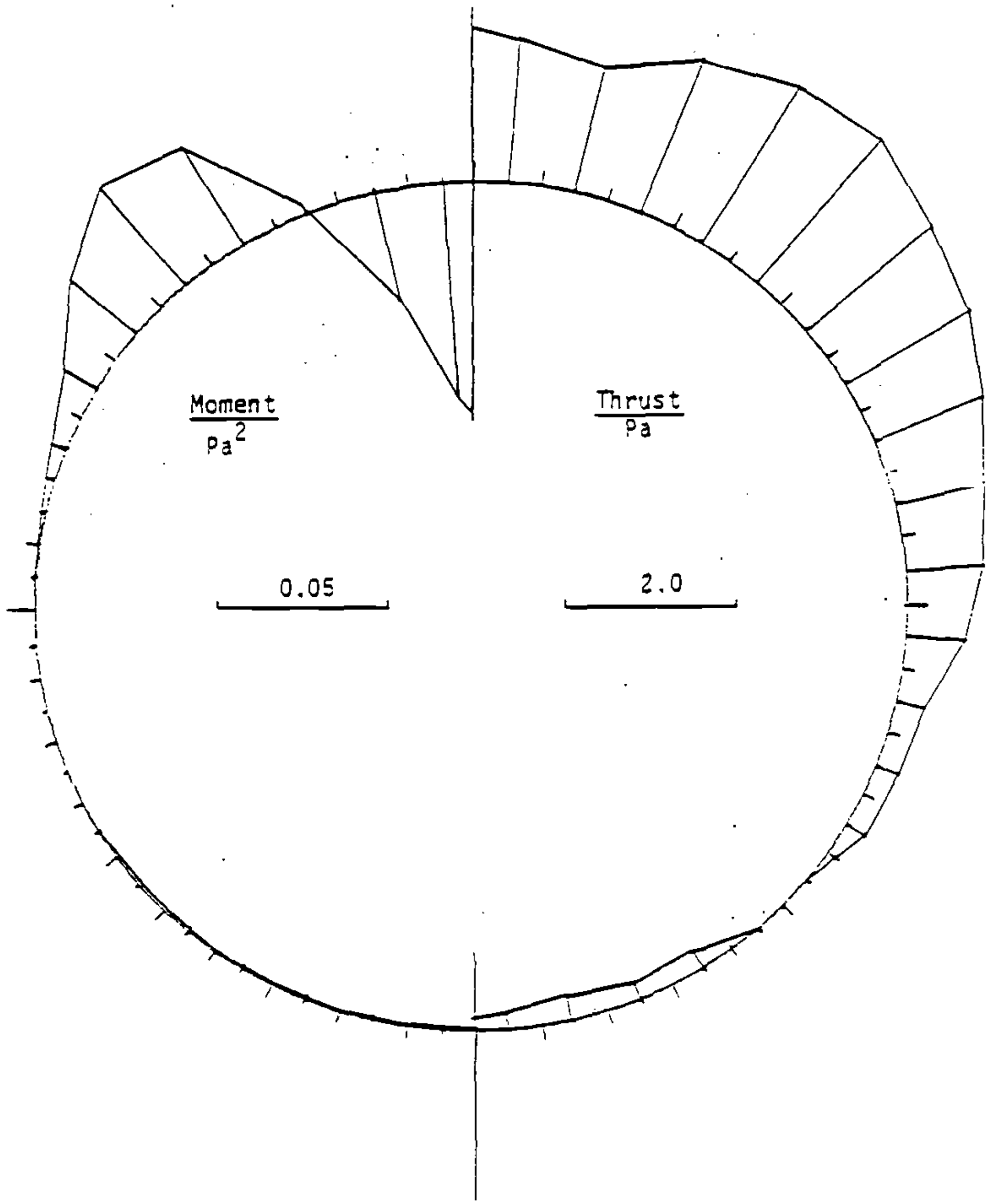

FIGURE E.14

Approximate Maximum Moment due to "Loosening Load" as a Function of Assumed Stiffness of Loosened Zone

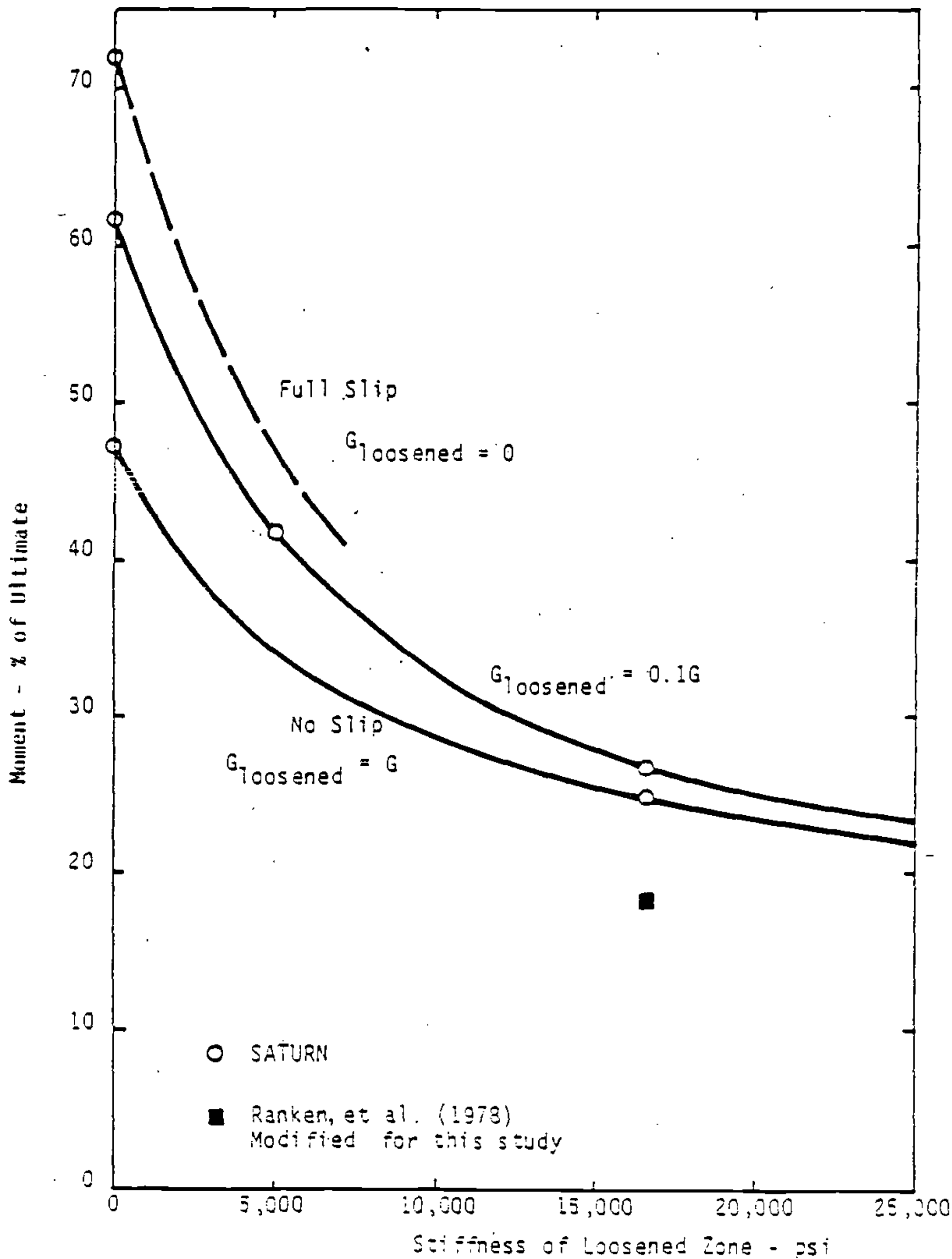

FIGURE E.15

Variation of Approximate Diameter Change with Flexibility Ratio for Loosening Load

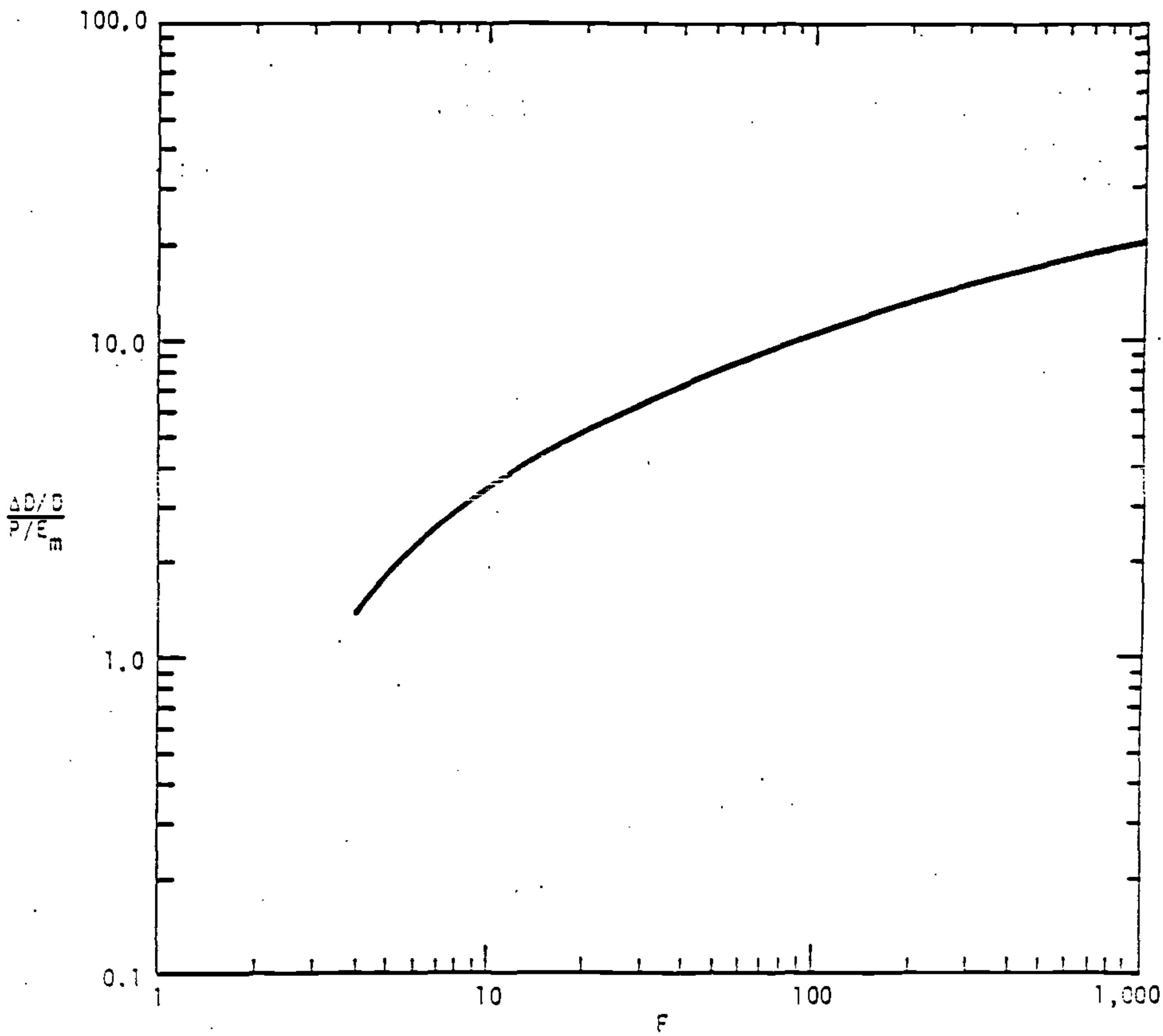

F = Flexibility Ratio (See Peck et al (1972))

P = Intensity of Loosening Load, Assumed to be a Triangular Distribution over a Central Angle of 90°. (for γ = 120 pcf and R = 9.5 ft., P = 3.5 psi)

E_m = Modulus of Elasticity of Medium

ΔD = Diameter Change of Cylinder

D = Diameter of Cylinder

FIGURE E.16

Variation of Vertical and Horizontal Diameter Changes with Flexibility and Compressibility Ratios (α =180°)

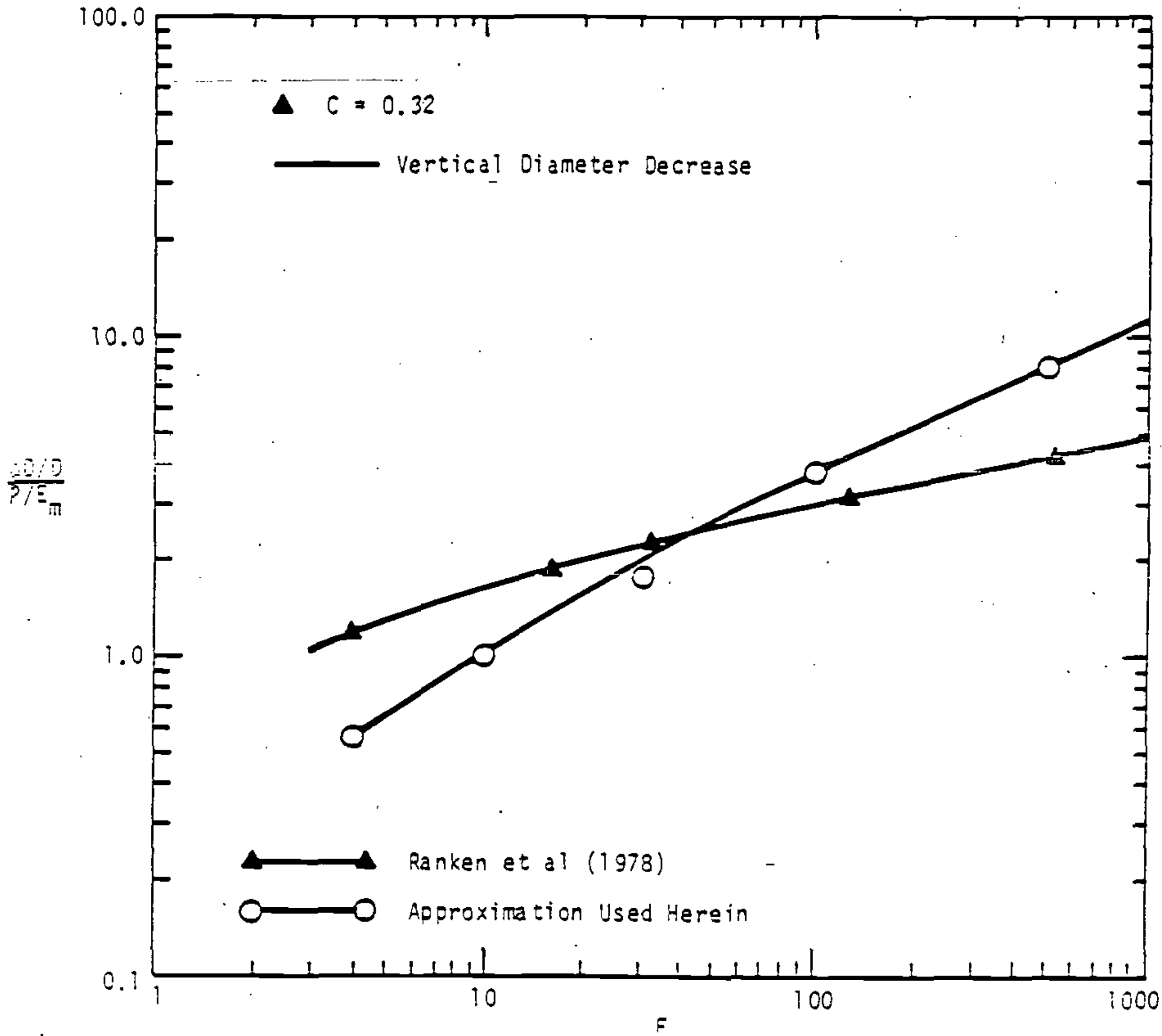

REFERENCES:

E.1 O,Rourke, T.D. editor (1984), "Guidelines for Tunnel Lining Design," Underground Technology Research Council, American Society of Civil Engineers, N.Y.

E.2 Peck, R.B., Hendron, A.J. and Mohraz, B. (1972), "State of the Art Soft Ground Tunneling," Proceedings, First North American Rapid Excavation and Tunneling Conference, Chicago, Vol. 1, pp. 259-286.

E.3 Ranken, R.E., Ghabousii, J. and Hendron, A.J. (1978), "Analysis of Ground-Liner Interaction for Tunnels," U.S. Department of Transportation Report No. UMTA-IL-06-0043-78-3, University of Illinois at Urbana-Champaign, Oct.

E.4 Sweet, J. (1979), "SATURN - A Multi-Dimensional Two-Phase Computer Program which Treats the Nonlinear Behavior of Continua Using the Finite Element Approach," Report No. JSA-79-016, Joel Sweet and Associates, September.

ANNEX F

PREDICTION OF STRAINS IN SELECTED SOIL COLUMNS RESULTING FROM EARTHQUAKE EXCITATION - TIME HISTORY ANALYSIS

ANNEX F

PREDICTION OF STRAINS IN SELECTED SOIL COLUMNS RESULTING FROM EARTHQUAKE EXCITATION - TIME HISTORY ANALYSIS

Introduction

The prediction of the stain in tunnel walls in an earthquake environment has been addressed by several authors with Kuesel (1969) and Yeh (1974) being typical examples. The approach utilized in previous studies is to apply the theoretical solution for simple wave propagation configurations to a more general situation by superimposing individual wave-type solutions.

The complexity of this problem forces the engineer to make conservative assumptions when utilizing the approach of Kuesel and Yeh. However, without a more detailed analysis, it is impossible to assess the degree of conservatism in the solution. The purpose of this study is to investigate the influence of different layered geologic configurations as well as the influence of the use of actual earthquake time history records on the peak strain induced.

It is implicitly assumed here, as is the case throughout this set of guidelines, that the tunnel walls experience the same strain as that in the immediately surrounding medium. As shown earlier in Annex D, this is generally a conservative assumption. It also simplifies the problem because it allows use of solutions where the wave propagates only in the medium.

Problem Configuration

Assuming that the geologic material is defined by a single material characterized by its P-wave and S-wave velocities, Yeh (1974) presents equations for the prediction of stresses in tunnel walls due to both oblique shear and compressional waves. These equations (Equations 16 and 23 of Yeh) are converted to strains and repeated as follows:

$$\text{S-wave strain} = \frac{\cos\theta_s}{c_s^2}\left(c_s\, v_s\, \sin\theta_s + R\, a_s\, \cos^2\theta_s\right) \qquad \text{Eq. F.1}$$

$$\text{P-wave strain} = \frac{\cos^2\theta_p}{c_p^2}\left(c_p\, v_p + R\, a_p\, \sin\theta_p\right) \qquad \text{Eq. F.2}$$

where R is the radius of the tunnel (assumed to act like a slender beam), c's are the seismic velocities, v's are the earthquake maximum velocity levels, a's are the earthquake maximum accelerations, and the subscripts p and s refer to the P-wave and S-wave terms. It is important to note that the equations of Yeh (1974) have been generalized to include differences between the angle of incidence of the P-wave and S-wave excitations. These angles are influenced by the P-wave and S-wave seismic velocity configurations and thus should be considered independently (see Figure B.1).

Equations F.1 and F.2 are derived by utilizing the fact that displacements transverse to the tunnel axis produce a bending strain and the displacements parallel to the tunnel axis produced axial strains. Also, it has been recognized that an oblique shear wave results in an apparent compressional wave of amplitude $A_s \sin\theta_s$ plus an apparent shear wave of amplitude $A_s \cos\theta_s$, both propagating with an apparent wave velocity of $c_s/\cos\theta_s$. Similarly, an oblique compressional wave is equivalent to an apparent compressional wave of amplitude $A_p \cos\theta_p$ plus an apparent shear wave of amplitude A_p $\sin\theta_p$, both propagating with an apparent wave velocity of $c_p/\cos\theta_p$. The terms A_p and A_s are the amplitudes of the compression and shear waves, respectively.

Since even for a single wave-type the maximum velocities and accelerations usually occur at different values of time for typical earthquakes, the superposition used in Equations F.1 and F.2 as well as the superposition of these equations can be overly conservative. Also, the influence of actual geologic layering has not been included. The approach used in this study has the objective of treating the superposition and geologic layering questions. These topics are treated by analyzing the earthquake motions in the time domain using typical soil geologic material configurations. The five configurations utilized here are illustrated in Table F.1.

The approach used applied an actual earthquake accelerations to a finite element mesh which represents the geologic layering configurations of Table F.1. To make the problem tractable, this problem is assumed to be divided into the P-wave and S-wave solutions.

These solutions, in turn, are derived by applying an acceleration record at a depth of 200 feet to finite element mesh with a free surface boundary condition at 0 feet. The P-wave solution utilizes the P-wave velocity of Table F.1 and 1940 El Centro Earthquake (Caltech, 1972) vertical acceleration. The S-wave solution utilizes the S-wave velocities of Table F.1 and El Centro East-West acceleration record (see Figures F.1 through F.3). The SATURN finite element program (Sweet, 1979) has been used to generate the time history solutions.

The approach defined above also has its inherent difficulties. Actual earthquake are, of course, much more complicated than the superposition of one-dimensional P-wave and S-wave solutions. It is not suggested here that this approach represents actual ground motion environments. It must be remembered that the intention of this study is to investigate several of the assumptions utilized in the earlier approaches by assessing their degree of conservatism and represents the next step in theoretical sophistication.

The utilization of the P-wave and S-wave solutions to predict the strain environments closely follows the approach of Kuesel (1969) and Yeh (1975). Namely, these solutions are assumed to be appropriate for a zero angle of incident and solutions at oblique angles are defined by reducing the amplitudes of the signal and modifying the time scales according to the geometry represented by the angle of incidence. Thus, the P-wave solution produces both compressional and shear wave contributions of reduced amplitude. These solutions (defined by a spatial distribution of displacements) can then be used to define the strain environment due to both axial and bending contributions. The S-wave one-dimensional solution is similarly treated to produce its contribution to the time history prediction of the strain in the tunnel wall. The total strain is then defined as the summation of the P-wave and S-wave solutions. Since the computations use time intervals which are very small compared to the smallest periods inherent in the wave, the effective "sampling rate" assures picking of several values along each leg of each spike within the wave. Thus, the time histories represented by the superposition process are an accurate reflection of all temporal characteristics in the input waves.

Numerical Results

The approach outlined above has been applied to the five geologic configurations of Table F.1. Velocity records as a function of depth for the P-wave solution, 3.1, and S-wave solution, 3.2, can be seen in Figures F.4 and F.5. Also, the surface velocity records for each of the P-wave and S-wave configurations defined in Table F.1 are shown in Figures F.6 and F.7.

The axial and bending strains at several depths resulting from these one-dimensional solutions are summarized in Figures F.8 through F.14. These solutions are the "zero angle of incidence" contributions and results from scaling the surface velocity records of Figures F.6 and F.7 to the maximum design earthquake (MDE) levels of 2.1 (P-wave) and 3.2 (S-wave) ft./sec. The superposition of these time history solutions is governed by the P-wave and S-wave angles of incidence. Typical tabulated results for both the MDE and operating design earthquake (ODE) are summarized in Tables F.2a and b, respectively.

Discussion

The results presented in Table F.2a and b are, for the most part, in agreement concerning several general behavioral trends. As an example both approaches are more sensitive to the maximum velocity rather than the maximum acceleration level as far as the prediction of strain is concerned. Also, the relative effect of different seismic velocities is in general agreement. As an example, Material #3 has the largest S-wave velocities and both Yeh's equations and this time history analysis predict that the strain is minimized for this configuration.

Yeh's equations predict that, similar to the seismic velocity distributions, the tunnel strain decreases with depth. The time history results, however, show an opposite trend for all cases except for Material #1. Finally, the superposition approach from Kuesel (1969) and Yeh (1974) results in an over-prediction of the strain in the tunnel wall by a factor of generally 2 or more compared to the time history solution utilizing the El Centro records as shown in Table F.3.

It is obvious by studying Table F.3 that use of the "Yeh approach," as reflected in Table B.1 of Annex B, produce strains for design which maybe conservative by a factor of approximately 2. Thus, even though no load factor or capacity reduction factor is used in the guidelines, the resulting design will be adequately conservative.

TABLE F.1

Definition of the Five Layered Geologies of This Study

The P-Wave velocities are defined as equal to two times the S-Wave velocities above the water table and equal to 5,000 ft./sec. below the water table.

LAYERED GEOLOGY CONFIGURATIONS
(S-Wave Velocities in ft./sec.)

Depth In Ft.	Material #1	Material #2	Material #3	Material #4	Material #5
0					
25	800	1200	1200	1200	1200
50	990	1200	1200	1200	1200
75	1120	1900	1900	1900	1900
100	1300	1900	1900	1900	1900
130	1500	1900	2500	1900	1900
200	2000	1900	2500	1900	1900
Water Table Location	25	25	25	100	200
P-Wave Calculation Solution No.	3.1	3.3	3.3	3.6	3.7
S-Wave Calculation Solution No.	3.2	3.4	3.5	3.4	3.4

TABLE F.2

Comparison Between Time History Solution and Results Using Yeh's Expressions (Yeh (1974)) for the Strain in the Tunnel Wall

Results are presented for the maximum design earthquake (MDE) and the operating design earthquake (ODE) for the five material configurations of Table F.2. The term Yeh-strain is derived by utilizing Equations 16 and 23 of Yeh (1974) with a radius of the tunnel equal to 9.5 feet and the local seismic velocities from Table F.1.

The MDE and ODE levels are defined as follow:

Table 2a - MDE:	Vertical Velocity	= 2.1 ft./sec.
	Horizontal Velocity	= 3.2 ft./sec.
	Vertical Acceleration	= 0.4 G's
	Horizontal Accleration	= 0.6 G's
Table 2b - ODE:	Vertical Velocity	= 1.0 ft./sec.
	Horizontal Velocity	= 1.4 ft./sec.
	Vertical Acceleration	= 0.2 G's
	Horizontal Accleration	= 0.3 G's

TABLE F.2.a

DEPTH EQUALS 150. FEET - M.D.E. - MATERIAL CONFIGURATION NUMBER 1

THETA-S DEGREES	THETA-P DEGREES	YEH-STRAIN PER CENT	STRAIN-MAX PER CENT
5.	5.	.0602	.0128
5.	15.	.0577	.0117
5.	30.	.0501	.0131
5.	45.	.0396	.0109
5.	60.	.0290	.0102
5.	75.	.0213	.0070
5.	85.	.0188	.0069
15.	5.	.0859	.0159
15.	15.	.0834	.0195
15.	30.	.0758	.0149
15.	45.	.0653	.0156
15.	60.	.0547	.0171
15.	75.	.0470	.0148
15.	85.	.0445	.0149
30.	5.	.1140	.0253
30.	15.	.1116	.0277
30.	30.	.1039	.0303
30.	45.	.0934	.0273
30.	60.	.0829	.0268
30.	75.	.0751	.0262
30.	85.	.0726	.0260
45.	5.	.1233	.0392
45.	15.	.1209	.0388
45.	30.	.1133	.0391
45.	45.	.1028	.0387
45.	60.	.0922	.0365
45.	75.	.0845	.0352
45.	85.	.0819	.0353
60.	5.	.1116	.0489
60.	15.	.1092	.0500
60.	30.	.1015	.0440
60.	45.	.0910	.0454
60.	60.	.0805	.0449
60.	75.	.0727	.0421
60.	85.	.0702	.0432
75.	5.	.0818	.0487
75.	15.	.0794	.0512
75.	30.	.0718	.0535
75.	45.	.0613	.0489
75.	60.	.0507	.0510
75.	75.	.0429	.0479
75.	85.	.0404	.0471
85.	5.	.0556	.0510
85.	15.	.0532	.0486
85.	30.	.0456	.0463
85.	45.	.0351	.0464
85.	60.	.0245	.0501
85.	75.	.0167	.0477
85.	85.	.0142	.0481

TABLE F.2.b

DEPTH EQUALS 150. FEET - O.D.E. - MATERIAL CONFIGURATION NUMBER 1

THETA-S DEGREES	THETA-P DEGREES	YEH-STRAIN PER CENT	STRAIN-MAX PER CENT
5.	5.	.0282	.0060
5.	15.	.0271	.0055
5.	30.	.0234	.0061
5.	45.	.0184	.0050
5.	60.	.0134	.0047
5.	75.	.0097	.0031
5.	85.	.0085	.0030
15.	5.	.0394	.0071
15.	15.	.0383	.0087
15.	30.	.0347	.0066
15.	45.	.0297	.0069
15.	60.	.0246	.0077
15.	75.	.0209	.0064
15.	85.	.0197	.0065
30.	5.	.0517	.0111
30.	15.	.0505	.0122
30.	30.	.0469	.0134
30.	45.	.0419	.0120
30.	60.	.0369	.0118
30.	75.	.0332	.0115
30.	85.	.0320	.0114
45.	5.	.0557	.0173
45.	15.	.0545	.0171
45.	30.	.0509	.0173
45.	45.	.0459	.0171
45.	60.	.0409	.0160
45.	75.	.0372	.0154
45.	85.	.0360	.0154
60.	5.	.0505	.0216
60.	15.	.0493	.0222
60.	30.	.0457	.0193
60.	45.	.0407	.0200
60.	60.	.0357	.0198
60.	75.	.0320	.0184
60.	85.	.0308	.0190
75.	5.	.0374	.0214
75.	15.	.0363	.0226
75.	30.	.0326	.0237
75.	45.	.0276	.0215
75.	60.	.0226	.0225
75.	75.	.0189	.0210
75.	85.	.0177	.0206
85.	5.	.0259	.0224
85.	15.	.0248	.0213
85.	30.	.0212	.0202
85.	45.	.0162	.0203
85.	60.	.0111	.0220
85.	75.	.0074	.0209
85.	85.	.0062	.0210

TABLE F.3

Comparisons of Maxima by Yeh (1974) and Time and Space History Approaches

Mat'l Config.	Depth ft.	Max. by Yeh (1974) %	Max. by current approach %	Ratio: Yeh: current
Maximum Design Earthquake				
1	75	0.17	0.09	1.9
1	150	0.12	0.05	2.4
1	175	0.12	0.06	2
2	75	0.13	0.03	4.3
2	150	0.13	0.06	2.2
2	175	0.13	0.07	1.9
3	75	0.13	0.03	4.3
3	150	0.11	0.03	3.7
3	175	0.11	0.04	2.8
4	75	0.14	0.04	3.5
4	150	0.13	0.06	2.2
4	175	0.13	0.07	1.9
5	75	0.14	0.04	3.5
5	150	0.14	0.06	2.3
5	175	0.14	0.07	2
Operating Design Earthquake				
1	75	0.08	0.04	2
1	150	0.06	0.02	3
1	175	0.06	0.03	2
2	75	0.06	0.01	6
2	150	0.06	0.03	2
2	175	0.06	0.03	2
3	75	0.06	0.01	6
3	150	0.05	0.02	2.5
3	175	0.05	0.02	2.5
4	75	0.06	0.02	3
4	150	0.06	0.03	2
4	175	0.06	0.03	2
5	75	0.06	0.02	3
5	150	0.06	0.03	2
5	175	0.06	0.03	2

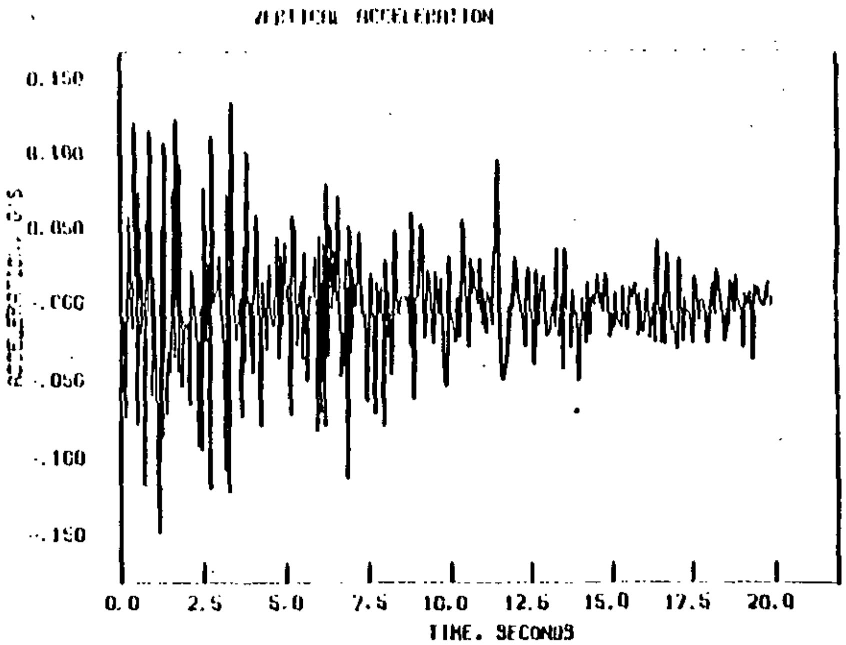

FIGURE F.1

1940 El Centro Earthquake Acceleration Records (Caltech (1972)). Vertical and East-West Acceleration Records are Utilized for the P-wave and S-wave Solutions, respectively. Both Acceleration Records are Applied at a Depth of 200 Feet for the Layered Geologies of Table F.1.

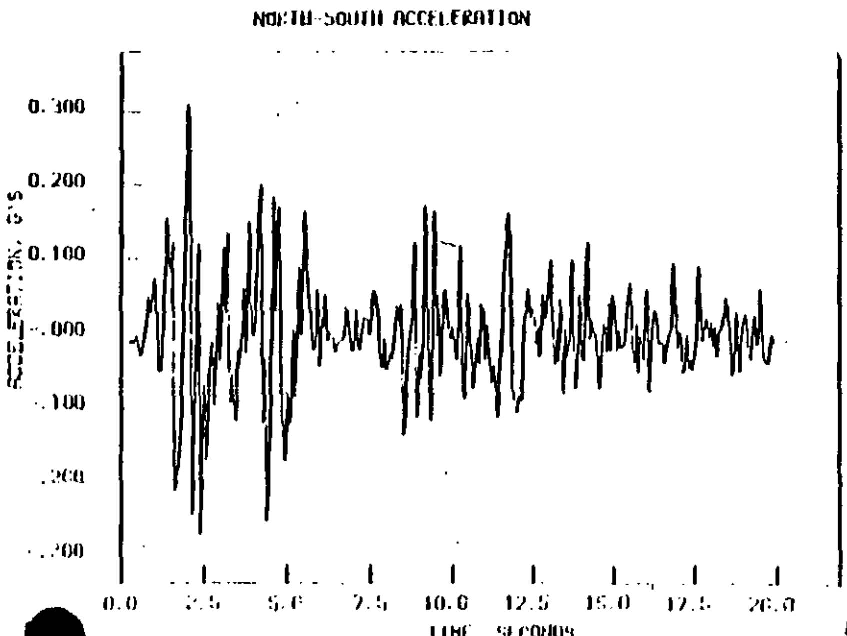

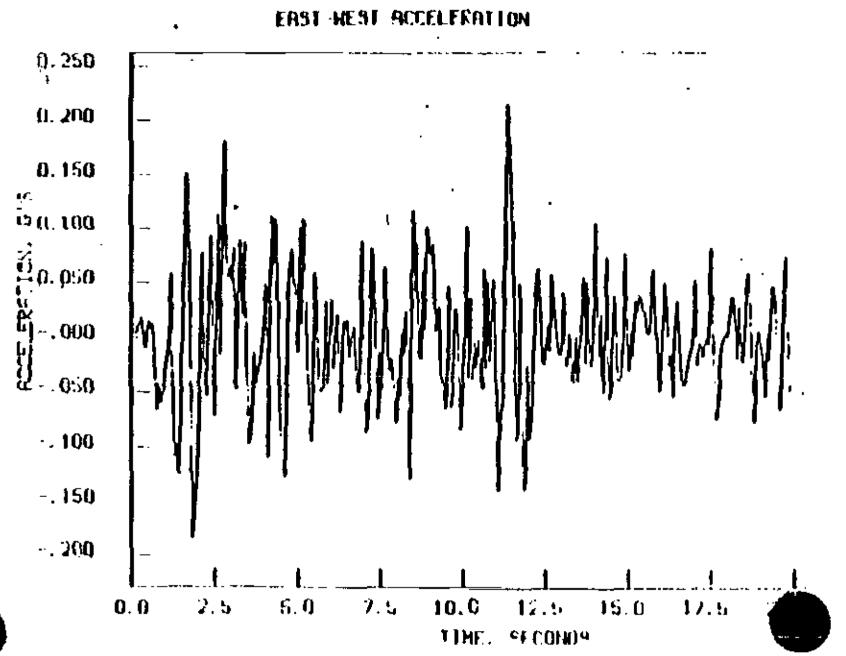

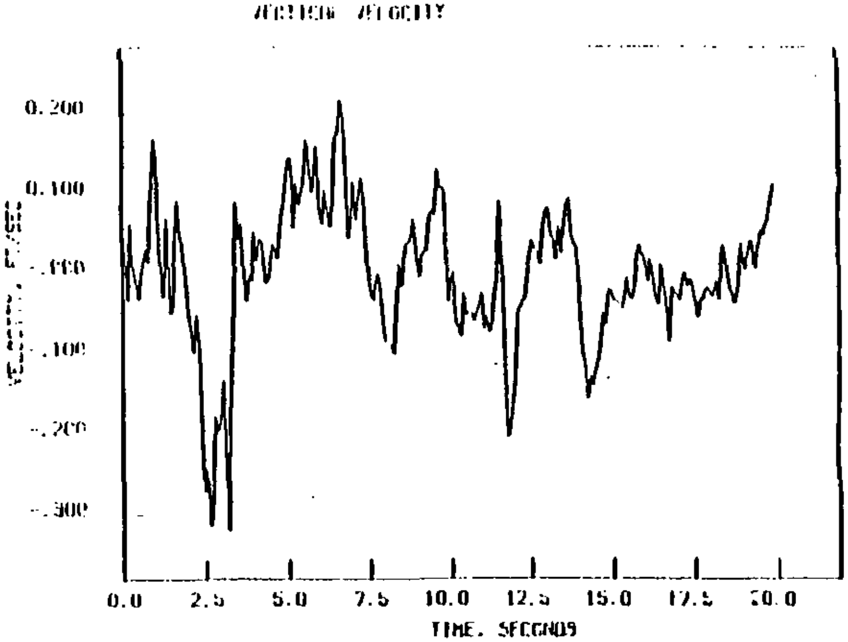

FIGURE F.2

El Centro Velocity Records From Caltech (1972)

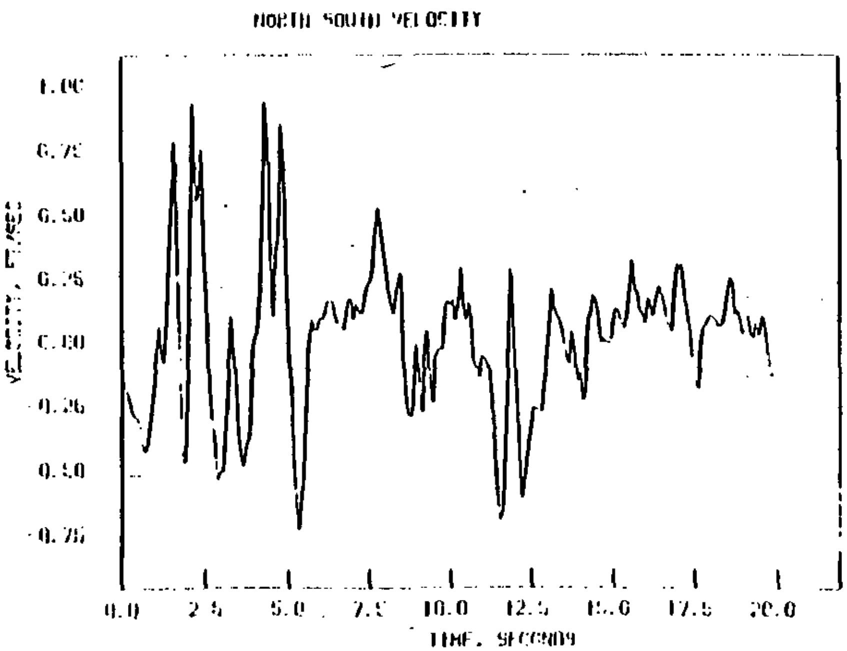

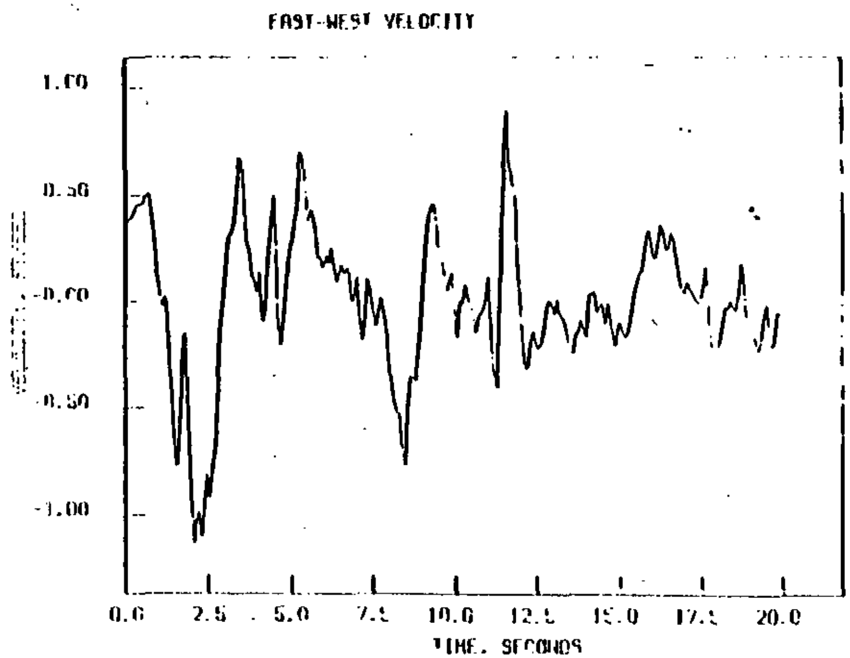

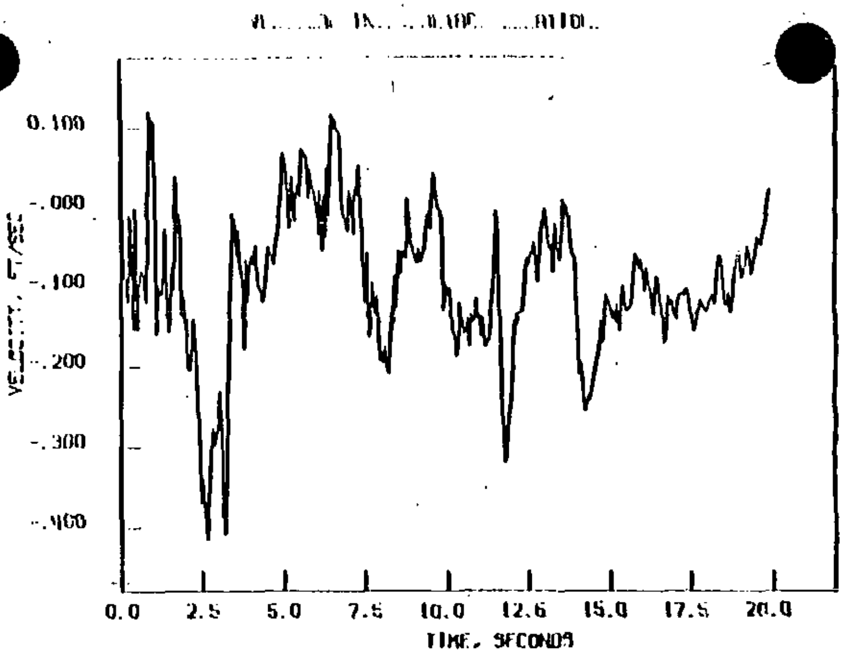

FIGURE F.3

Velocity Records Resulting From The Integration of the Acceleration Records of Figure F.1. These Records Are Indicative of the Velocity Behavior of the Finite Element Mesh at 200 ft.

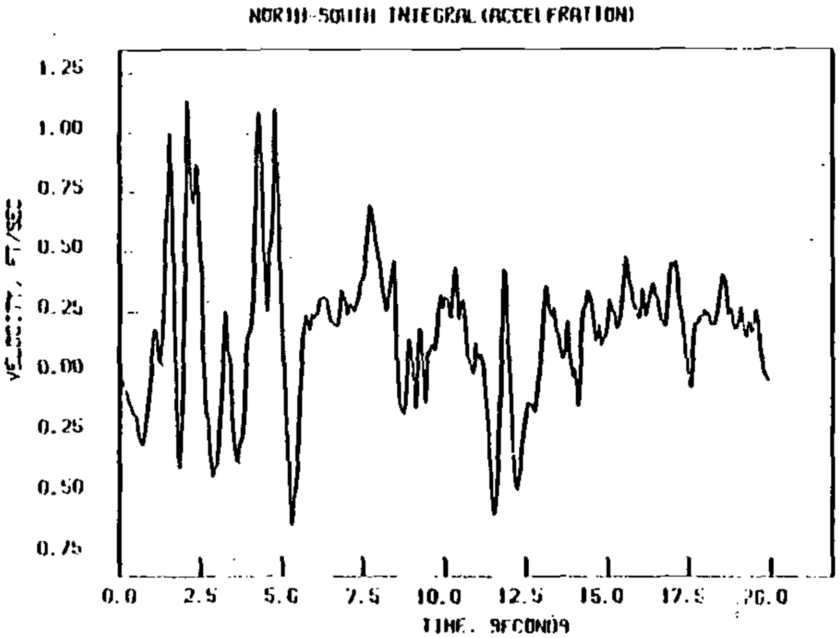

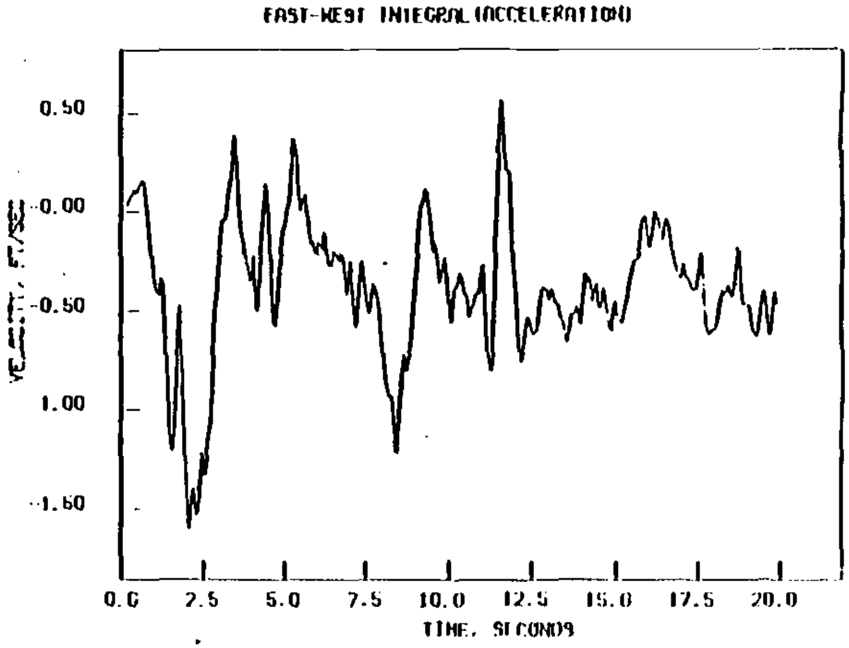

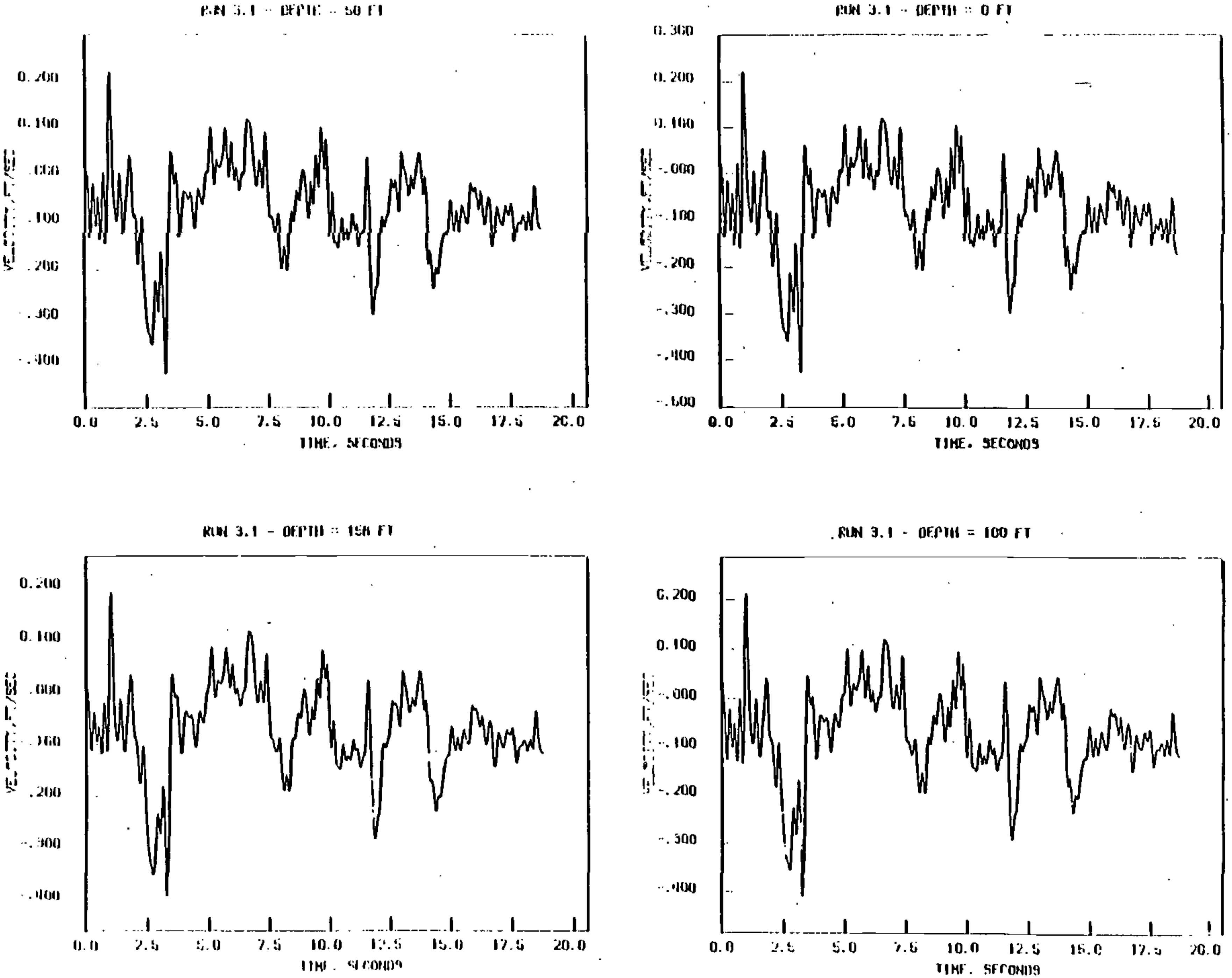

FIGURE F.4 P-wave Velocity Records at Various Depths for the Calculation 3.1 (See Table F.1)

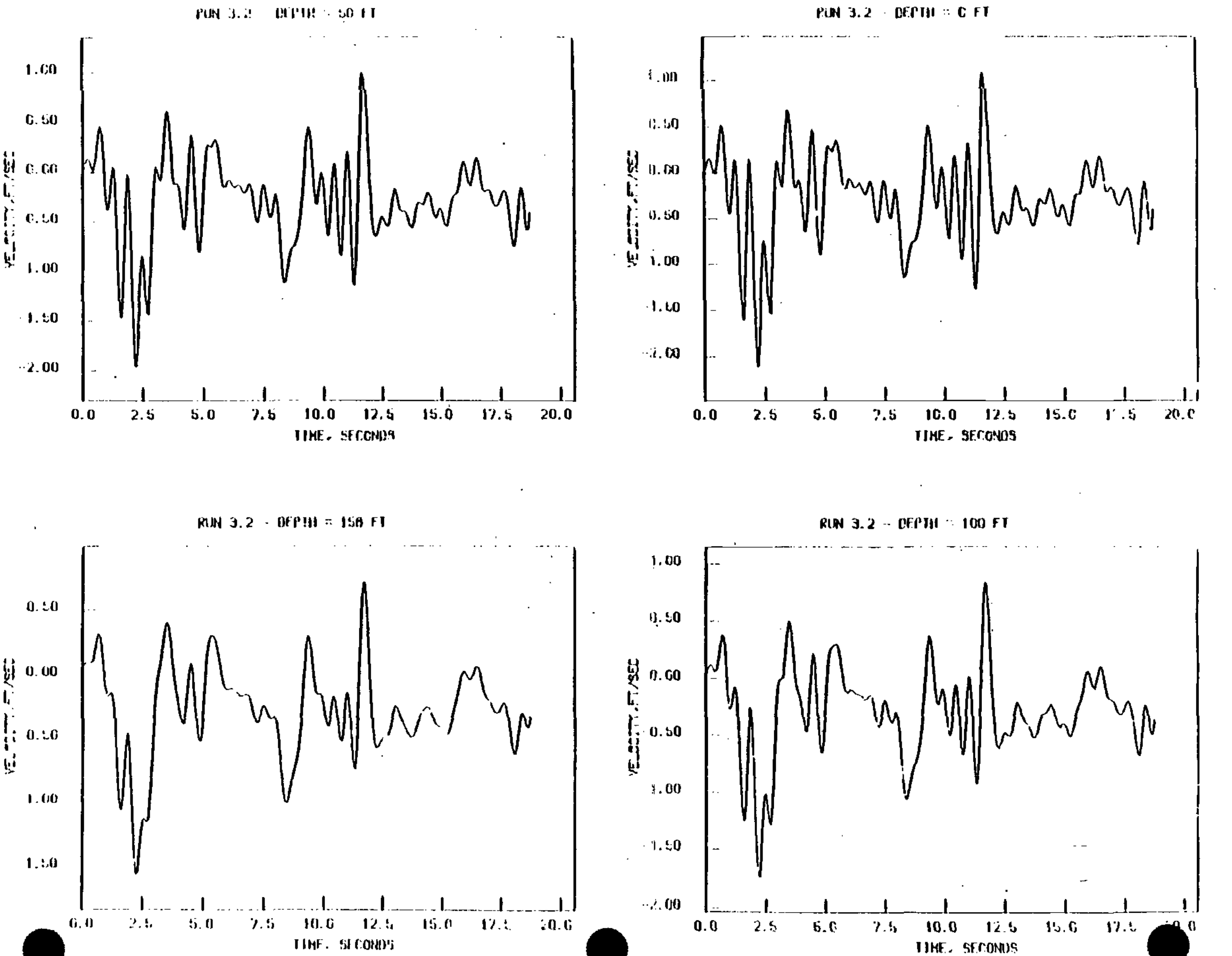

FIGURE . . S wave Velocity Records at Various Depths for the Calculation 3.2 (See Table F.1)

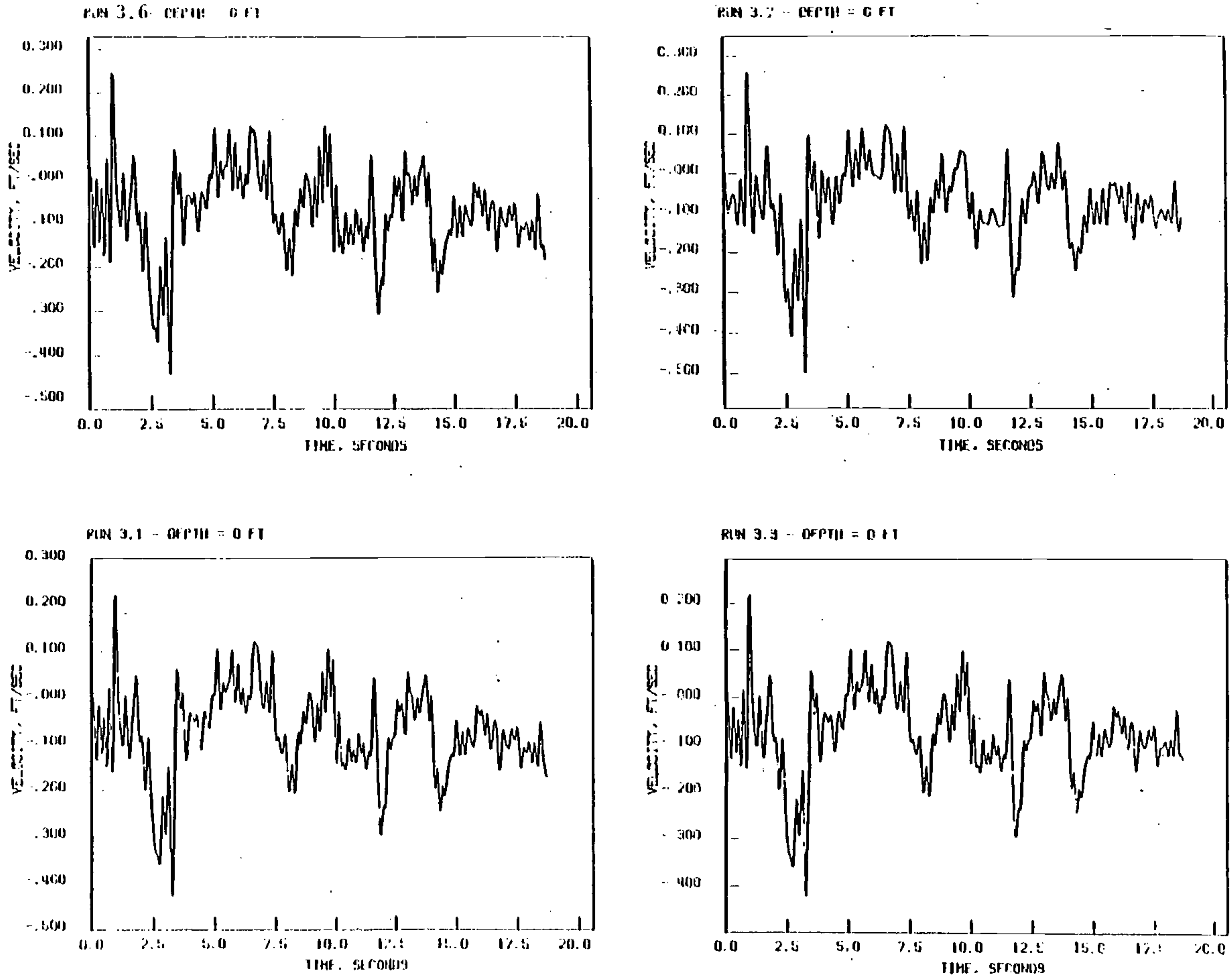

FIGURE F.6 Surface Velocity Records for the P-wave Solutions of Table F.1

FIGURE F.7

Surface Velocity Records for the S-Wave Solutions of Table F.1

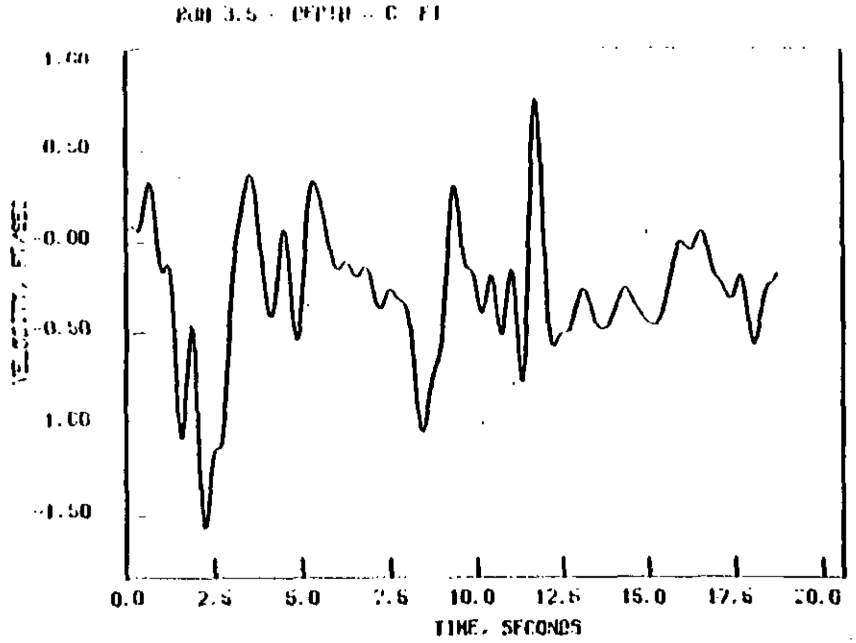

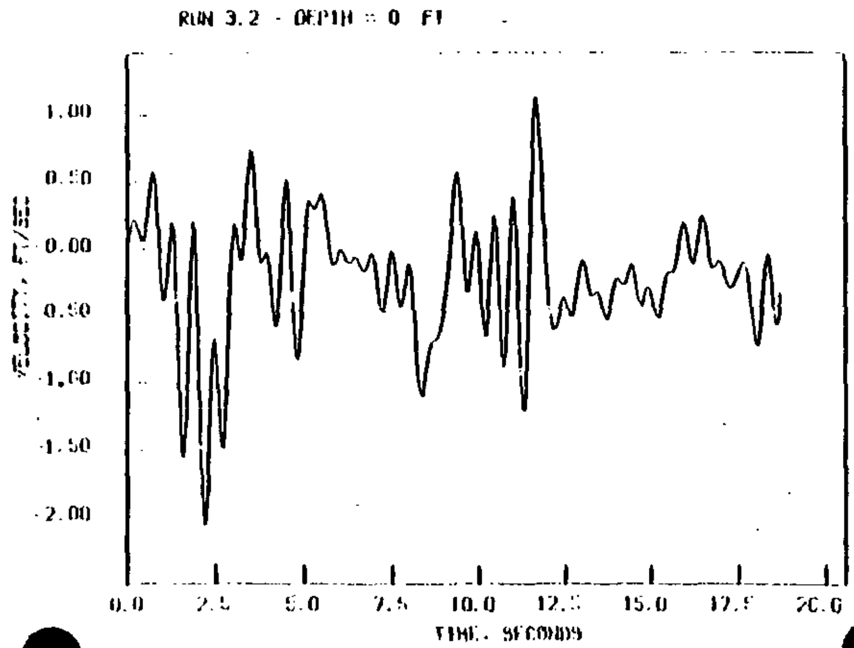

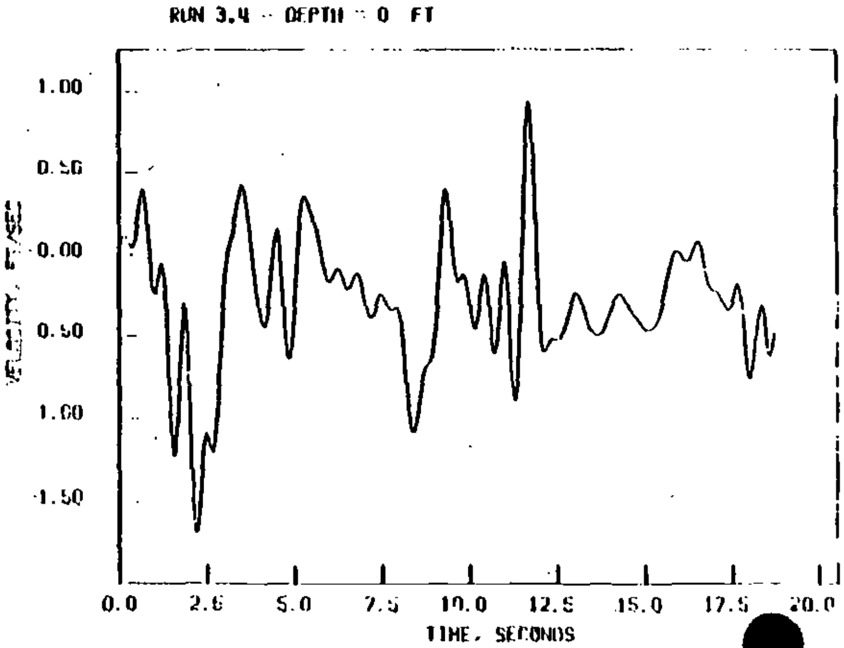

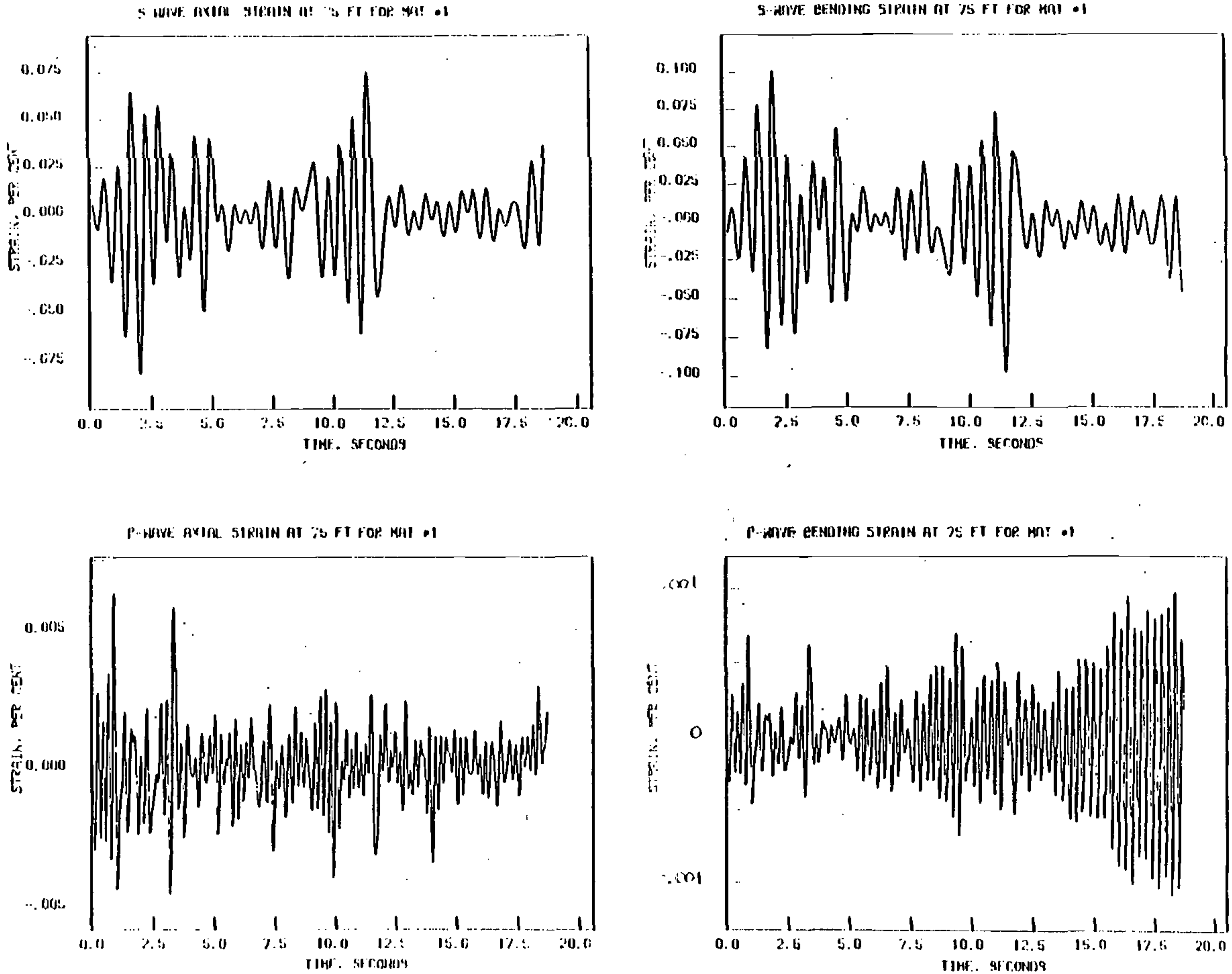

FIGURE F.8 Material #1 Strains at 75 ft. After Scaling P and S Surface Velocities to 2.1 and 3.2 ft./sec.

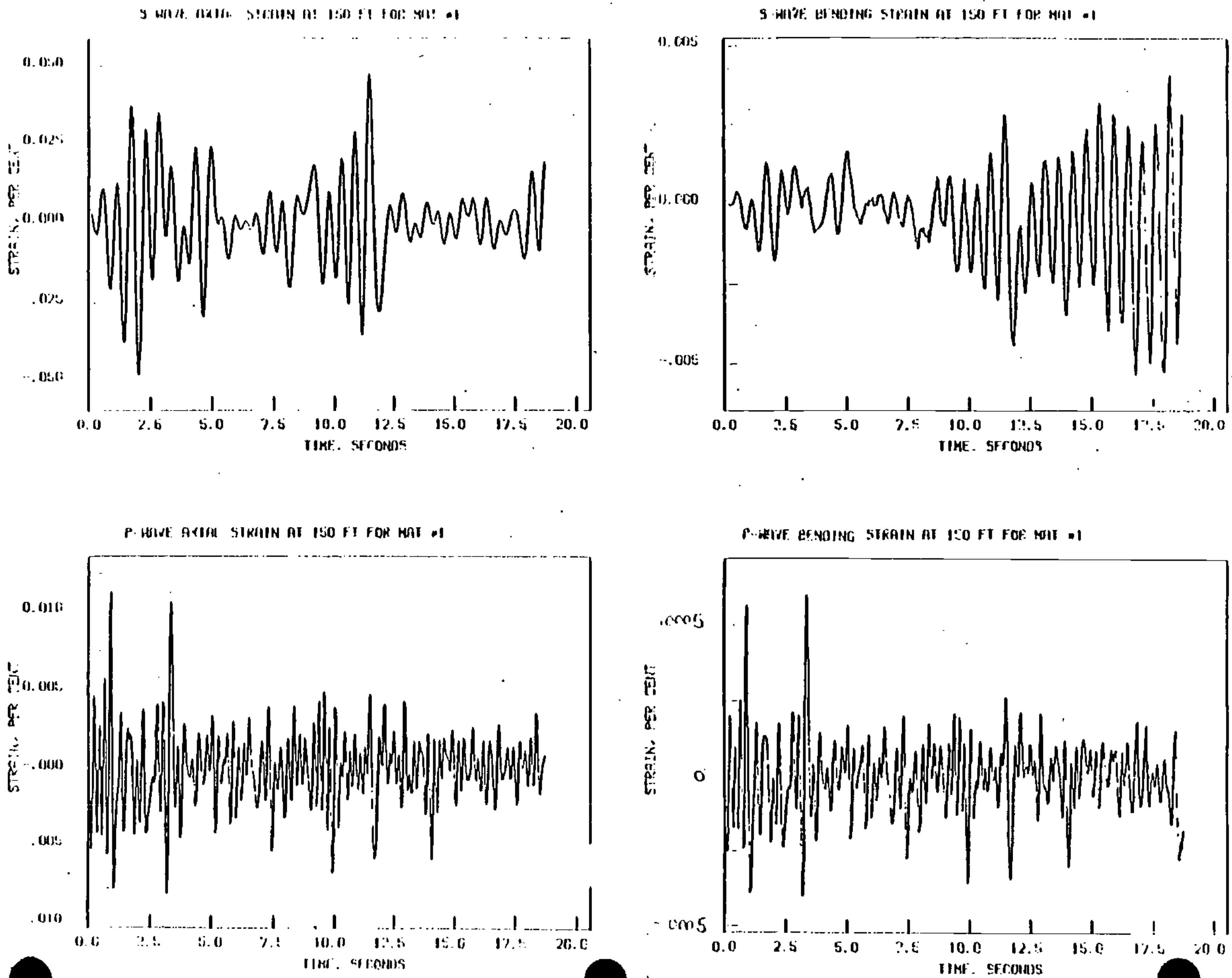

FIGURE F.9 Material #1 Strain at 150 ft. After Scaling
P and S Surface Velocities to 2.1 and 3.2 ft./sec

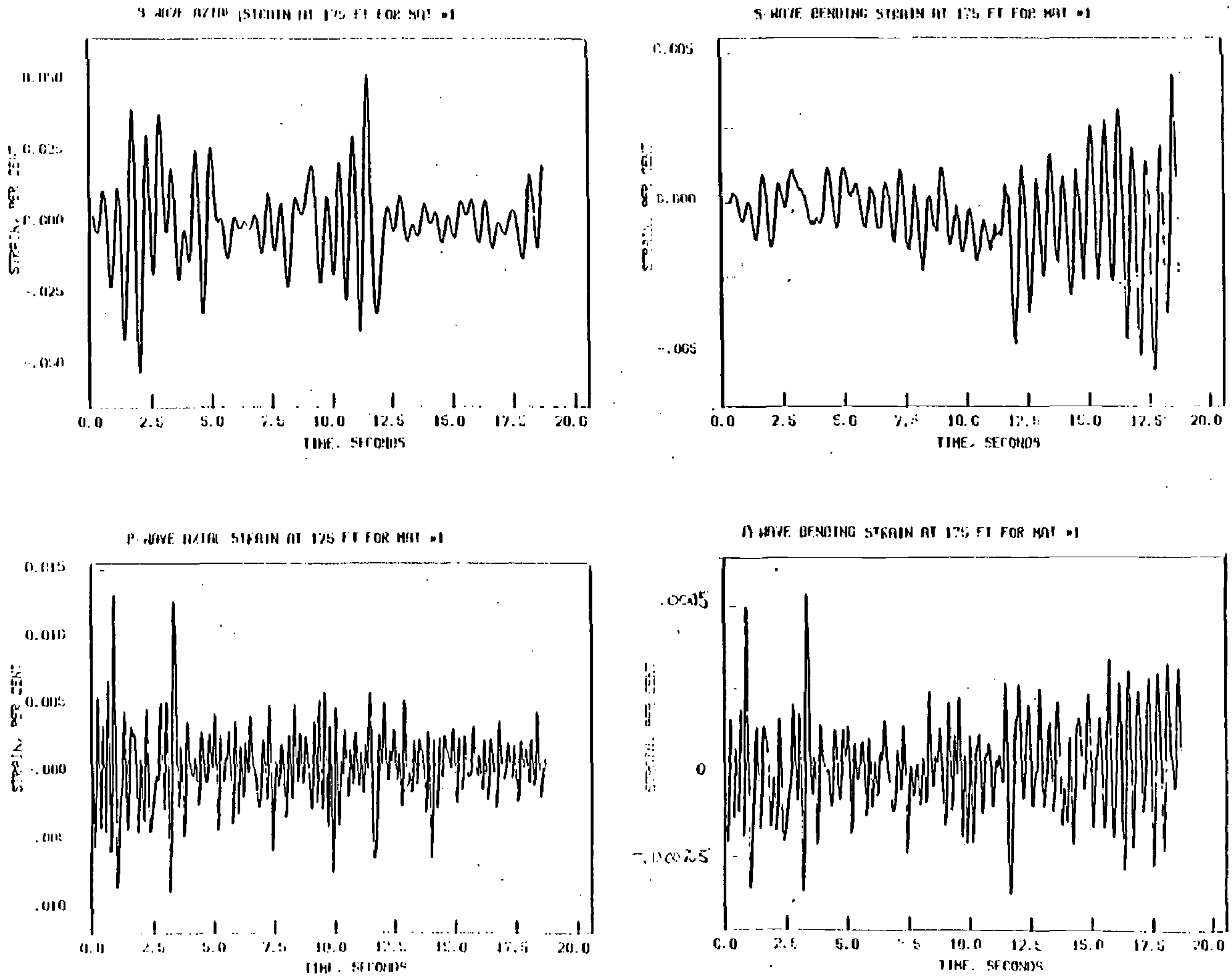

F-21

FIGURE F.10 Material #1 Strains at 175 Ft. After Scaling
P and S Surface Velocities to [illegible]

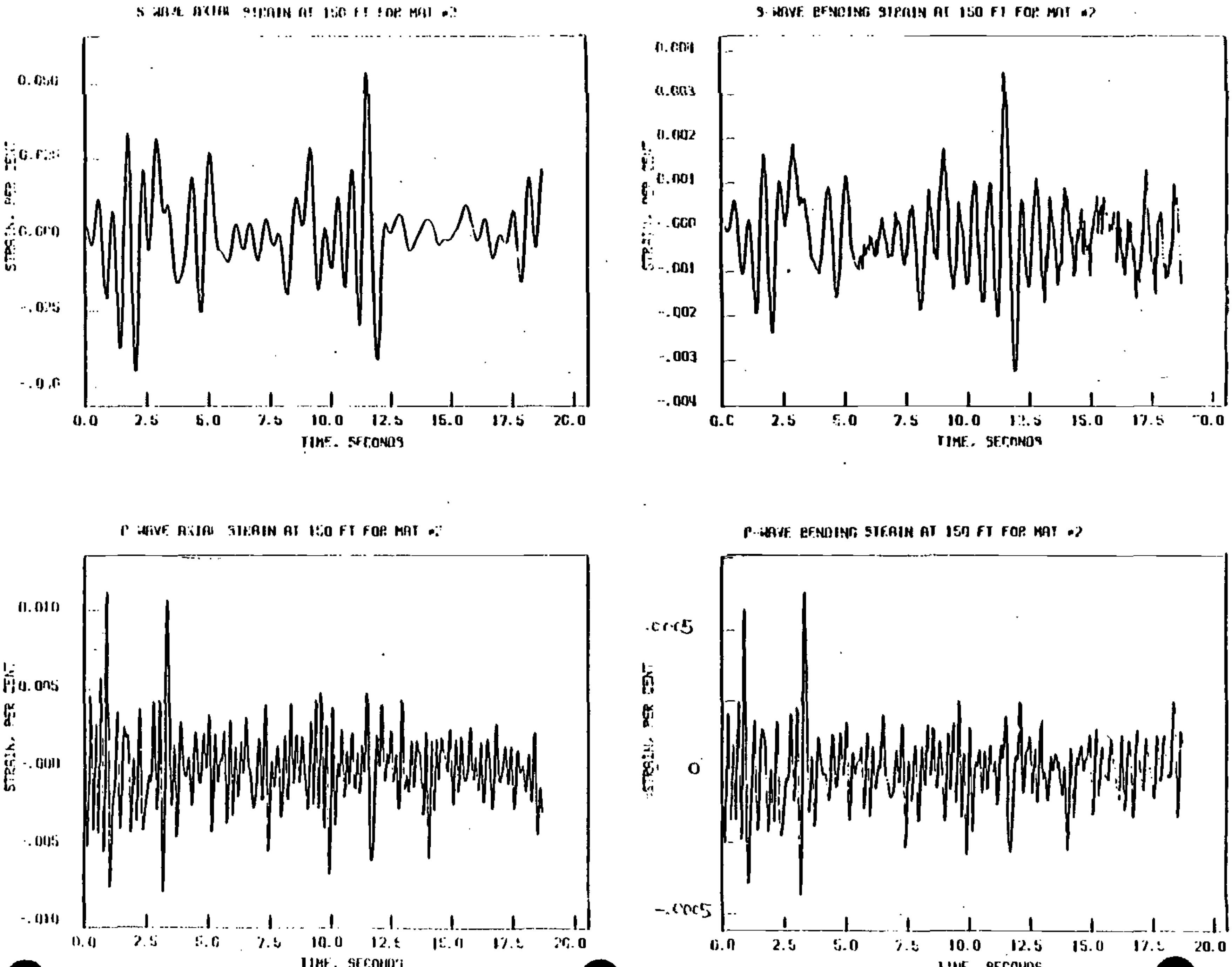

FIGURE F.11 Material #2 Strains 150 ft. After Scaling

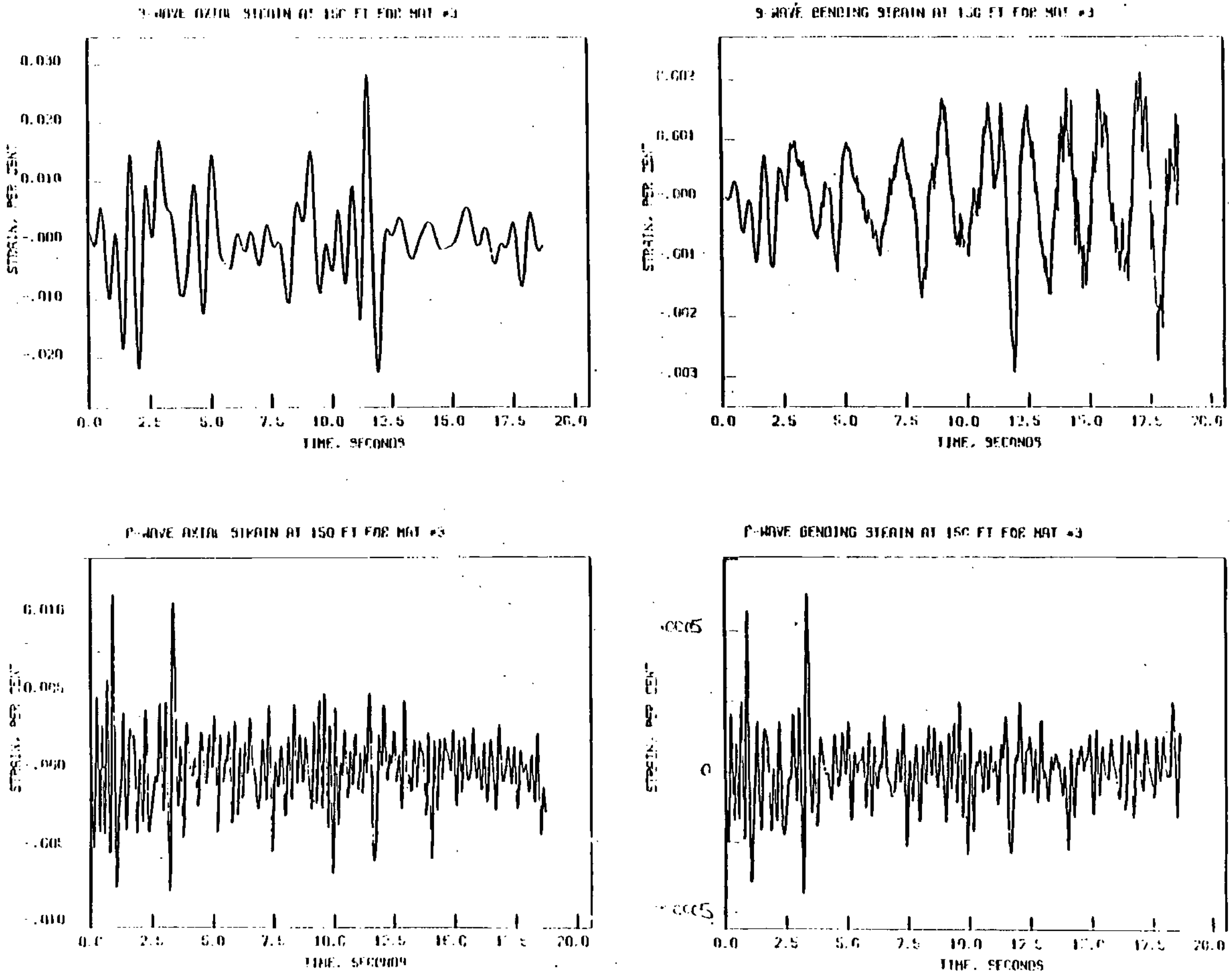

FIGURE F.12 Material #3 Strains a 150 ft. After Scaling

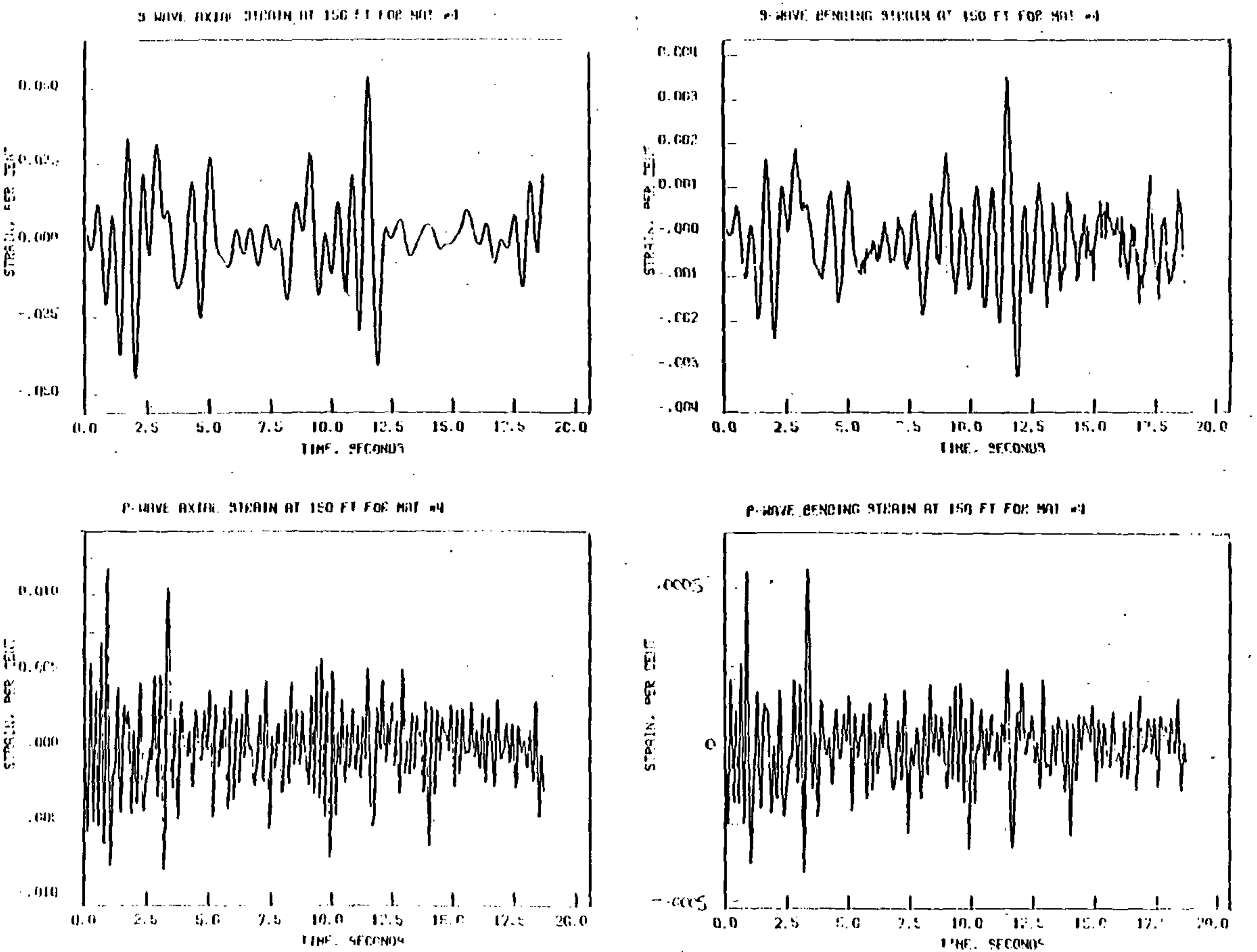

FIGURE F.13 Material #4 Stra at 150 ft. After Scaling P and S Surface cities to 2.1 and 3.2 ft./sec.

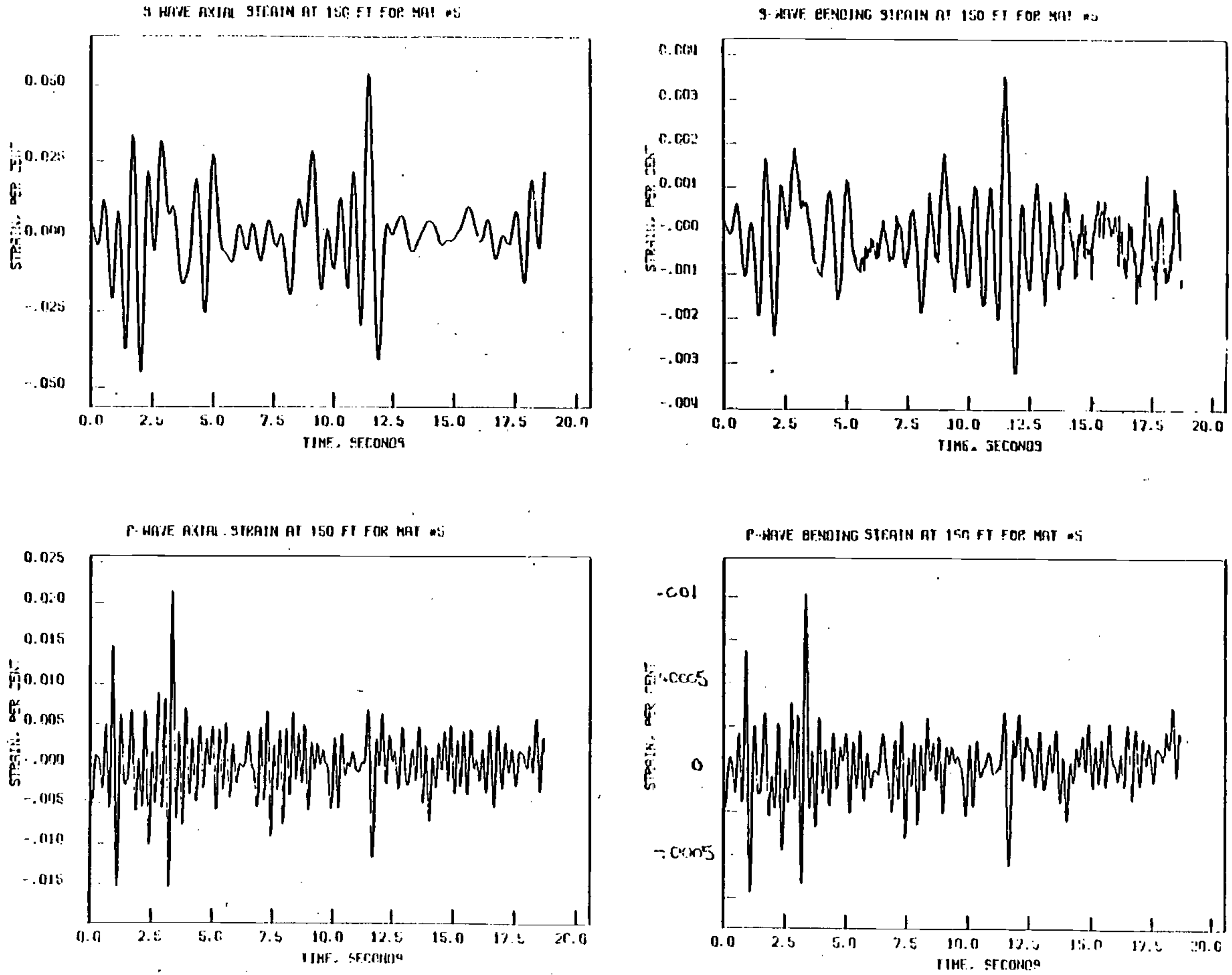

FIGURE F.14 Material #5 Strains at 150 ft. After Scaling P and S Surface Velocities to 2.1 and 3.2 ft./sec.

REFERENCES

F.1 Kuesel, T.R. (1969), "Earthquake Design Criteria for Subways," J. Struct. Div. Am. Soc. Civil Eng., V. 95.

F.2 Yeh, G., (1974), "Seismic Analysis of Slender Buried Beams," Bull. Seism. Soc. Am., V. 64, No. 5.

F.3 Caltech (1972), "Analysis of String Motion Earthquake Records," Report EERL 72-80, August.

F.4 Sweet, J., (1979), "SATURN - A Multi-Dimensional Two-Phase Computer Program which Treat the Nonlinear Behavior of Continua Using the Finite Element Approach," Joel Sweet and Associates Report No. JSA-79-016, September.